2014-02-10

The Development of a Sensitive Manipulation End Effector

Catherine Coleman
Worcester Polytechnic Institute

THE DEVELOPMENT OF A SENSITIVE MANIPULATION END EFFECTOR

By

Catherine Coleman

A Thesis

Submitted to the Faculty

of the

WORCESTER POLYTECHNIC INSTITUTE

in partial fulfillment of the requirements for the

Degree of Master of Science

in

Robotics Engineering

by

_____

January 29, 2014

APPROVED:

_____

Dr. Eduardo Torres-Jara, Advisor

_____

Dr. Gregory Fischer, Thesis Committee Member

_____

Dr. Taskin Padir, Thesis Committee Member

Abstract

This thesis designed and realized a two-degree of freedom wrist and two finger manipulator that completes the six-degree of freedom Sensitive Manipulation Platform, the arm of which was previously developed. This platform extends the previous research in the field of robotics by covering not only the end effector with deformable tactile sensors, but also the links of the arm. Having tactile sensors on the arm will improve the dynamic model of the system during contact with its environment and will allow research in contact navigation to be explored. This type of research is intended for developing algorithms for exploring dynamic environments. Unlike traditional robots that focus on collision avoidance, this platform is designed to seek out contact and use it to gather important information about its surroundings. This small desktop platform was designed to have similar proportions and properties to a small human arm. These properties include compliant joints and tactile sensitivity along the lengths of the arms. The primary applications for the completed platform will be research in contact navigation and manipulation in dynamic environments. However, there are countless potential applications for a compliant arm with increased tactile feedback, including prosthetics and domestic robotics. This thesis covers the details behind the design, analysis, and evaluation of the two degrees of the Wrist and two two-link fingers, with particular attention being given to the integration of series elastics actuators, the decoupling of the fingers from the wrist, and the incorporation of tactile sensors in both the forearm motor module and fingers.

Acknowledgements

This project has vastly expanded my engineering skills and knowledge. This project would never have come close to completion without the help and support from countless people. I would like to begin by thanking my adviser Professor Eduardo Torres-Jara for his continuous support and guidance throughout this project. You gave me the best possible opportunity to grow as both a person and an engineer. Thank you so much for the opportunity to work on such a educational and fulfilling project.

I would also like to thank my committee members, Professor Gregory Fischer and Professor Taskin Padir. Thank you for taking the time to review my paper and give me feedback on my project.

I also need to thank Ennio Claretti. You are responsible for getting me involved in academic research and motivating me to stay for my Masters. I couldn't have done this project without your support. Thank you for constantly pushing me to expand my horizons and be a better engineer. The time you spent teaching me about manufacturing, mechanical design, and electronics was invaluable. My project is better because of the hours we spent brainstorming together the best solution for the different joints and mechanical problems I ran into. I would also like to thank you for all the time you spend reviewing my design and creating boards for this project. I hope that I get a chance to work with you again in the future.

Nigel, it was a pleasure working with you. Thank you for designing the base of the arm and for the dynamic model of the arm. It was a great working with you in lab and on this project.

Thank you Tracey! Your effort was invaluable in getting everything I needed for this project. You relieved so much stress from my life by correcting wrong parts for me and chatting with me when I needed a break. Thank you also for helping me navigate through the graduation and requirements paper work.

To Keven Arruda and Matt DiPinto, thank you, thank you, thank you, for being so patience with me in the machine shop. I really didn't know anything about machining when I first approached you guys for help. By the end of the project you had taught me well and I felt confident using all of the manual tools and some of the CnCs. Hopefully I was not too much of an annoyance.

And finally to all my friends that helped me and had to deal with me during this project, thank you. Dan Lanier thank you for proof reading my thesis paper, and keeping me motivated enough to write it. Victoria Coleman, thank you for also taking the time to look through my thesis paper. James Kingsly, thank you for helping me come up with a better method to tighten the tensioners on the wrist. Carly it was a pleasure to work in lab with you. And thank you to everyone else who helped me on this project who I may have missed.

Table of Contents

List of Figures

List of Tables

Chapter 1 Introduction

Robots are historically suited for tasks that are dull, dirty, dangerous, or in areas inaccessible to humans. They are used to automate tasks that humans could perform but for a variety of reasons would rather have the task done for them. In an assembly line, the tasks involved are repetitive and dull. Because of this, assembly lines were one of the first locations that robotics was applied to supplement human labor. Robotics relived human factory workers from extremely mundane tasks, while increasing the efficacy of the production system. Currently, there are over 1.5 million industrial robots in use worldwide with 159,346 new robots shipped in 2012 according to the International Federation of Robotics (1). In a factory setting, the product being manipulated is fairly consistent and the process is well defined. Because of this, most manipulation is accomplished with either a basic two-finger pincher mechanism or custom end effectors with task specific sensors. The success of these robots in the structured industrial setting has inspired the reapplication of robotics to dull tasks in more dynamic and unstructured environments. For example as personal assistance robotics equipped with sensitivity for helping the elderly. The robots found in the industrial setting focus on precision, accuracy, and speed, all of which require a very stiff, fast moving mechanism with only the required level of sensitivity to accomplish the particular task (2). This type of system raises many safety concerns for the robot, the operating environment, and potentially humans in the case of collisions. It also focuses on task specific manipulation and sensing which cannot be applied seamlessly into unknown manipulation and navigation tasks.

For a robot to successfully perform tasks in a dynamic environment without being a hazard to itself and other objects, such as people in its environment, it needs to be

adaptable. In order to be adaptable, it needs to be aware of its environment so that it can react according to stimuli instead of simply following a simply preset set of instructs. These types of interactions are more event driven instead of procedural. Therefore, a flexible, compliant robot with a combination of both visual and sensory force feedback would be necessary. Humans are a good example of a flexible and compliant system that pairs vision and haptic feedback to interact with their environment and can serve as an inspiration for further robotics development in this field.

Humans have flexible ligaments that add natural elasticity to their joints, which allows for compliant contacts with the outside world. This compliance makes overextending or spraining an ankle more common than breaking a bone. This compliance protects the joints and bones from injury. This is especially evident in the fingers. After having extended the fingers as far back as possible, they can still be pulled back further without pain or damage. In a robotic system, compliance has the added benefit of simplifying the force control equation. Instead of using a complex equation that requires an accurate model of the system, the compliant element can be used to measure the joint torque and drastically simply the control equation. Having force control allows tasks like inserting a peg in a hole to become significantly easier. Humans easily perform this task by using force control to 'feel' for the edges of the hole in order to place the peg. Without force control, the robot would need to know exactly where the hole is and the orientation of the peg (2).

Human rely on their sense of vision more than any other sense. For example, in the Mcgurk effect humans will hear different sounds based on the image they are shown of the person making the sound when in reality the same sound is played when both images are

presented (3). Vision is capable of overwriting any of the other sensors. Consider the sensation of walking on a broken moving walkway or escalator. Despite the fact that it is not moving, we still trip a little when entering and exiting. Vision, while not addressed directly in this project, will be applied to the platform in later experiments combining vision and contact based navigation and manipulation.

Humans are also covered tactile sensors. These sensors have a range of resolutions depending on the location on the body. The fingers have the highest resolution and are able to detect separate impacts less than 5mm apart. When manipulating in the dark or in an area where there is no line of sight, humans relay heavily on this sense of touch. They work by exploring their environment using contact to map their environment. Tactile sensors in the skin are also important when doing fine manipulation. Johansson and Wrestling studied the feedback response of skin when grasping objects and how that affects finger control. They found that even with full vision, participants found grasping and manipulating objects difficult without tactile sensing. Tactile sensing was removed by forcing the participants to wear thick gloves. Despite the richness of information that can be gathered from tactile sensors, significantly more research has been done with vision (4). The tactile research that has been conducted mostly examines tasks being completed in controlled environments (5) (6).However, sensitive manipulation is capable of proving a much more complete solution to both dynamic manipulation and navigation (7) (8) (9).

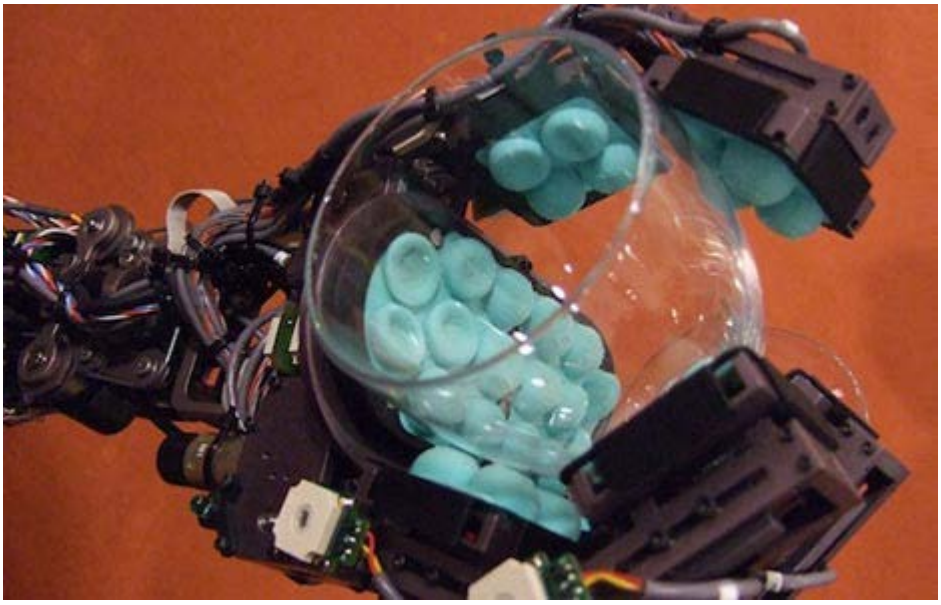

Figure 1 Tactile sensors applied to the inside of a hand (Torres-Jara E. , 2007).

Sensitive manipulation has been explored on the inside of a hand (8), on the foot of a biped robot (10), and on the tips of the fingers of a robot (7). This project will expand this area of research by completing the six-degree of freedom arm (11) with a 4 degree of freedom, two finger gripper at the end. This platform will expand research on the benefits of increased tactile sensitivity by applying tactile sensor onto the exterior of the links of the arm and to all of the faces of the fingers, not just the inside. This thesis covers the design and prototyping of the arm with the two-degree of freedom wrist and the gripper platform specifically designed for sensitive manipulation. The platform developed during this project will use only joints with incorporated elastic and tactile sensor coverage integrated into the design. This thesis addresses the details behind the design, analysis, and evaluation of the two degrees of the Wrist and two two-link fingers, with particular attention being given to the integration of series elastics actuators, the decoupling of the fingers from the wrist, and the incorporation of tactile sensors in both the forearm motor module and fingers.

1.1 Literature Review

Robotic manipulators have a wide variety of applications and are a major focus of research. They have applications spanning across many different industries, from industrial applications to domestic applications. This section provides a comprehensive review on the history of robotics manipulators, series elastic actuators and tactile sensors.

1.1.1 Robotics Manipulators

Dr. George Devol and Dr. Englberge invented the first robotic hand for industrial applications in 1959 for use with their industrial 'Unimate.' Robotic Hands and automated industrial machines were developed in parallel. This gripper was a very simple 'grab-release' style, two prong manipulator that is still used in industrial applications today. This style of gripper focuses on accuracy and precise manipulation (12).

The most common industrial applications for robotic grippers are in packaging and assembly, these applications being ideal for robotic manipulators as they require both precise grasping and placement. Robotic arms used in packaging are responsible for moving products, usually from a conveyor belt into a larger box for shipping. The gripper is a critical element in this process because it needs to be able to reliably control the product without damaging it and place it in its correct new location. It also needs to be capable of removing it from the conveyor belt safely. The most common grippers used for this type of application are the two prong manipulators mentioned above (13)and suction cups. The other common industrial application for grippers is assembly. During this process the gripper needs to be able to move components into the correct position for assembly or to

move products between different assembly steps. Most of this work is usually done with specifically engineered fixtures or suction cups. An example of an industry that uses robotics heavily for assembly is mass production circuit board assembly. This thesis develops a platform for sensitive manipulation capable of working in an unstructured dynamic environment with a variety of different objects, which is very different from the goals of its industrial predecessors.

The first 'sensitive' gripper appeared in 1961 and was created by Hinrich Ernst at MIT (14). Like the manipulator on the Unimate (15), it had two fingers that pinched; however this gripper had pressure, photodiode, and touch sensors. Having a 'sensitive' gripper provides feedback and a closed-loop system to increase the accuracy of the gripper because it was able to 'feel' when it was grasping an object. Previously, if the robot failed to grasp a product or the product slipped out of the gripper, it would not be aware and proceed as if the motion had been successful. By adding sensitivity, the gripper is also able to detect the amount of force it is applying to the product and if it is lined up properly, reducing product drop rate and breakage (16).

A summary of the following 51 years of history is in Table 1. Over the next 51 years, robotic manipulators have further developed to be capable of completing more complex manipulation tasks with a higher level of autonomy and intelligence because of a combination of advances in both design and controls. Manipulators with different levels of sensitivity and flexibility and with different numbers of fingers in different orientations, have all been explored for different applications.

Table 1: Historical Time Line (17)

Year	Invention	Summary

1959	Unimation	First industrial gripper
1961	MH-1	First sensitive mechanical hand
1961	Unimation	First industrial gripper installed in a facility
1963	Rancho Arm	First gripper not made for industrial applications
1974	Silver Arm	First autonomous gripper that used feedback from touch and pressure
1976	Shigoe Hirose	First Soft Gripper that could conform to shape of grasped object
1978	Nachi	First electromotor-driven robot hand
1982	Salisbury hand	Three finger hand Build at Stanford University
1983	N/A	66,000 Industrial robots in operation
1987	Shadow hand	First commercially available humanoid robotics hand
1991	Haptic hand	First Haptic system implemented on a Multi finger hand
1998		
2005	Luke Arm	First fully functional prosthetic Arm and Hand
2008	Robotiq	First flexible and adaptive three finger gripper on commercial market
2009	Switzerland	First Prosthetic hand that can ‘feel’
2010	Universal Gripper	First gripper that doesn’t have digits

1.1.2 Contact navigation

One of the applications for this platform is contact navigation. Contact navigation is a new topic in robotics. The majority of the research done in this field has been at Georgia Tech. Their primary goal has been to use contact navigation to detect human-robot contact and implement force-following algorithms that respond to tactile cues provided by humans. Detecting human-robot contact is also important when this contact interferes with the robots task, because it can ensure the safety of the human. Their work broke tactile human robot interactions down into three topic areas: human contact that interferes with

the robots task, human contact that contributes to the robots task, and human contact that develops or modifies the robot task (18). Contact that interferes with a robotics task is important because it can effects the safety of the human involved. Contact that contributes to the robots includes assistive robotics, where a task too difficult for a human is assisted by a robot. For example, if a heavy load needed to be moved a robot arm could move it while being directed by a human operator. The final category of conduct includes conduct that is used for instructing or teaching a robot about its task. This includes developing new tasks for the robot or modifying the current ones.

Another group explored the benefits of adding a tactile 'skin' of sensors to a robot arm by investigated how knowing the contact locations and determining the external wrench forces being applied to the system could help create a more complete dynamic representation of its interaction with the environment (19). The focus of this work was on determining external forces and didn't investigate the methods for planning motion based on this information. Another field of research using skin on a robotic arm focused on using force feedback to navigate in a cluttered environment. This research focused on how tactile information from the arm could be used to help solve path planning problems. This research platform seen in Figure 1 was conducted on an arm that was not capable of manipulating objects. The platform being created in this thesis will be used for research on unintentional collisions and on using contact for navigation and gasping tasks. Unlike the other platforms used for this type of contact research, this platform uses tactile sensor capable of detecting shear forces as well as normal forces. This capability allows this platform to detect the difference between a sliding contact and a static contact.

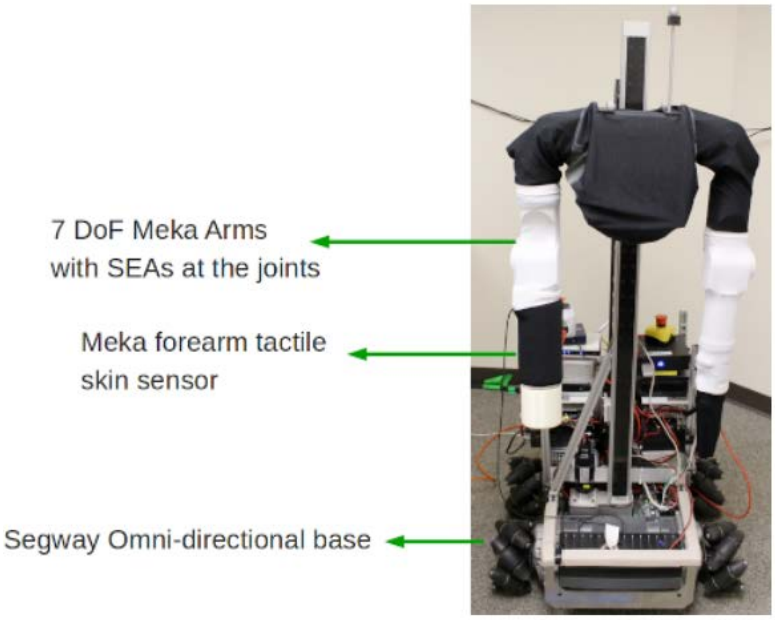

Figure 2: Meka Arm with Tactile Skin

1.1.3 Traditional Grasping

Traditional grasping is based on having an accurate model and assessing whether the grasp on a target meets certain desirable criteria including robustness, reliability and stability. Most of the work on robot grasps planning focuses on pre-grasp analysis, which includes the location of the object to be grasped and the tasks that need to be considered to create a list of grasping candidates (20). Most of the research in this field falls into two different categories: determining the conditions to immobilization the object in particular configurations and computing stable configurations for a given object. These approach focuses on immobilizing the object being manipulated with fixtures and external forces, and therefore determining the quality of the grasp is critical. For example Nguye and others found that large friction cones are produced by grasping contact at the edges or vertices of an object. This explains why humans grasp objects at the edges as well (21). This also

explains why human fingers are soft enough to conform around these edges instead of being hard. This was an example of how the location of the grasp can affect its quality. This quality can also be measured using a variety of sensors, which are also used to determine the exact model. Many of these sensors are contact based, but some rely on visual input and proximity.

Vision is the most popular and suited sensor for determining the locations and basic orientations of objects in the workspace because it provides the richest amount of information. It can also be used to track the relationships between different moving objects in the workspace, including contacts (20). However vision is not completely reliable and needs other sensors to supplement it to account for sensing errors, calibration errors, and so on. It can also be more expensive than the other types mentioned and have specific size and positioning requirements. The raw data produced by vision can also be extremely complex to analyze and can require massive computational resources. Contact based sensors are used both to supplement vision systems and to be used on their own. Proximity sensors are frequently used but are the least common.

New trends in sensor fusion are replacing the traditional strategy done with kalman filters. These new trends are based on a hybrid control that integrates the sensor signals from a variety of sensors at the control level, like vision and tactile readings. This approach is more appropriate for dealing with the disparate sensors. Vision, tactile, and force sensors all produce different qualities and quantities of information compared to traditional sensors where the sensors were equated to a common representation and then integrated. Newer approaches develop a sensor hierarchy where different types of information are weighted above others. For example tactile information is usually weighted above visual.

Traditional grasping favors an accuracy, repeatable, and payload capably systems, which are all weaknesses of a compliant manipulators. Compliant devices also can suffer from a weakened grasp, vibrations, and energy loss during dynamic loads. However there are also several key advantages to using a compliant system for manipulation when properly controlled and anticipated. Compliant manipulators can automatically correct of misalignment errors mechanically, decreasing the need for precision. For example this compliance could be helpful during assembly operations, peg into hole tasks, deburring tasks, or tasks in dynamics environment like with a prosthetic (2). Stiffer manipulators also tend to be heavier than their complaint counterparts. This negatively affects stiffer manipulators' dynamic performances and power consumptions (20). These advantages and disadvantages usually result in an optimal trade-off solution between stiffness and compliance in both the mechanical design and controls being identified for each application.

1.1.4 Compliant Grippers

More sensitive and compliant manipulators have numerous advantages over their blind counterparts. More sensitive and compliant manipulators are capable of reacting to changes and uncertainties in their environment. As technology develops more there has been a trend towards developing more responsive gasping manipulators compared to the original ones that had stiff motions and relied on precision programming. Within a few years of the first industrial manipulator being created the first sensitive industrial manipulator was created. Same goes for fully functional prosthetics.

Having a degree of flexibility in a gripper is also very important. Human ligaments add flexibility to human joints. This flexibility protects the joints during high impact collisions. In Robotics applications flexibility in the joints can compensate for inaccuracies in manipulation and reduce the damage caused during unintentional collisions. This flexibility was originally accomplished by having pneumatic powered grippers that had a slight amount of give to them, and allowed them to pick up imperfect objects (12). Pneumatics use pressurized air to actuate pistons that move the joints. Since air is compressible, when fully actuated, the pivot has some give to it under high impact since the pressurized air compresses further. In the past, a variety of different strategies been implemented to achieve a variety of levels of flexibility. For example grippers with multiple weaker fingers have been created it increase the a more flexible and capabilities of the system, with the same gripping strength as a basic two finger manipulator. The JPL Designed Spiny-Finger Gripper is a good example of this seen in Figure 2, this gripper uses lots of little grippers to grab on the rocks for drilling (22).

Figure 3: NASA's Jet Propulsion LAb (JPL) Spiny Finger Grippers

iRobot was challenged by the government to make a hand that was “more capable, more robust, more dexterous, and [can be built] at a lower cost than any hand available on the market right now,” explains Mark Claffee, the principal robotic engineer at iRobot Research (23). They answered this challenge with a compliant three-fingered system. The compliance was added by having hard plastic links connected by rubber joints as seen in Figure 3.

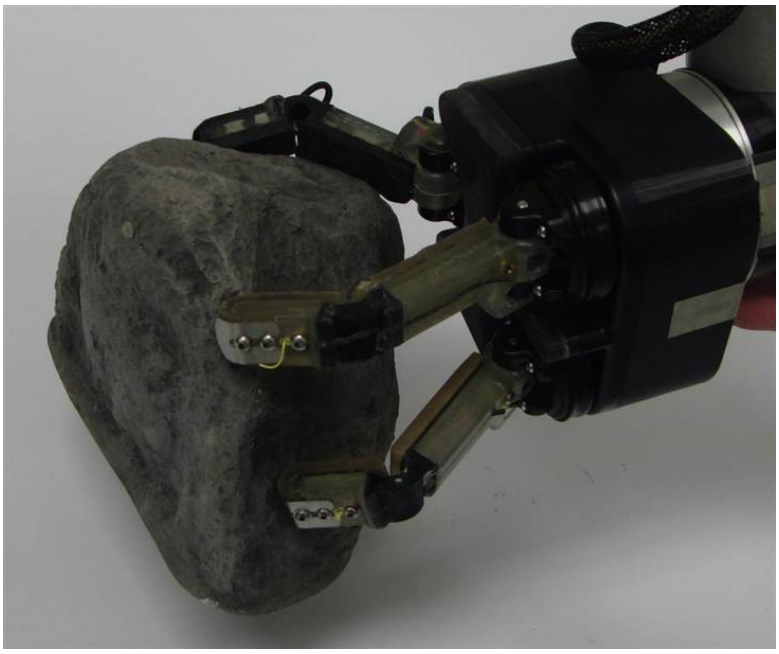

Figure 4: iRobot compliant hand being developed for the military.

Compliance has also been added to grippers through the use of pressure sensors, motor current monitors (2), and various control algorithms. When the pressure sensors are activated, the system knows that contact has been made and the normal force interaction can be monitored and controlled. Or if a spike in motor current is measured, the system knows that extra torque has been placed by an outside force, like a collision. By regulating the current the contact interaction can be monitored and controlled. However this approach is also limited because motors are used in conjunction with gear boxes. These gear boxes contain numerous gears that increase the torque and reduce the speed of the motor, which adds significant friction and momentum to the system resulting in a large impedance. They also rely on a software controller that can add a slight delay to the response; however this approach is limited. Therefore, direct drive systems are ill-suited for situations requiring fast reaction times to the sensor information. This down side to

direct drive system and the advantages associated with using series elastics made them an idea choice for this project.

1.2 Series Elastic Actuators (SEA)

Series Elastic Actuators have an elastic element the decouples the motor and the load. A block diagram of this concept can be seen in Figure 4. Having this elasticity between the motor and load can allows for greater shock resistance, lower inertia, better environment interactions, and more stable force control, at the cost of precision motion.

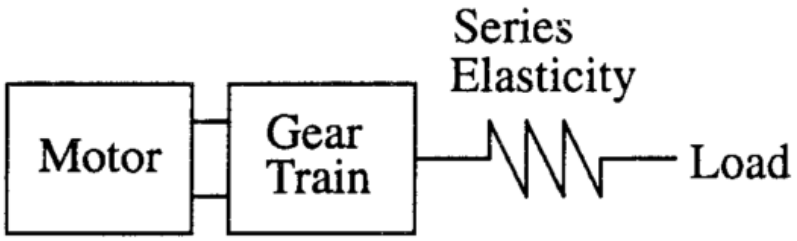

Figure 5: Simple Diagram of Series Elastics (24)

Additionally, elastic joints can compensate for minor irregularities in predicted contact locations, by flexing slightly on contact. These elastic elements also serve as a low pass filter for vibrations by reducing minor shock loads and torque ripples, which reduces wear and tear on the system and increases the stability of the controller . By measuring the displacement of the elastic element, force control becomes as easy as position control.

Impedance, stiction and bandwidth are key characteristic of an actuator that can be used to measure their quality. Mechanical impedance refers to how much a structure resisted the load placed on it. Mechanical impedance can be thought of as the opposite of mechanical mobility. Stiction is the static friction that needs to be overcome to enable motion of a stationary object. Stiction sets the minimum force the actuator will produce

with motion. Bandwidth is the frequency that the force produced by the motor can accurately produce. An ideal actuator has zero impedance, zero stiction and an infinite force bandwidth. Based only on these key characteristics a human muscle is the closest actuator to this ideal actuator. SEA's are the second best actuators in these categories having low impedance, low friction, and decent bandwidth.

Series elastic actuators simplify and stabilize the usually complex task of force control at the expense of precision. They take the complex force control problem and translate into a simple mechanical equation. Because there are springs incorporated into every joint, the force of a joint can be measured using Hooke's Law, show in the equation below, where F is the force on the joint, k is the spring constant on the elastic element, and x is the measured displacement of the elastic element.

$$\boldsymbol{F = k * \Delta x} \qquad (1)$$

Instead of having to interpolate the current of the motor and relate it to the produced force, the displacement on the elastic element, the value of the spring constant, and the location of the force can be used to find this seam value. In traditional systems the force equations needs to account for the dynamics of the system including its inertia, the coriolis effect, and friction in the actuators. These equations are computationally more expensive and difficult to generate without a completely accurate model of the system. A completely accurate model of an robotic system is difficult to create, especially because this model would have to reflect changes that occur in the system during use.

There are three main techniques for implementing series elastics. The first is based on torsion springs and works on rotary motion. The second uses compression springs and working in a linear motion with a ball and screw. The third method is a hybrid of the first

two and uses compression springs off the rotary motion at the joint. There are also numerous implementations of these three basic types.

1.2.1 Torsion Springs and Rotation

The first technique for implementing series elastics is more traditional is has been used mostly in older robotic system. This rotary SEA uses a custom torsion spring to decouple the joint and motor. These custom torsion springs are difficult and expensive to fabricate which makes this technique expensive. Torsion springs are much smaller than compression springs, however they are also stiffer. This additional stiffness reduced the amount of deflection that can be measured under force. This small amount of deflection is traditionally measured with strain gages which are very fragile. The biggest advantage to this technique is that they are smaller, can be directly mounted to the motor output shaft, and has good modularity. A schematic of its implementation can be seen in Figure 5.

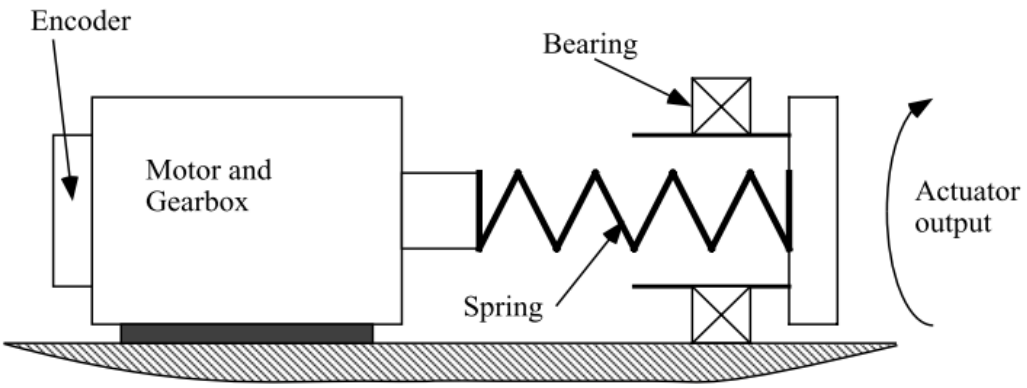

Figure 6: Torsion Spring SEA (24)

1.2.2 Compression Springs and Linear

The second technique translates the rotational torque of the motor into a linear force acting on the cable and series elastic element with linear rails and a ball and screw. This system is also expensive because of the precision required for smooth linear motion

without jamming. Typically the compression springs are then integrated into this bus that pulls on the cables as see in Figure 6. A pushing force will result in the compression of the springs on the lower half, and a pulling force will result in a compression on the springs in the upper half. When the system is not experiencing any forces both sets of springs are at half compression. This system is completely modular and can be pre-compressed outside of the assembly.

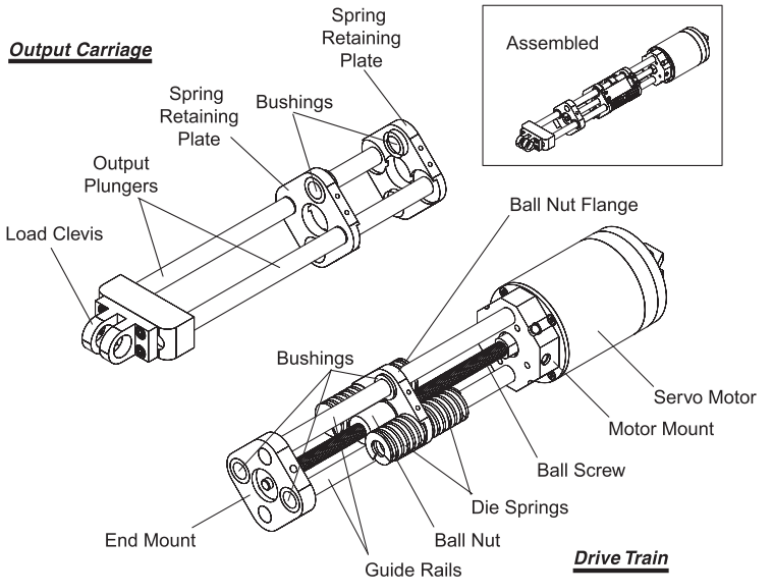

Figure 7: Linear SEA Assembly (2)

1.2.3 Compression Springs and Rotation

The final technique is a hybrid between the previous two. Unlike the others, the series elastic component for this style is located at the joint instead of the motor. At the joint the linear motion of the compression spring is directly translated to the rotation at the joint as seen in Figure 7.

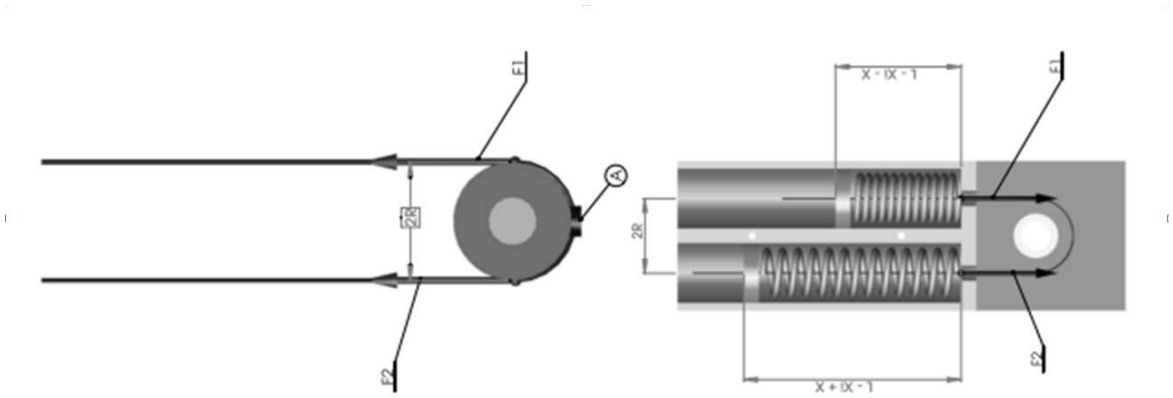

Figure 8: Simplified SEA module (25)

Like the second technique the springs are at half compression when no load is present. The primary advantage to this technique over the other two is that it uses off the shelf components and doesn't require expensive linear systems or custom torque springs. While being more scalable and smaller than the previous style, this technique is less compact than the torsion spring setup. The disadvantage to this technique is that there is constant tension on the cable equal to at least half the length of the spring multiplied by the spring constant. This constant tension needs to be considered in the design and provide sufficient support of the cable path.

Another variation on this technique is to build the series elastic module directly into the joint as seen in Figure 8 instead of as a separate modular module as discussed previously. This method is more difficult to assemble because the springs need to be compressed halfway before cabling can be completed on the robot instead of separately. The springs are compressed by running the motor one direction until one of the springs is half compression, then pinning it. Next the motor is run in the other direction half compressing the other side, completing the cabling. This means that the motors are necessary for the cabling and tensioning process.

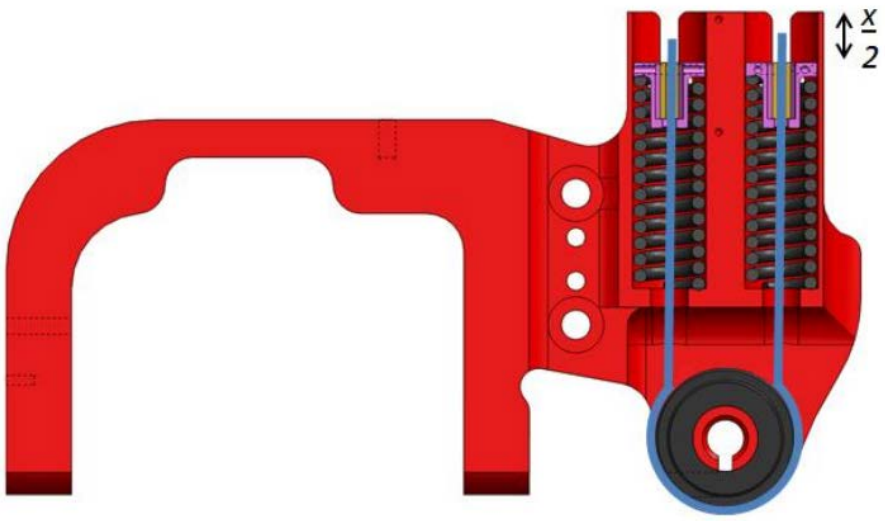

Figure 9: Cutaway section view of the Series elastic module integrated into the joint (10)

1.2.4 Series Elastic Actuator Summary

In summary, series elastics are good in applications where unintentional collisions are frequent and where force control is more important than position control. They are also good for working near or with humans because the elastic element can be tuned to be safe around humans. Since the manipulator being developed in this project is intended for human environments, series elastics will be incorporated into every joint. As this platform is additional intended for research in tactile manipulation, it needs an accurate force controller to respond to the contacts. As a result of the primary requirements of modularity and low cost, the hybrid version of SEA's will be used.

1.3 Tactile Sensors

An important aspect of manipulation is tactile sensing. The accuracy and precision of fine manipulation is greatly increased with the use of force and tactile sensor, because it allows an adaptive closed loop controller to be used. This effect can be seen in human manipulation as well. It becomes difficult to manipulate object accurately when (26).

Several studies have been done to understand the importance of somatosensory input (force and touch) on manipulation. Johansson and Wrestling studied the feedback response of skin when grasping objects and how that affects finger control (27). This study found that even with full vision, participants found grasping and manipulating objects difficult without tactile sensing participants found grasping and manipulating objects difficult. Tactile sensing was removed by forcing the participants to wear thick gloves.

While compliant spring based manipulators can be used to successfully grasp objects despite locational errors, there is a potential for large forces to be unintentionally applied. These large forces are caused by errors causing large deflections on the passive spring joints. Depending on the gasping location, as well as the object's geometry, friction, and mass distribution, these forces have the potential to displace the object before it is grasped, changing the gasping problem (5). Limiting these large forces would increase the number and variety of objects that can be grasped. This characteristic of compliant manipulators makes them a good application of tactile feedback. Using tactile sensors, the earliest stages of contact can be detected and responded to correctly, rather than letting large contact forces build up at only one point of contact. When using tactile sensing in the approach phase of grasping, they are used to detect the exact location of the object, so that the arm can then center the hand on its actual location instead of the estimated position. Having the hand centered on the object increases the stability of the grasp, and decreases unbalanced contact grasping forces.

Tactile sensors can also play a critical role during the actual grasping phase. They can determine the stability of the grasp and if there is unbalanced force contacting the object. Tactile sensors that are capable of detecting shear forces can also be used to

determine if an object is sliding. If any object is sliding in a grasp this could indicate that the object is not being grasped firmly enough or that it is in contact with an external object. In both cases, application of tactile feedback is mostly being used for event-driven manipulation, and plays a large role in determining the actions the robot performs and how it assesses its progress.

1.3.1 Types of Tactile and Contact Sensing Technologies

Several different technologies have been developed for contact or tactile sensing (27). Contact sensing and tactile sensing refer to two similar but distinct concepts. Tactile sensing includes skin-like sensing that measure information like pressure distribution, temperature, texture, compliance, etc. Contact sensing only refers to the perception of forces and torques generated during point contacts. Each of these types of sensors rely on different electrical engineering principles to gather comparable information that can be used to measure contact interactions. Each of the types described in this section have different advantages and disadvantages.

Resistive Sensors

The most common type of tactile sensor used on the market today is the resistive-based sensor. These sensors change in resistance in response to the force being applied to the area. They are most commonly used in pressure sensing 'buttons' but have also been applied to robotics. They have an average sensitivity range but are also cheaper and less accurate than the other technologies. They are also rugged enough to operate satisfactorily in moderately hostile environments. The biggest disadvantage to this type of sensor is that they have size limitations. They have a very limited and set size range they can be made,

and the reading they produce doesn't give an indication of where on the pad the force was applied, only that it exists somewhere.

Quantum tunneling Composite (QTC)

QTC is a flexible polymer that is normally a near-perfect electrical insulator, however when deformed it becomes a metal like conductor. QTC based sensors are good for soft circuits and they can be used in a variety of different sensor geometries. They are also more sensitive than the resistor based technology. The disadvantages of this technology are they need to be allowed to return to their normal state and they also cannot withstand high forces.

Capacitive

Capacity sensors rely on the principle that the capacity between two plates is a factor of the distance and surface area. So the applied force either changes the distance of the effective surface area of the capacitor. As the size is reduced to increase the spatial resolution of this type of sensor the sensor's absolute capacitance decreases. Because of this there is an effective limit on the resolution and size of this type of sensor. Capacitive sensors are overall very sensitive but if placed near the end effector or the robots earthed metal components it can experience severe hysteresis and stray capacity.

Optical-based tactile sensors

Optical-based tactile sensors work by changing the intensity of light by moving an obstruction into the lights' path or by using photoelasticity which is a phenomenon where stress or strain causes birefringence in the translation photoelastic material, which rotates the polarization and the intensity of the light with the applied force. These sensors are very sensitive, flexible, and fast. They are intrinsically safe, and since they use optical fibers, the

actual sensors can be located a distance away from the optical source and receiver. Unfortunately this type of sensors is extremely bulky.

1.3.2 Tactile Sensing in Humans

Many different robotics applications have biological inspirations, like robotic snakes and stereo vision. Humans have also been an inspiration for the development of touch sensors. Mechanoreceptors are human receptors, seen in Figure 9, in the skin that sense contact and can detect a shapes, size, texture, temperature and position. These sensors were used as an inspiration for the tactile sensor used in this thesis.

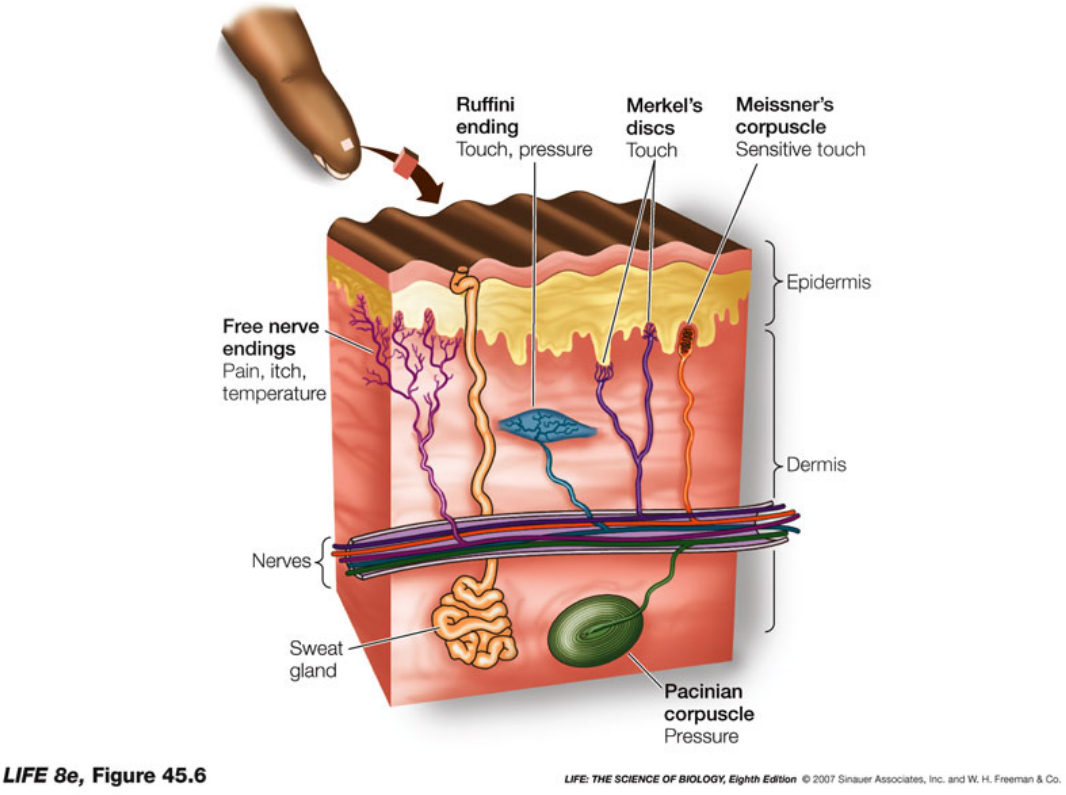

Figure 10: Mechanoreceptors in Human Skin (27)

Deformable Tactile Sensors by Eduardo Torres-Jara

Eduardo Torres-Jara developed a deformable tactile sensor based on the human Mechanoreceptors that gives a more complete understanding of the object in contact. This type of sensor is more suited for tactile sensing in an unstructured environment. This type of sensor has been proven effective in a number of humanoid robots platforms including Obrero and Go-bot seen in Figure 10 and Figure 11.

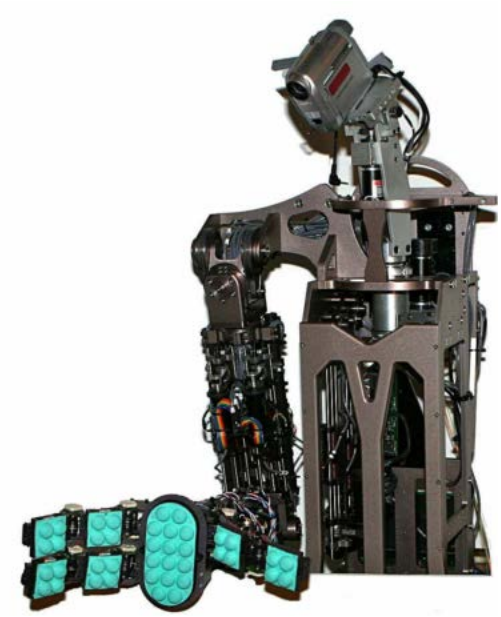

Figure 11: Obrero Robot (8)

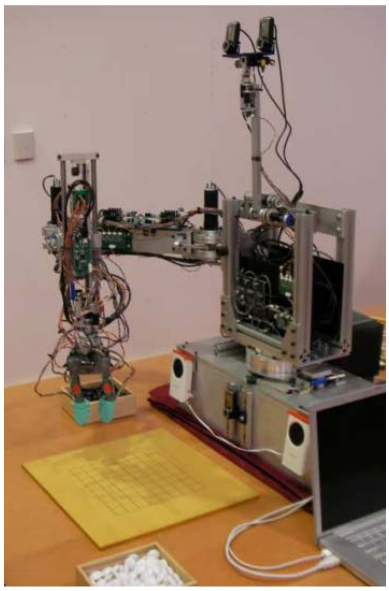

Figure 12: Go-bot Robot (7)

The tactile sensor modules are the green domes located on the fingers. The tactile sensor used in Obrero is composed of a magnet encapsulated in the membrane of a flexible hemispherical dome which is tracked using four hall-effect sensors to localize its position. This sensor technology was improved and used on Go-bot. The new version used four phototransistors and one infrared led which measured the diffractions off the hemisphere dome. This upgrade decreased the size of each dome, weight of the board, and the cost of each module. It also eliminated the interference that ferrous materials had on the sensors and simplifies the assembly process. The illustration of the sensor used on Go-bot can be

seen in Figure 12. This sensor is inspired by the ridges on human fingerprints, and is capable of detecting both normal and shear forces, so unlike the other sensors it gives an indication of the direction of the force.

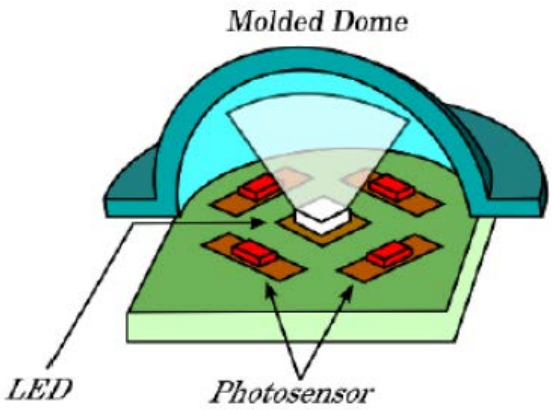

Figure 13: Optical Deformable Tactile Sensor (10)

Limited attention has been given to the advantages of having tactile feedback on the entire surface area of the platform so that all of the interaction with the environment can be monitored and controlled. The goals of this project are to create a platform that can be used in contact navigation and for navigation in locations in which vision based sensing is difficult, like in a box.

1.4 Contributing Projects

Several previous projects under the advisement of professor Torres-Jara at WPI laid the groundwork for this project. Below, we will provide a brief summary of each project, including the portions that are relevant to this project and the results of each project. It is noted below how each project furthered research within the field of sensitive manipulation. For more information on each of the projects below, consult the project reports.

1.4.1 Obrero

Obrero is an upper body humanoid robot consisting of a hand, arm, and head designed to provide high level haptic and tactile feedback. Each joint on the manipulator provides intrinsic elasticity and force feedback using series elastic actuators. The arm has 6 degrees of freedom: three in the shoulder, one in the elbow, and one in the wrist. The manipulator consists of a palm, thumb, middle, and an index finger. The exterior of the hand is covered in tactile sensors which provide a sensitive, deformable interface when gripping objects. The completed assembly of Obrero can be seen in Figure 13.

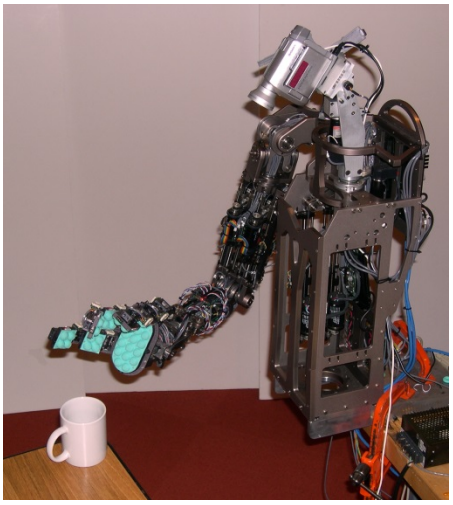

Figure 14: Obrero Robot reaching for an object (9)

The series elastic actuators in the arm are based on the second method using linear rails and ball screw. The series elastic elements in the fingers are based on the optimized version of series elastic actuators. The hand has low mechanical stiffness to soften contact with objects during grasping and increased the sensitivity. It is also under actuated and the seven joints are driven by only five motors. This hand was the first applied application for the deformable tactile sensors seen on the hand.

This platform was used to prove that the use of haptic feedback enhanced the robots ability to interact with an unstructured environment intelligently. This platform was used in a routine that allowed it to grasp objects without any prior knowledge about their shape or location. Instead of focusing on precision, it focused on the potential advantages of exploration and sensitivity. This routine identified both the arm and object based on motion and then moves the hand close to the object. Using a depth, hover, and pushing behavior the object was found using the tactile feedback. Obrero only failed seven out of the 104 trails using four different unknown objects.

1.4.2 Go-Bot

The Go-Bot, developed by Dr. Eduardo Torres-Jara and Gabriel Gomez, represents a precursor to this project. The project used sensitive manipulation coupled with series elastic actuators to perform delicate manipulation of small components. Goals of this project included showing that sensitive grippers can allow for more delicate manipulation in dynamic environments and to show that they can compensate for the inaccuracy induced by compliant grippers. The project showed this by designing the robot used in the project to play the game Go. Accomplishing this goal required the robot to execute 3 tasks: pick up a stone from a bowl, place a stone on the board, and pick up a stone from the GO board.

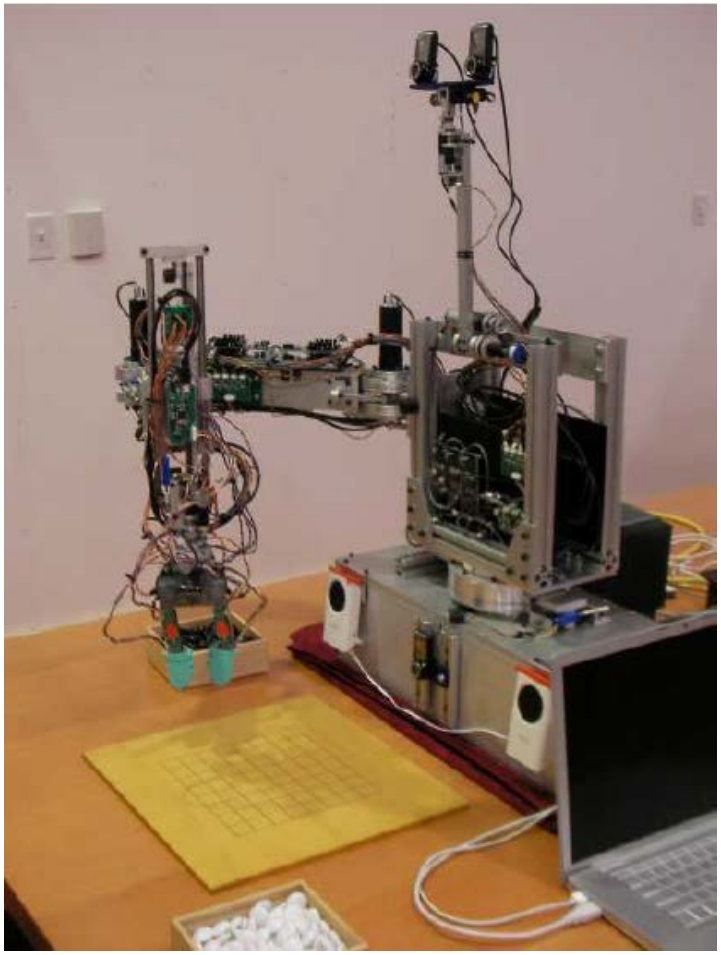

Figure 15: Go-Bot Robot platform

The robot designed for this purpose uses a SCARA style arm, with two horizontally joined links and a single vertical axis of motion. Compliance was added to each joint using series elastic actuators. Like in this project, the tips of the fingers were sheathed in the tactile deformation sensors. These were used to provide the tactile feedback that allows the gripper to act as a sensitive manipulator. The gripper was not specifically designed to manipulate Go pieces, but was instead a general-purpose hand made for detailed manipulation using tactile feedback. The robot used cameras for the rough localization of the target stone and then used contact based navigation to localize the stone and grip it.

This project laid the groundwork for this thesis, which follows up on the work done on Go-bot and Obrero. This project will continue the manipulation goals of the Go-bot with a higher payload, greater range of motion through an improved base arm, and a significantly larger portion of the arm covered by tactile sensors. This project will also not be integrated into a task-oriented robot, instead serving as a general platform for research.

1.4.3 Sensitive Arm Platform

The manipulator developed in this project was mounted to an arm designed in a previous thesis project which also incorporates tactile feedback. This arm, developed by Nigel Cochran in 2013 and referred to as the Sensitive Arm Platform, incorporates compliant joints and a shell that detects tactile input. The Sensitive Arm Platform is a four degree of freedom arm with a rotating base, two link arm, and rotating wrist joint. For a full description of the project, please see the report.

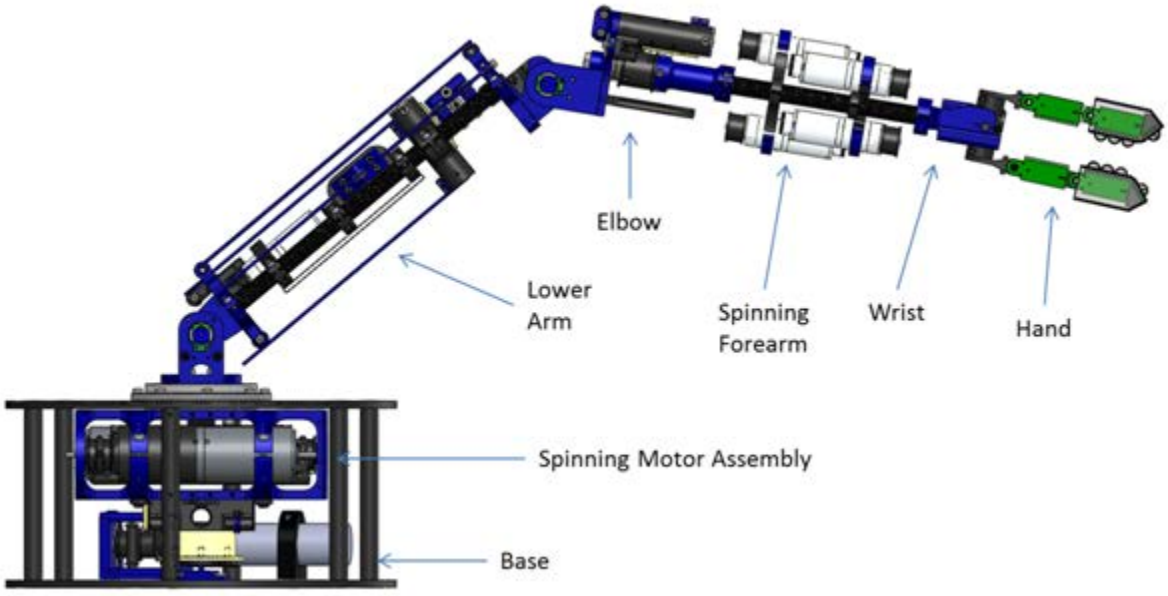

Figure 16: Compliant Sensitive Arm displaying a previous iteration of the wrist and hand modules developed in this thesis (11)

The compliance in the shoulder rotation joint was created using springs at the terminating ends of the cables. These springs also acted as tensioners on the cables. The two pivot joints utilized an isolated module attached to the links to create the compliance. This module isolated the cable attachment point from the component that the cable is acting on using a set of springs to either side of the attachment point and a guiding case. The case keeps the force of the cable acting on its original vector while the springs add compliance to the input along that vector. This module served as the inspiration for the finger modules, but in the fingers it was miniaturized and made into an integrated part of the link that is being moved as a opposed to a separate module.

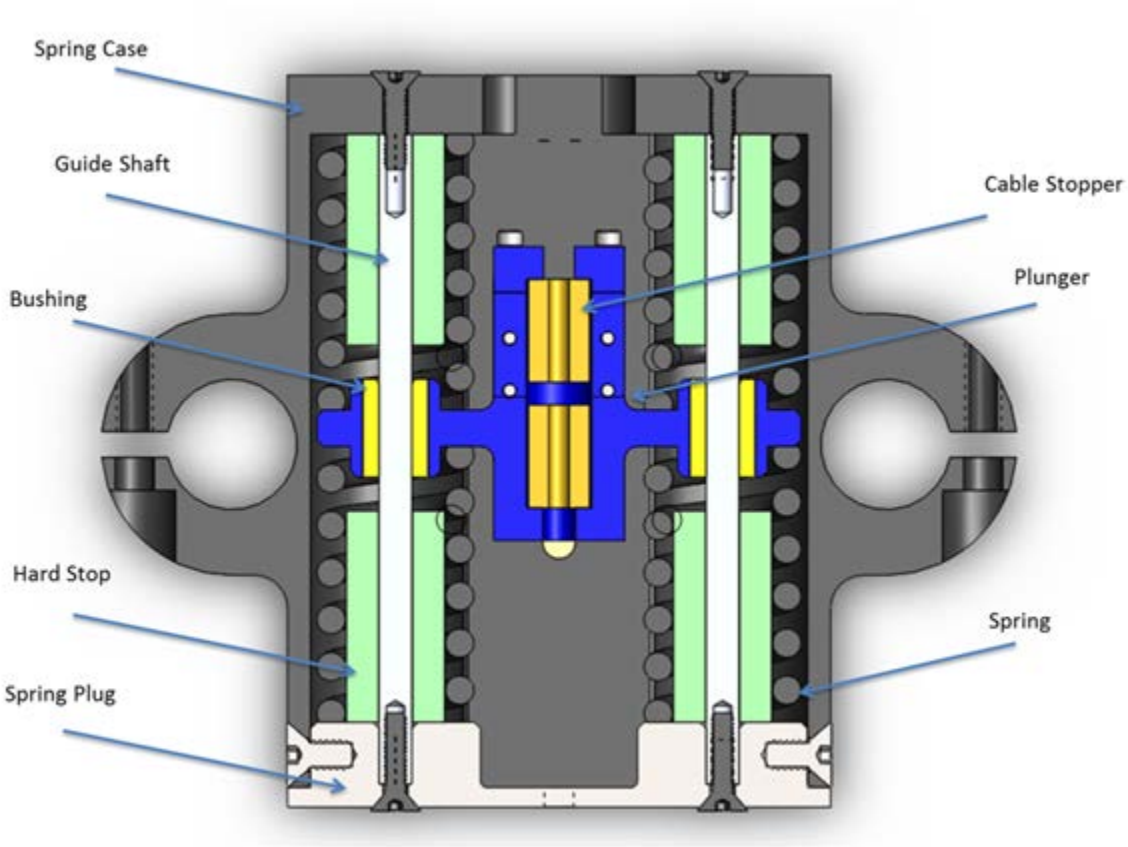

Figure 17: Shoulder Pivot SEA pivot spring box (11)

Tactile feedback was designed to be provided by a network of deformable tactile sensors attached to a shell around the two links of the arm. Figure 17 shows a CAD of the arm including an outdated version of both the wrist and fingers, which were developed in this thesis. This shell was designed and constructed, but the sensors themselves were not implemented as part of the project. These sensors can detect both normal and shear forces, allowing the arm to detect and move around obstructions without harming them. This, combined with the compliance in the mechanisms, would create an arm that can work in crowded and human occupied environments without worrying about damaging people, surrounding, or itself.

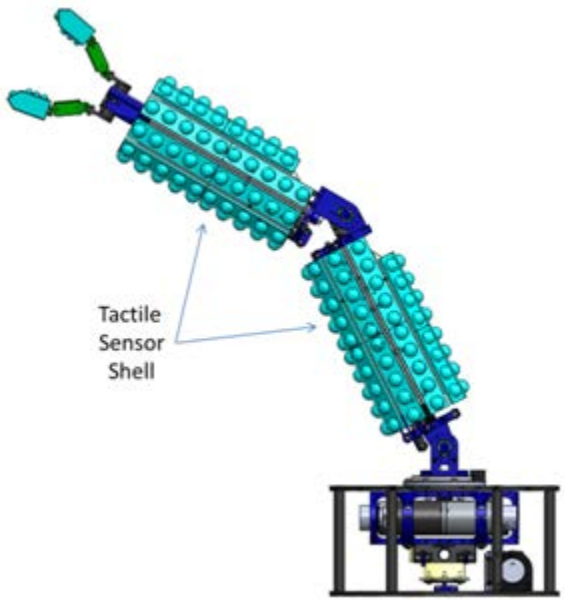

Figure 18: Complete Arm CAD of a previous iteration of the entire design, including the finger and wrist components from this thesis (11)

This arm interfaces with the manipulator above the wrist rotation joint. The manipulator incorporates two carbon fiber rods similar to those shown in Figure 18. These serve as the interface point. The manipulator designed in this project can takes full

advantage of the arm's original four axis.

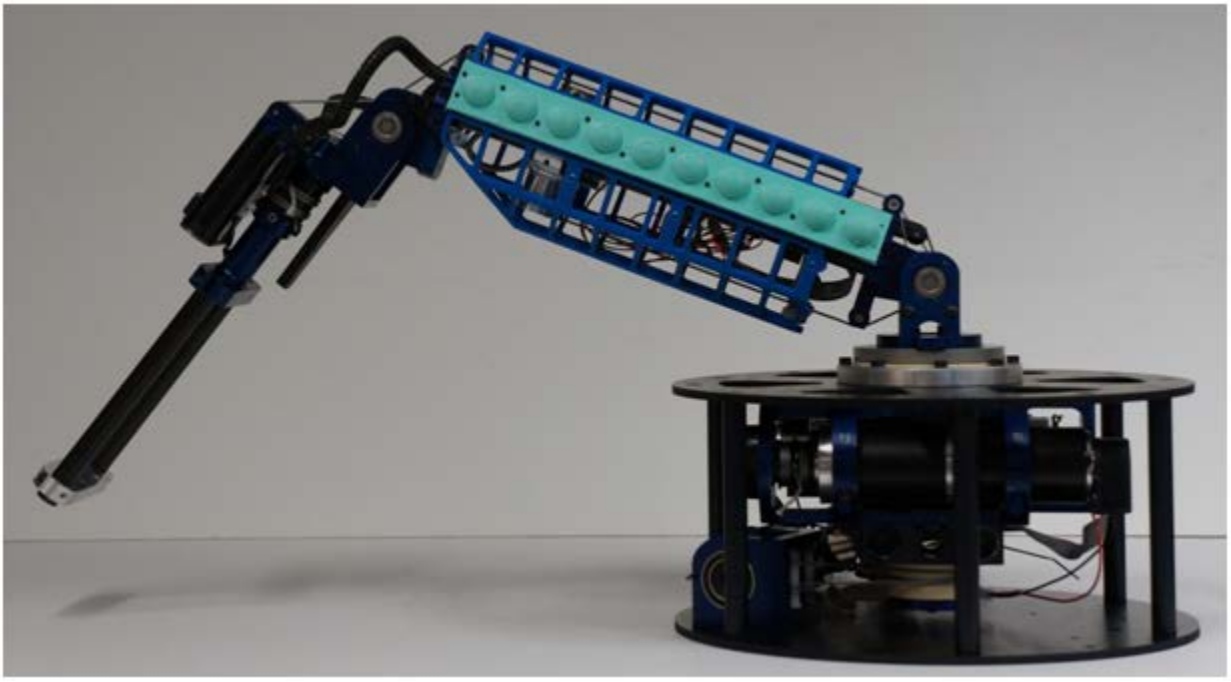

Figure 19: Completed Assembly of the arm and elbow portion of the Sensitive Arm Platform to be attached to the fingers and wrist of this thesis (11)

1.5 Thesis Contributions

This thesis completes the Sensitive Arm Platform that created the first four links of the total six degree of freedom arm seen in Figure 15. The primary contributions to the project are the final two degrees of freedom of the arm: the two axes of the wrist and the manipulator consisting of two fingers with high mechanical compliance. This project also examines methods of incorporating and utilizing the feedback from series elastic actuators and tactile sensors in robotic manipulation. The ultimate contribution of this thesis is to complete the Sensitive Arm Platform so that it can be used in researching control algorithms to best utilize tactile feedback. These control algorithms will utilize both the

force information from the series elastic elements and from the tactile sensors. In this thesis, basic force and position control algorithms were developed and implemented. Previous research has mostly focused on using information from only one or the other of these sources. A pioneer research to investigate the effect of having both series elastics and tactile sensor when detecting contact during path planning did not investigate manipulation as well. The robot Obrero also combined tactile sensors and series elastics (9), but the surface area covered by the sensors was minimal and only could be helpful during grasping. This thesis combines manipulation with contact path planning.

The primarily focus of this thesis is the mechanical design, analysis, and assembly of the wrist and fingers and the sensor selection. A cabling system with tensioners and series elastic elements was developed to control joint articulation of the wrist. Sensors were natively integrated into the design for position and joint force feedback. For the fingers, the babbling system was designed tin integrate tensioners, flexible cable support and guidance tubing with multiple spring series elastic elements. Because the system is meant as a research platform, it was designed to be as inexpensive and for easy assembly and manufacturing. Furthermore, it acts as a convenient infrastructure to support integration and maximized tactile feedback sensor coverage to provide ample sensory input for future tactile driven control development. This thesis also created methods and mechanisms to detect force applied to the joint through deformation of the series elastic elements. The electronics and software architecture are not the focus of this particular thesis and will be the subject of follow up research using this platform. The software written for this project was developed primarily for testing and basic control.

1.6 Thesis Layout

The body of this thesis paper is organized to cover the design, analysis, parts selection, assembly, tensioning, and testing of the robotic platform. Chapter 2 addresses the mechanical design including the design requirements, justifications for design decisions, and component selection. Chapter 3 outlines the electrical architecture of the system and the selection of sensors. Chapter 4 discusses Tactile Sensor Integration for both the sensors on the fingers and on the Motor Module. Chapter 5 goes through the system validation and how each of the design requirements and goals were tested during this project through experimental validations. Chapter 6 summarizes the entire thesis and offers suggestions for future work on the project.

Chapter 2 Mechanical Design

The major contribution of this project to the field of robotics is a platform for sensitive manipulation. A successful platform relies heavily on a good mechanical design oriented towards the task. This Chapter of the report covers the mechanical design. First Design requirements for this project are covered. A good Mechanical design is, conscientious of the Design requirements, while still being aesthetically pleasing and machinable. Next the mechanical design is broken down into details including the analysis and selection calculations. Finally the design of the tactile sensor shell is covered.

2.1 Design Requirements

Before developing an initial design a list of design constraints was identified for the wrist and Fingers. This list of constraints included:

1. The wrist and fingers must be able of manipulating a 1kg payload
2. The arm must have at least a tactile sensor spatial resolution of 40 mm., which is that of a human
3. The fingers need to have the highest spatial resolution physically possible given the chosen sensors
4. The Wrist must have 2 Degrees of Freedom that are arranged as a gimble
5. There must be two, 2 DOF fingers attached to the wrist.
6. Each joint of the wrist and fingers must have series elastic actuators
7. Each SEA must be inexpensive and easy to assemble.
8. All of the Motors for the Wrist and Fingers must fit in a 5 inch long 3.5inch diameter tube

9. Robotic Wrist and Hand need to be easily integrated into the Sensitive Arm platform
10. The fingers need to be able to deflect easily on contact but be strong enough to support payload.
11. Wrist will not deflect more than 8 degrees during maximum dynamic load
12. The fingers need to be a comparable size to a humans.
13. The range of motion of the Wrist and fingers needs to be comparable to the equivalent human joint.

[Req 1] This robotics appendage was designed for research purposes. This research focuses on contact navigation, the interaction between the robot and other objects, and how robots use the sense of touch to explore their world. These research goals don't require the wrist and fingers to be extremely strong so a 1 kg payload was determined to be sufficient for this application.

[Req 2] As the focus of this project is on sensing, having an adequate coverage of tactile sensor on the fingers and wrist is required to meet that goal. In order to better mimic the human body, which has different levels of sensitivity on the arm and the hand, different size sensors will need to be used for these different areas. Since this project mostly focuses on the platform, the board construction and design for the tactile sensors are not included. However the support shell for the arm and the molds for the sensors are included as they relate to the hardware design of the arm itself.

[Req 3] The human wrist forms a mock spherical wrist with the rotation of the forearm. Since this rotation is enabled by the arm, the wrist must have two inline degrees of freedom that allow it to emulate this type of motion and maneuverability. The dexterity

of a 6-axis arm is mainly due to the final three axis, which have to concentrate the final three axes of rotation into a compact space, while the entire length of the robotic arm is mainly responsible for positioning the wrist. [Req 8] Also as the manipulator is relying on the arm for its ability to rotate, it must be able to easily integrate with the arm. [Req 4] Unlike the human hand and more similar to industrial robotics, this platform must have two fingers that will allow it to pinch objects. In order to be able to explore the effect of different types of contact, at least 2 Degrees Of Freedom are necessary in the fingers. According to statistical studies, from 60 to 70 % of man's grasping of objects of cylindrical, parallelepiped, and pyramidal shapes is performed with only two fingers [4, 13].

[Req 7] The wrist and fingers must aesthetically match the arm of the robot all of the motors need to fit within the fore arm and match the tube like form of the rest of the arm. So that it looks like it was cohesive extension. Because of this all of the motors must fit in the a 5 inch diameter tube.

[Req 11] This research is going to be conducted in dynamic environment and is based on human biology. To most closely represent human interactions with their environment the fingers need to be a comparable size to a human. Since human hands have three joints and the fingers in this project only have two the combined length needs to be comparable to the sum of all the joints in a human finger.

[Req 12] Not only is this robot intended for research in a human environment, but it also needs to have a similar range of motion and reflect the same capabilities of a human wrist and individual finger. This means that one of the pivots of the wrist needs to be able to rotate 150 degrees, and the other pivot needs to be able to rotate 60 degrees. The first

link of the finger needs to be able to rotate 150 degrees, and the second joints needs to be able to rotate 90 degrees.

[Req 5] Finally every joint must incorporate series elastic actuators. The benefits of series elastic actuators were highlighted in the background section. However their primary purpose in the arm is to add compliance to the system. [Req 9] In the fingers, not only are the SEAs adding compliance but they are also adding sensitivity. This sensitivity was accomplished by detecting deformation in the SEA. This means that the SEAs must deform when light contact is encountered, but still be rigid enough to support the required load. [Req 10] To avoid excess compliance in the wrist, the requirement that it shall not deform more than 8 degrees during maximum dynamic loading was also added. This ensures that the wrist is compliant, but also rigid enough to perform its required function.

[Req 6] Many series elastic platform have complex and expensive series elastics elements. One of the goals of this platform is to avoid that, while still maintaining true series elastics properties.

2.2 Design Summary

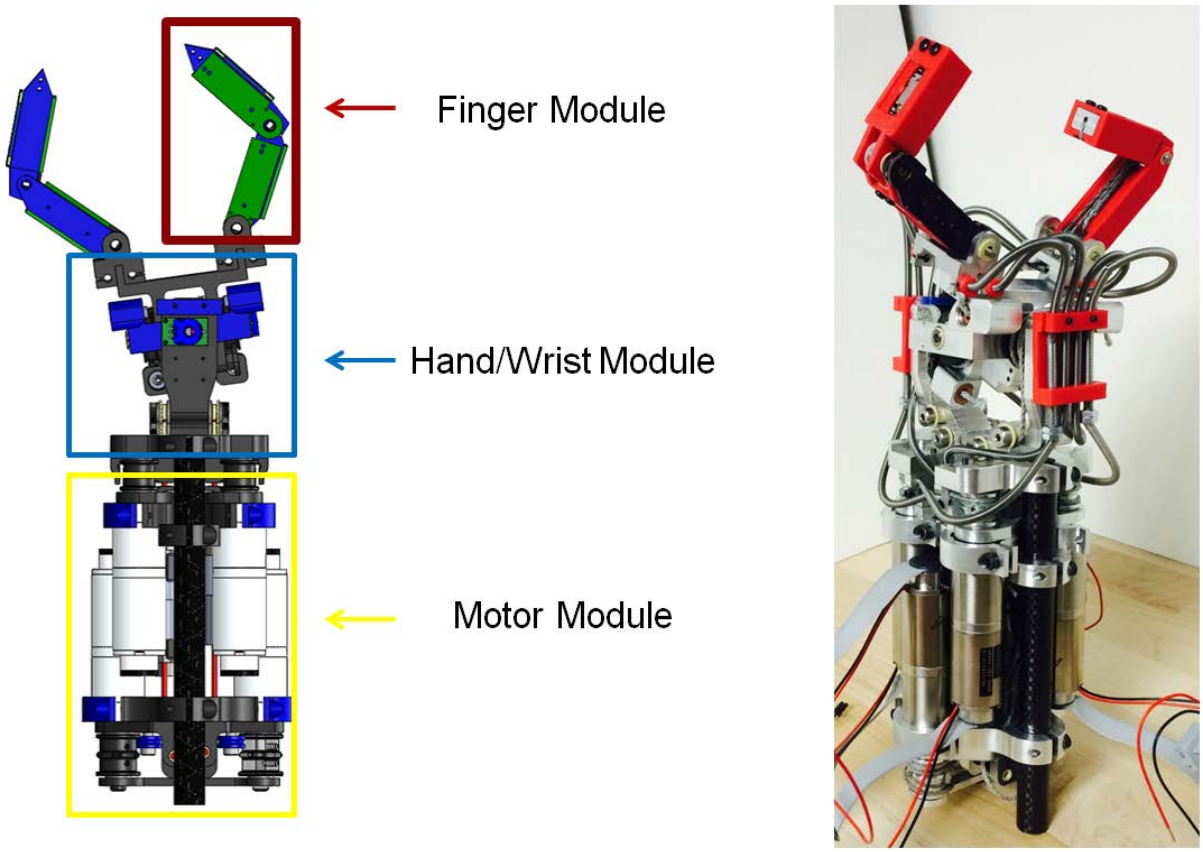

Figure 20: The image to the left is the CAD of the entire system developed in this thesis with the modules described depicted. The image to the right is of the completed system.

The final assembly can be broken down into three different modules, as seen in Figure 19: the motor module, the wrist rotation, and the fingers. The motor model houses the 6 motors that actuate the joint in the other models. This model is mounted directly to the elbow joint on the arm. The major components in this module are two parallel carbon fiber tubes that are clamped by the elbow joint of the Cochren arm, two motor supports that are attached to the carbon fiber tubes, the 6 motors, and a 3D printed shell. The shell is a cylindrical grid that completely contains the motor module. The motors are spaced evenly in a circle with three motors on each side of the carbon fiber tubes. The first motor support is closest to the elbow and supports two of the motors and their respective pulleys. The

second motor support is near the wrist module and supports the other 4 motors and their respective pulleys.

The Wrist module has two degrees of freedom; pitch and yaw seen in Figure 19.Two support pieces attach the wrist gimbal to the motor module. These pieces support the outside of the gimbal. A middle gimbal skeleton pivot in relationship to these outer support skeleton pieces and provides the pitch axis of rotation. The final piece rotates in the center of these skeletons and provides the yaw axis of rotation. The two finger modules are attached to this center pivot piece. Unlike a standard gimbal both of these joint incorporate the series elastic elements at the joint.

The finger modules have two links each. These links are 3D printed modules with a metal slider in the middle and a metal cap. The body of each link of the finger contains the springs for the series elastic element. The controlling cables for these joints are attached to the sliding metal piece that pushes against the internal springs. The links of the fingers are connected to the wrist by a metal piece that routes the cables from the finger joints into the Bowden tubes. Bowden tubes are flexible tubes that route control cables around other joints so that they maintain their independence.

The entire assembly consists of six powered joints; two for the wrist and two for each of the two fingers. The first joint in the wrist is independent from any of the other joints. The second joint of the wrist is in line with the wrist and is dependent on the first joint. Combined with the rotation from the last joint on the arm they create a motion similar to a ball-and-socket joint. The Bowden cables keep the joints of the fingers independent of the motion of the wrist. The first joint in the fingers is independent and the second joint is dependent on the motion of first.

2.3 Wrist Module

The wrist module is the section of the manipulator containing a pitch joint and a yaw joint, located above the motors and below the fingers. This module provides the last two degrees of freedom for the six axis arm and provides a mounting point for the gripper seen in Figure 20. This section discusses the requirements, material selections, and cable routing. Also addressed is the modeling of the system and its effect on motor selection. The description of the wrist concludes with a discussion of the design of the series elastic actuators used in this module, a discussion of the assembly and tensioning methods used during arm construction, and evolution of the module's design during the course of the project.

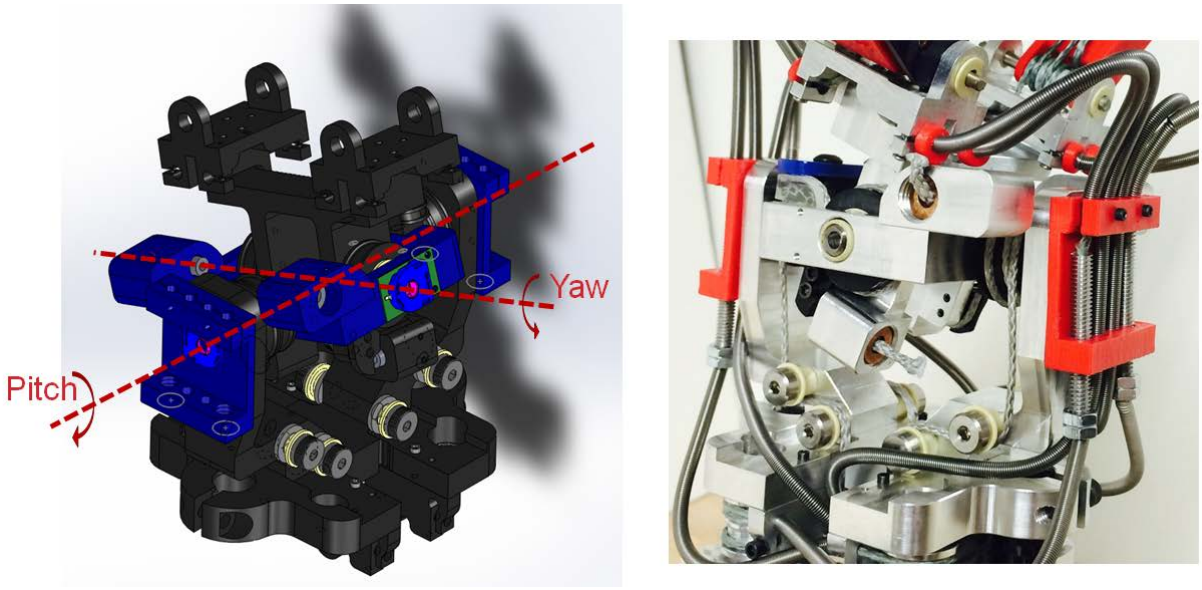

Figure 21: Depictions of the wrist module. The image to the left is a CAD of the system with the axis of rotation depicted while the right is the actual produced system

2.3.1 Design Requirements

Based on the design requirements this module needed to have two in-line series elastic joints capable of manipulating a 1 kg payload. The series elastic element also needs

to deflect a maximum of 8 Degrees based on the desired requirments for the platform, be inexpensive in both the materials and manufacturing process and be easy to assemble. The additional requirement for this model is that the motors that power it be located as close to the Cochran arm as possible. The motors are located away from the joints to reduce the torque requirements on the arm. Because the motors are not directly in-line with either of the joints cables were selected to translate the motion of the motors to the joints. Cables were chosen over chains or belts for the power translation because of their flexibility and ability to be routed three dimensionally instead of in a plane.

2.3.2 Material selection and Manufacturing

The structural components for this module where all milled from 6062 Aluminum and all the components that come in contact with the cable were machined from Delrin Plastic. Aluminum was chosen because it of its balance of strength and weight. Delrin was chosen for the pulleys and cable redirectors because of its low coefficient and easy machinability. Before being Machined all of the components were checked using Finite Element Analysis (FEA) and were checked for machinability. The number of set up required for all of the pieces combined was also considered during the design process. Having fewer total set ups reduces the machining cost and the number of required pieces. Having few parts reduces the weight of the assembly and the torque requirements on the arm.

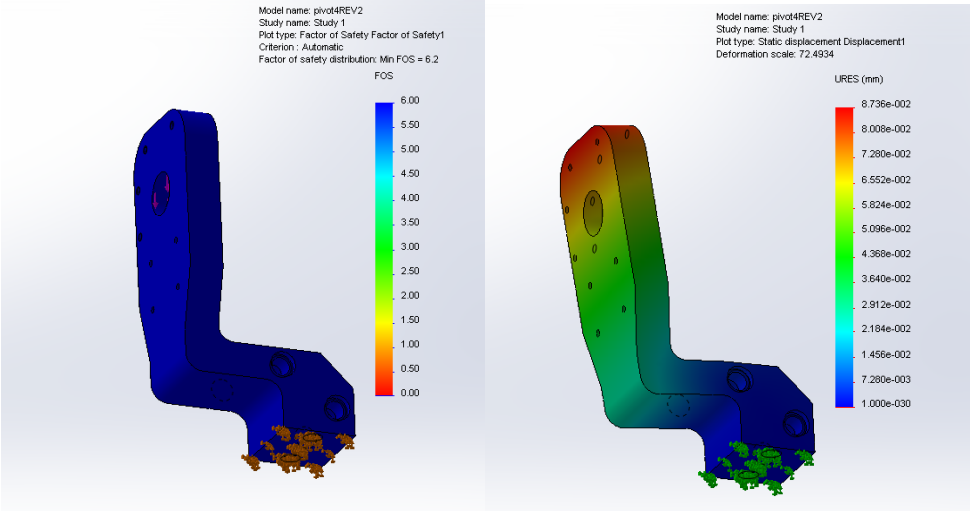

Figure 22 FEA of Wrist support piece

2.3.3 Cable Routing

The cables for the first joint, the pitch axis, come from the motor facing down the upper arm in the motor module. This cable is then routed through the center of the upper arm and then to the rotation pivot. This .75-inch diameter pivot pulley and the .5-inches pulley at the motor further gear down the motor output. By gearing it down some in system it makes the requirements for selecting the motor easier to meet. After wrapping around the pulley the cable then grounds into the spring box, which is described in Section 2.3.7. This path can be seen in Figure 20 using the green and purple cables.

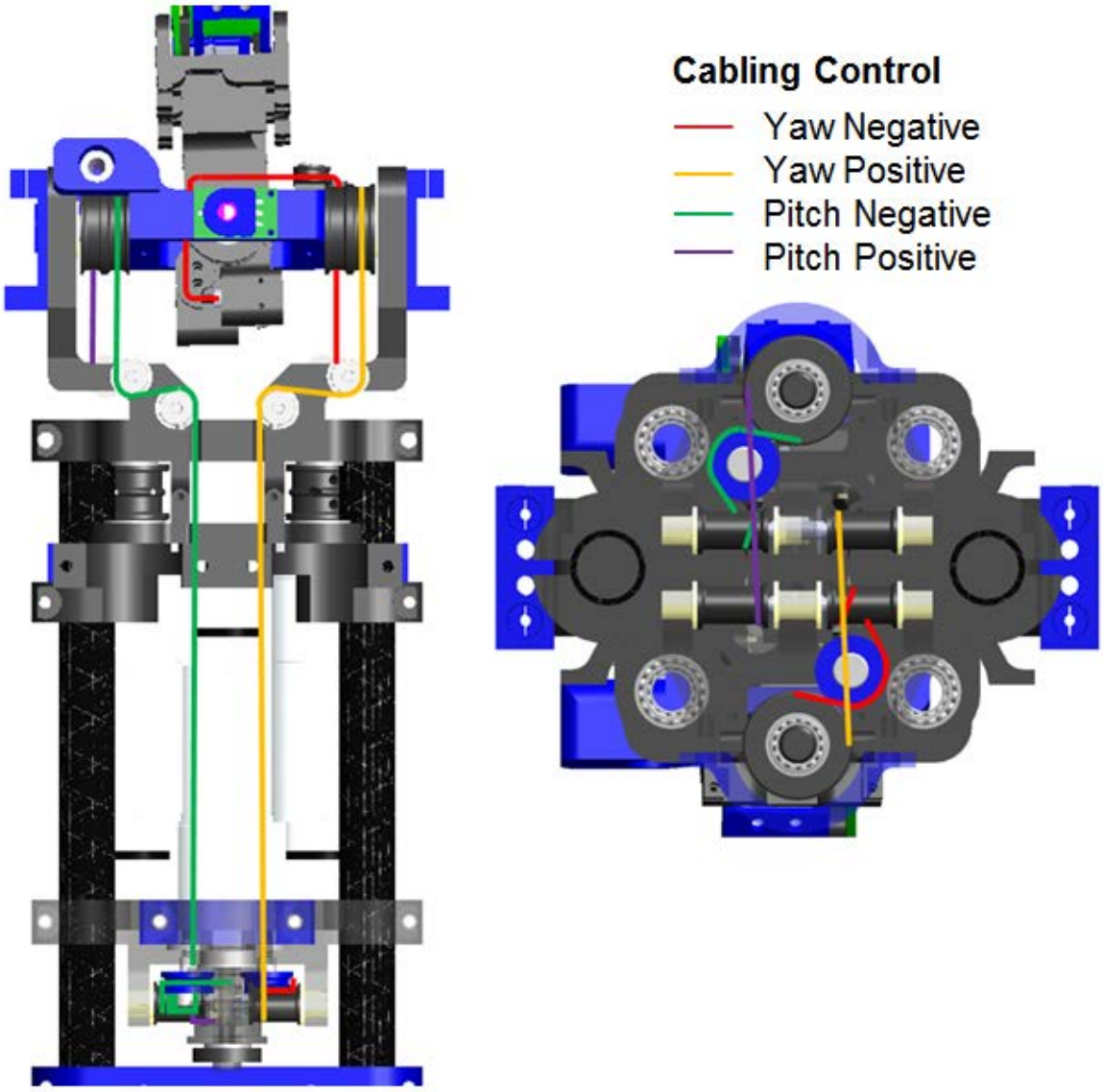

Figure 23: Cable routing for both joints of the wrist

The cables for the second joint, the yaw joint, follow a similar path to the previous joint. However, after wrapping around the pulley at the pivot point for the pitch rotation, it is then redirected by a Delerin piece to the pivot pulleys for the yaw joint. Instead of having a full pulley that would transfer the cable from the first joint pivot to the second, a small

Delerin piece is used because of space limitations. Using a pulley would reduce losses caused by friction, but a pulley takes up significantly more space. This space requirement would reduce the range of motion of the second yaw joint. Also, several other robotics hands use Dyneema sliding on Delerin, such as the hand on the Justin Robot in Germany, because of the low coefficient of friction between the two surfaces. Since the cable rotates around the pivot point of the previous joint, it is motion dependent on this joint. This relationship between the two joints needs to be considered when designing the controls. This cable routing for the second joint can be seen in Figure 20 in the red and orange cables.

After rotating about the second yaw pivot point the cables are then directed to its corresponding spring box by a second Delerin Director. Normally having a cable slide along a surface is an undesirable routing option. Because of this, most designs only have the cable touching pulleys that can freely and easily rotate on their respective axles. However, in this case it was impossible to have sufficient space for a pulley while still maintaining the size constraints on the platform. So instead Delerin redirectors were created. The additional friction produced by having the cable slide instead of on a pulley is reduced by the material selection for both the cable and the redirector. Both Delrin and Dyneema have a fairly small coefficient of friction. There are several other examples of other robotics applications, like the DLR robotics hand, intentionally sliding the cable along a plastic director because of size constraints.

2.3.4 Cable Selection

The cables used for the wrist module are the same cables that were used for the Sensitive Arm Platform. These cables are 12 strand, braided, 2mm Dyneema cable. Dyneema is a lightweight, high-strength, oriented-strand, low-stretch gel spun cable from Ultra-high-molecular-weight polyethylene. It has a comparable yield strength to steel, and a higher one than low-carbon steels. Dyneema fibers are commonly used in personal anti-ballistic armor, bow strings, climbing equipment, fishing lines, high-performance sails, and parachutes. Dyneema and Spectra are made from the same molecule using different spinning methods. Dyneema is produced in Europe and Spectra is produced in the US. Between the two, Dyneema is stronger and more stretch resistant, but is also more expensive and more difficult to source in the US. This cable was selected based on research done in past robotic projects in the lab (Caminante). Unlike the traditional steel cable commonly used in this type of application, Dyneema has a much higher strength ratio to weight, significantly smaller turn radius, and a much smaller coefficient of friction. These advantages allow it to be manipulated in smaller spaces and while reducing the inefficiencies caused by friction. This cable is capable of withstanding up to 950 lbs. of static load before breaking it, which makes it one of the strongest points in the system. This cable was also chosen because there is a known way of grounding the cable developed by Igus Corporation. This method is based on inserting a cone into the center of the Dyneema braid, then compressing the braid in between the code and a conical hole. This method of terminating the cable is used at all the ends. The brass pieces from Igus are used in the tensioning system, and a custom brass pieces is used in the series elastic end. Because of Dyneema's low coefficient of friction grounding the cable can be a very difficult task, with enough force it can slide through knots, traditional clamps, and crimps. Having a reliable

grounding method already in place reduces the amount of potential issues and engineering needed to use this type of cable in this application.

All of the joints in this module are D-shafts supported by bushings. Bearings and bushings are mechanical elements that reduce the friction between rotating parts and constrain the allowable motion. Bearings have three main components, an outer ring, an inner ring, and a roller element. Bushings are a low friction plastic ring. While bushings are not as frictionless bearings, they are much cheaper and smaller. They also don't require the same level of machine tolerancing that bearings require. The primary reason bushings were selected over bearings for the points of rotation was because of the size difference. D-shafts were chosen for the axles because they reduce the chance that the setscrew locking it will slide by increasing the surface area it makes contact with.

2.3.5 Kinematic and Dynamic Modeling

The kinematics and dynamics of the wrist alone are fairly straightforward to calculate as the wrist is simply equivalent to a spherical joint. The torque requirements on these joints are fairly low because of their proximity to the payload. The Peter Corke toolbox was used to calculate the joint torques of all six joints in the arm.

The Peter Corke toolbox uses the Newton-Euler method. This method starts at the bottom of the linkage and works its way up through each joint, solving for the linear and angular motion, and then works its way back down the arm using this information to solve for the joint torques. These dynamic equations were used to determine the tourque for selecting the motor. The elastic element is not considered because the elastic element are

more relevant when the hand makes contact with an object. The first step in this method defines the dynamic model seen in Equation (2).

$$M(q) * \ddot{q} + C(q, \dot{q}) * q + g(\dot{q}) = u \qquad (2)$$

q = Vector of joint variables

u = Vector of torques

M = Inertia matrix

C = Centrifugal and Coriolis terms

G = Gravity vector

Using the completed CAD, the following information was used to create the dynamic model necessary for the Newton-Euler approach.

Table 2 Dynamic Parameters

Link	Length (m)	Mass (kg)	CGx (m)	CGy (m)	CGz (m)	Ixx (kg* m²)	Iyy (kg* m²)	Izz (kg* m²)
Spinning Motor Assembly	0	3.34	0.00119	-0.08468	-0.00167	0.00722	0.00804	0.01099
Lower Arm	0.304	1.55	-0.16192	0.01293	0	0.00197	0.01378	0.01424
Elbow	0.021	0.45	0.008769	0.000223	0.056031	0.000209	0.000782	0.000795
Spinning Forearm	0.314	1.65	0	0.96270	0	0.00253	0.00701	0.00729
Wrist	0	0	0	0	0	0	0	0
Hand	0	1.15	0.06645	0	0.00130	0.00014	0.00041	0.00049

In addition to this information a trajectory $\hat{q} = \begin{bmatrix} q \\ \dot{q} \\ \ddot{q} \end{bmatrix}$, was also necessary. This trajectory was based on the starting position, and the average speed of human joints determined experimentally. Trajectories are used to generate the torque values . Joint 1 corresponds to the first shoulder, 2 to the second shoulder, 3 to the elbow, and 5 and 6

correspond to the two wrist joints. The arm joint is included because it affects the torque values on the wrist. The starting position was chosen to generate the highest torques. A visualization of the trajectories of the joints can be seen in Figure 22.

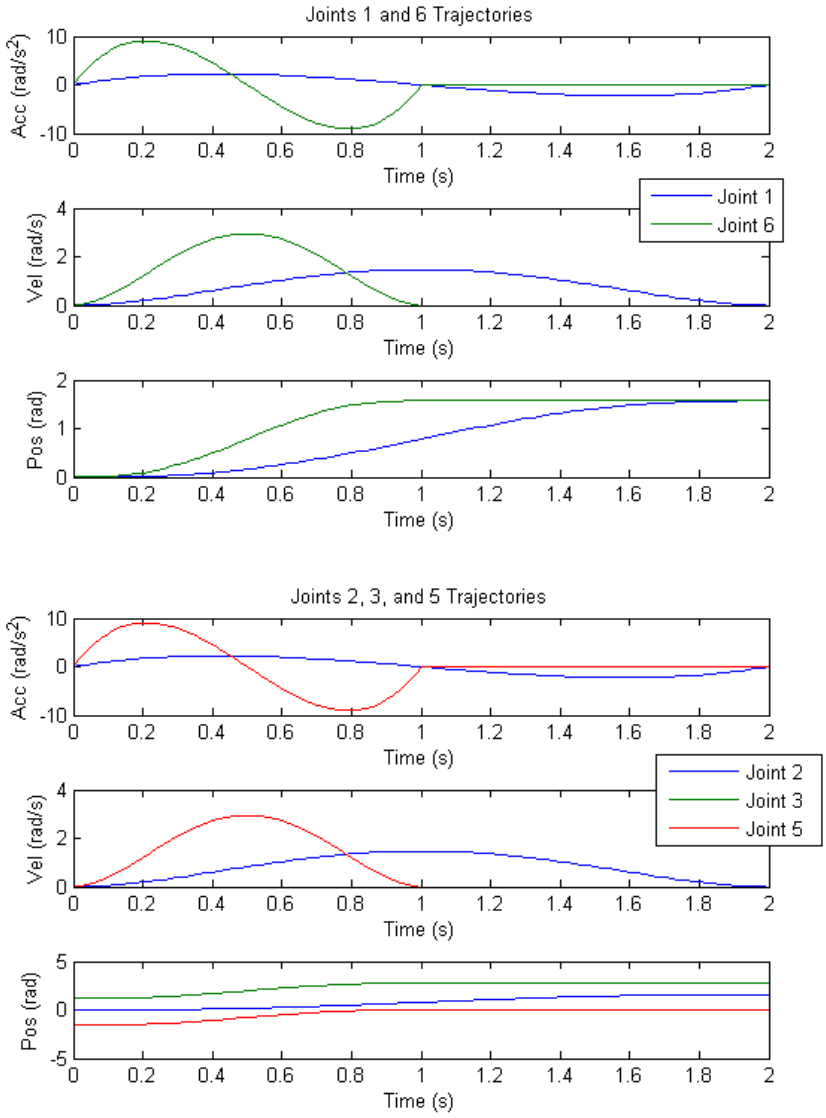

Figure 24: Trajectories used to determine the torques on the wrist joints. The joint numbers map to the system in the following way: . Joint 1 corresponds to the first shoulder, 2 to the second shoulder, 3 to the elbow, and 5 and 6 correspond to the two wrist joints.

The final result for the Matlab toolbox is displayed in Figure 23. The maximum dynamic joint torque for the joints of the Wrist is 1.18 Nm. They share the same joint torque because they share an origin.

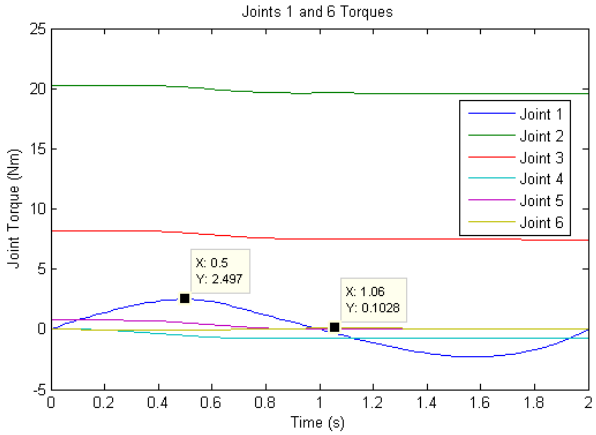

Figure 25 Joint Torques

As a comparison, the calculation for the maximum static torque was also calculated to compare the torque values. As seen in Equation (6), the static maximum torque is .585 Nm, which is about half as much as the dynamic maximum torque on the joint.

$$Length = 4in \tag{3}$$

$$Pulley_{Wrist} = \frac{.75}{2} inches \tag{4}$$

$$Pulley_{Motor} = .6\ inches \tag{5}$$

$$JW_{torque} = Length * g * load = .585\ Nm \tag{6}$$

2.3.6 Motor Selection

Motors for the wrist were selected based on dynamic torque and maximum static torque results from the previous section. These torques were then converted into the maximum tension on the cable, which has a stretch of 3% as latter discussed in detail in the tensioning section, and then back to the torque need by the motor. The required speed of

the motor was also calculated in order to help with the motor and gearbox selection process. The torque and speed requirements for the two wrists joints are identical because they are in line with each other. The equations for this are summarized below.

$$JW_{motor} = JW_{torque} * Pulley_{Motor} = 1.067\ N * m \quad (7)$$

$$JointSpeed = \pi\ rad \quad (8)$$

$$Speed_{Wrist} = \frac{Pulley_{Wrist}}{Pulley_{Motor}} * JointSpeed = 33.618\ rpm \quad (9)$$

The motor size was limited by the area that it needed to fit in. The most powerful motor and gearbox combination that would fit in the limited space and still meet the speed requirements were selected. The final motor requirements and the chosen motor specifications can be seen in Table 3. The motor selection process was iterative and worked closely with the mechanical design because the size of the pulleys used directly affected the required torque from the motor. The required torque in table reflects the required motors torque and not the calculated joint torque.

The Maxon brushless 4 pole DCX series motors were selected because of their high torque, high acceleration response, and high power density. The biggest advantage to the DCX series is that it delivers customized, high precision motors in only a few days. The selected motors have a max power output of 24W, a nominal torque 1500 mNm, a no load speed of 12400 rpm, and a maximum efficiency of 85.9%. To keep the motor operating in the peak range for this application, the motor was paired with a 243:1 gearbox.

Table 3: Selected Motors for the Wrist

Joint	Required	Actual	Safety

	Torque(Nm)	Speed(rpm)	Torque(Nm)	Speed(rpm)	
WristX	1.06	16.809	1.5	38.03	1.42
WristY	1.06	16.809	1.5	38.03	1.42

2.3.7 Series Elastic Actuators

The third style of series elastics discussed in Section 1.2.3 Compression Springs and Rotation of the Background was used in this joint, which relies on terminating the cable in a spring directly connected to the joint. Because the joint needs to move in both directions, two different cables are used which ground into two different spring boxes. These spring boxes consist of a bronze stopper that that the cable is locked into, the spring and the threaded case. The threading in the spring box is used during the cabling process to half compress the springs in order to position them for cabling. This spring box is broken down in Figure 23.

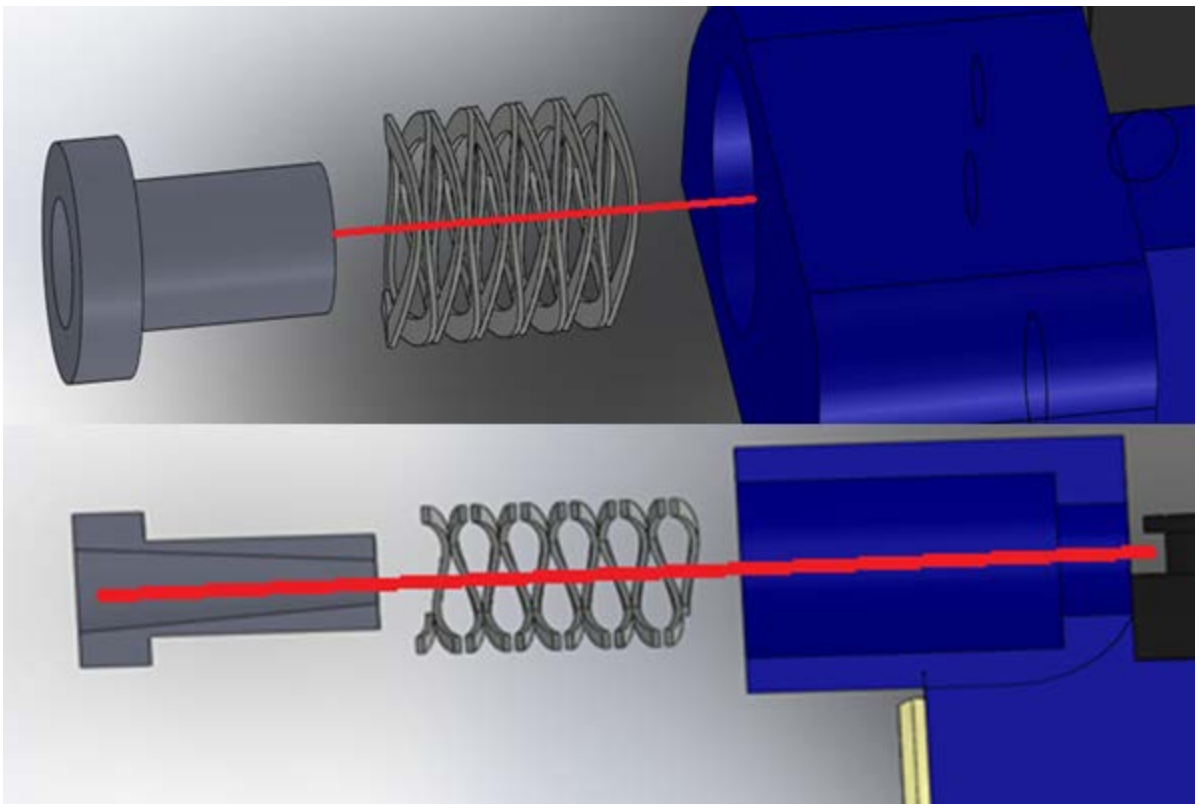

Figure 26 Exploded view of one spring box

2.3.8 Spring Selection

Based on the torques calculated earlier, the necessary spring constants to minimized deflection during dynamic motion could be calculated for the wrist. As seen in the equations below an equation of the spring constraint can be derived from the original F=K dx. Since 10 degrees of motion is equivalent to 0.065 inches of travel for the spring, the torque at the joint could be deviated by two times this displacement to calculate the spring constant as seen in Equation (16), where k is the spring constant, F is the force adding on the spring, and Δx is the displacement of the spring.

$$F = k * \Delta x \quad (10)$$

$$F = k * (x_0 + \Delta x) - k * \left(L - (x_0 + \Delta x)\right) \quad (11)$$

$$F = k * x_0 + k * \Delta x - k * L + k * x_0 + k * \Delta x \quad (12)$$

$$x_0 = \frac{L}{2} \quad (13)$$

$$F = 2 * k * \frac{L}{2} - k * L + 2 * k * \Delta x \quad (14)$$

$$F = 2 * k * \Delta x \quad (15)$$

$$k = \frac{F}{2 * \Delta x} \quad (16)$$

However since there are two springs compressed to half compression that keep tension in the cable in both direction of motion. The final equation is instead bellow. The final displacement must then be divided by two for the two different springs.

$$k = \frac{F_{cable}}{2 * \Delta x} \quad (17)$$

Wave springs are used in these spring boxes because of the high spring constants that can be achieved in a small package. As seen in the equations above, a spring constant of 44.912 lbf/in is required in order to have a maximum of 8 degrees of deflection during maximum dynamic torque. If compression springs were used, they would need to be eight times longer than the wave springs selected and would complicate the mechanical design significantly.

2.3.9 Assembly and Tensioning

An important design consideration is the assembly and tensioning process. Having fewer pieces in this module simplifies the assembly process. The first step in the assembly

process was to mount the center pivot into the middle pivot ring with the pulleys and D-shaft. Next, the small shafts on the sides of the middle ring pivot are added along with the pulleys. The two pivot pieces are then clamped between the two support base pieces and the bases of the support pieces are screwed into the motor mount module. Finally the three Delerin director pieces are attached to the pivots.

Having a well thought out and planned cable routing and tensioning system is an important part of making this a functional platform, since all of the joints rely on cables to transfer the motion and torque from the motor. The two most important things to consider when planning the cable routing and tensioning are the 3 percent stretch in the cable that will need to be accounted for and the Capstan equation effect. The capstan equation effect is Equation (18), where T_{load} is the applies tension, T_{hold} is the resulting force at the other side, and μ is the coefficient of friction between the rope and capstan materials and φ is the total angle swept by all the turns of the rope, measured in radians.

$$T_{load} = T_{hold} * e^{\mu\varphi} \quad (18)$$

Before cabling can begin, all of the springs need to be half compressed. If the springs are not at half compression, during maximum torque one of the sides of the cable will have no tension in it. When the spring has no tension, it has the potential to jump off of one of the pulleys. All of the spring boxes in the wrist are threaded so that a bolt can pre-compression the springs to half compression before cabling starts.

When cabling the joints, first one side is cabled as tightly as possible, then the motor is turned in that direction putting the full load and tension on the cable and spring. The other cable for the joint is then routed and attached as tightly as possible. Finally the cable tensioners are tightened and any additional slack that was in the cable is removed.

Since the cable is capable of stretching 3%, it is important that the tensioning mechanism is able to either elongate the path of the cable by that much or reduce its total length by an equivalent amount. Since the stretching is a plastic deformation, it does not add any compliance to the system. For the wrist joint, this extra tension was removed by shortening the cable. In the space between the motors in the upper arm four, 3-piece cable tensioners were added as seen in Figure 26.

Figure 27: In line three piece Wrist tensioners

These cable tensioners are tightened by removing the wrist motors then pulling a cable around them while holding onto the screw component. The friction between the cable and the steel threaded piece is large enough that pulling the cable rotates the piece as seen in Figure 27.

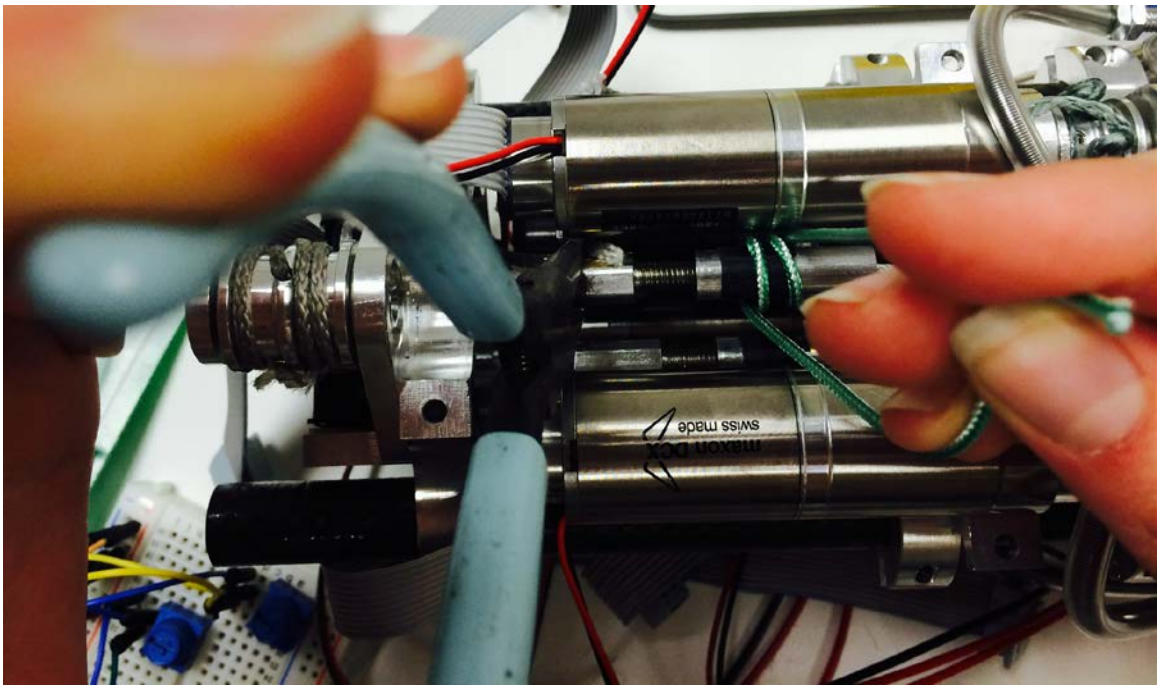

Figure 28 Tensioning method for Wrist

By screwing the two components together, the distance between them is reduced. The third component is a sleeve that locks the two pieces together and prevents them from untwisting during operation. Each of these tensioners can reduce the length of the cable by 10 mm. Their locations in the final assembly can be seen in Figure 28.

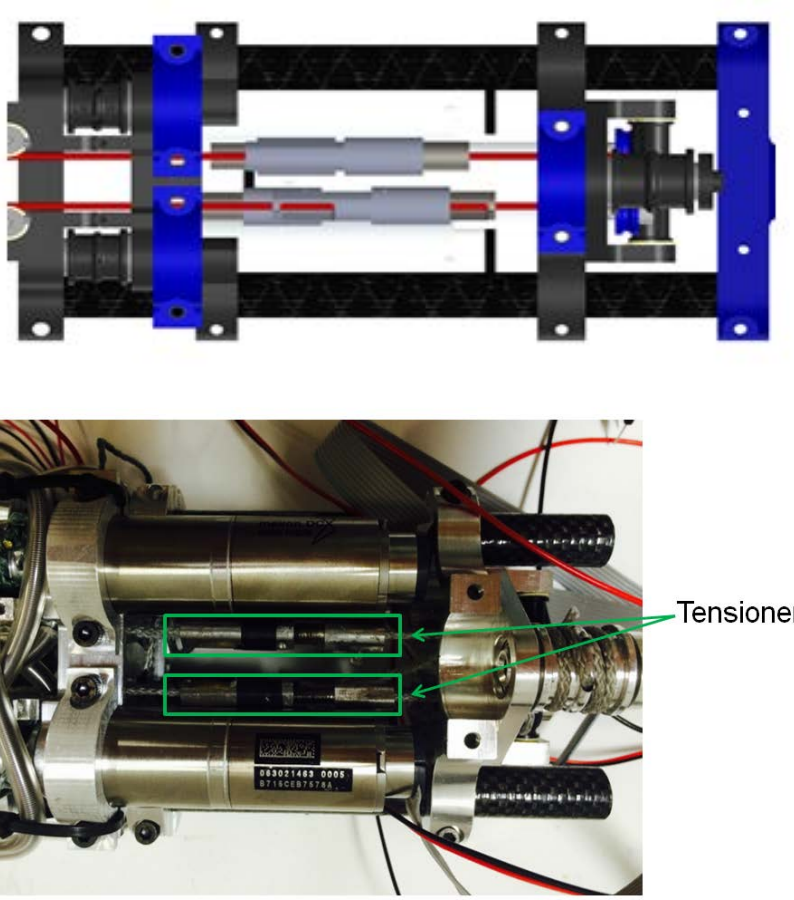

Figure 29: Wrist tensioner location

Capstan equation calculates the reduction in force on a cable bending around a curve. This means that three turns around a pulley will halve the amount of force output. While keeping this principle in mind, I focused on limiting the number of turns around idler pulleys in routing the cable. In most locations the cable only makes a maximum of one turn. Table 4 below shows how many extra turns the cable makes before reaching its final destination.

Table 4: Additional turns around idler pulleys

Joint	Additional turns (rad)
Positive First Wrist Pitch	5.75
Negative First Wrist Pitch	8.90
Positive Second Wrist Pitch	10.47

Negative Second Wrist Pitch	13.61

2.3.10 Evolution of Designs

This module went through several design revisions before reaching the final design discussed above. Each of the major revisions and reasons for the revision to this module are discussed in the sections below. All of the designs discussed are in-line joints consisting of three primary pieces; a base support skeleton, a middle rotation piece, and a final rotation piece.

Original Design

The original design for the wrist was similar to a typical Universal Joint with an 'X' shaped center. This design did not have series elastic joints. Instead, it had springs that applied forces to center the joints. Since it was a gravity compensation to make it more efficient, it did not give any direct information about the joint torque. It was decided that series elastics would be better mainly for this reason. Also, in this design the first joint was independent and the second joint was dependent. The dependency of the second joint meant a longer cable path which would increase the stretching distance. Another issue with this configuration, the second joint would move with the first, increasing the power demand and decreasing the efficiency of the system. The cables from the motors directly grounded into the pulleys at the joints and separate cables connected each joint to its

corresponding centering joint.

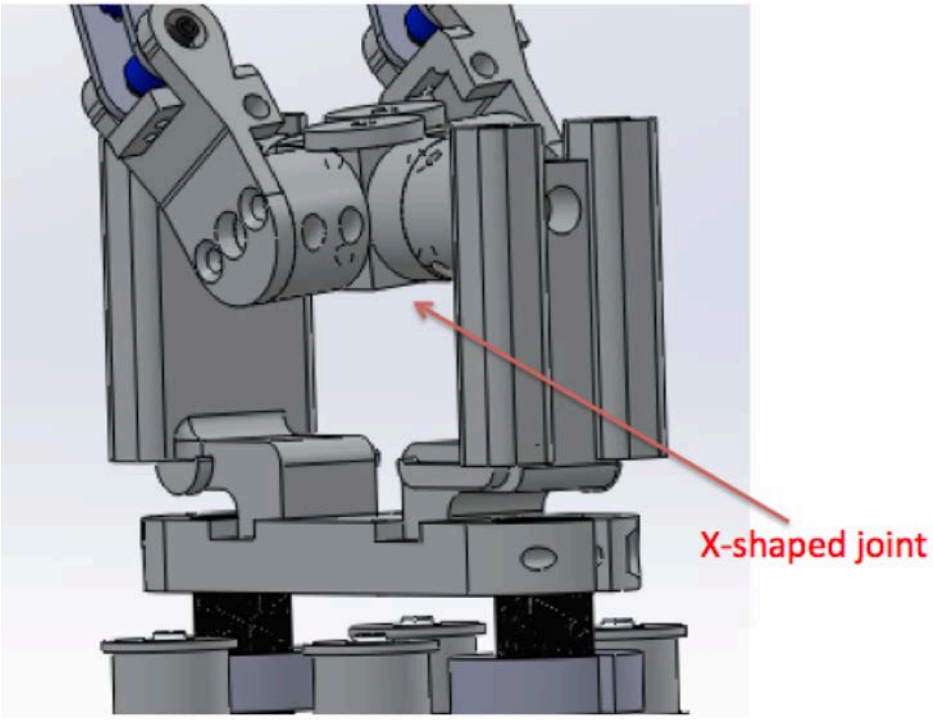

Figure 30: Self Centering Original Design without Series Elastics

Second Design

This design incorporates series elastics in the design. Instead of being an 'X' the first pivot became a cage around the second pivot, with the springs being stored under the cage show in Figure 30. The second pivot then was moved inside this cage and its springs were also placed underneath the pivot axial. Both of the pivots have the cables entering the spring box from the same side. A simple pulley is used to redirect the cables from around the first axis to the second. The major issue with this design was that it was extremely expensive to machine.

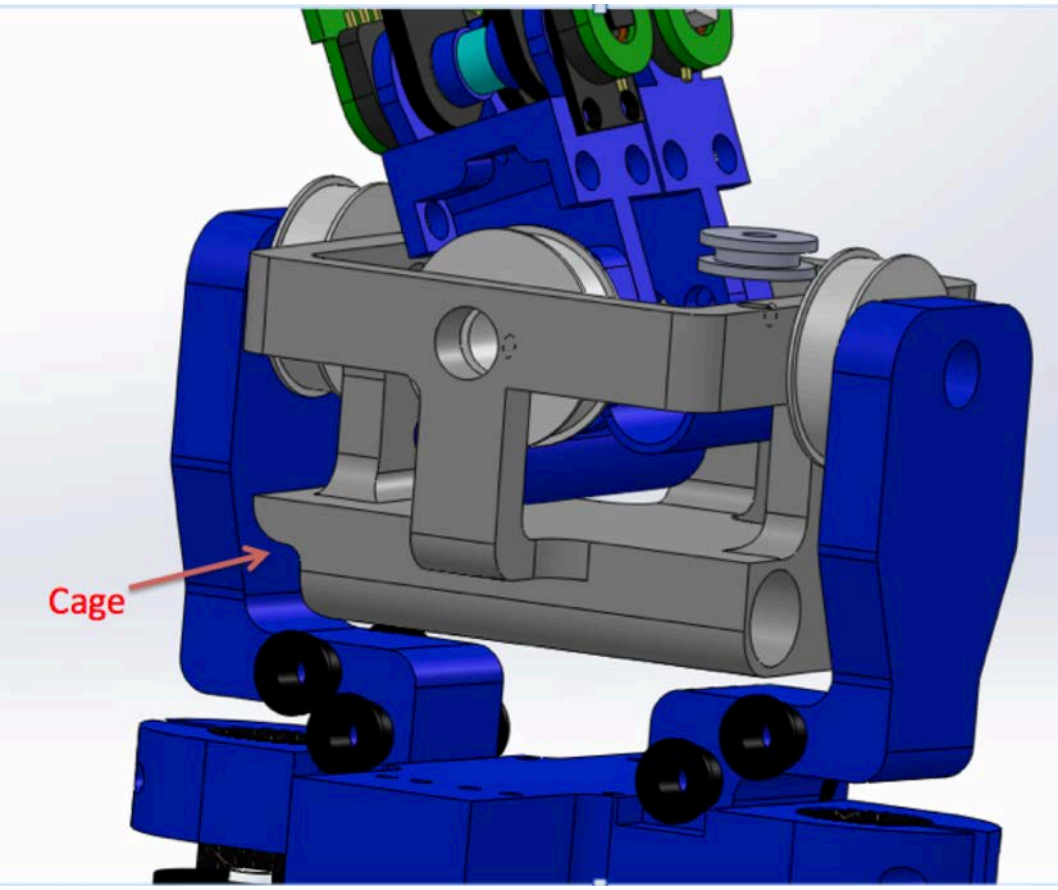

Figure 31: Second Wrist Design, incorporated SEA's

Third Design

In this design, the fingers are moved further apart so that they hover above the edges of the cage instead of directly above the pivot as seen in the figure below. This change was due to the fact that having the base of the fingers so close together limited the variety of the objects that could be grasped. Limiting the variety of objects it was capable of grasping would limits its usefulness as a research platform.

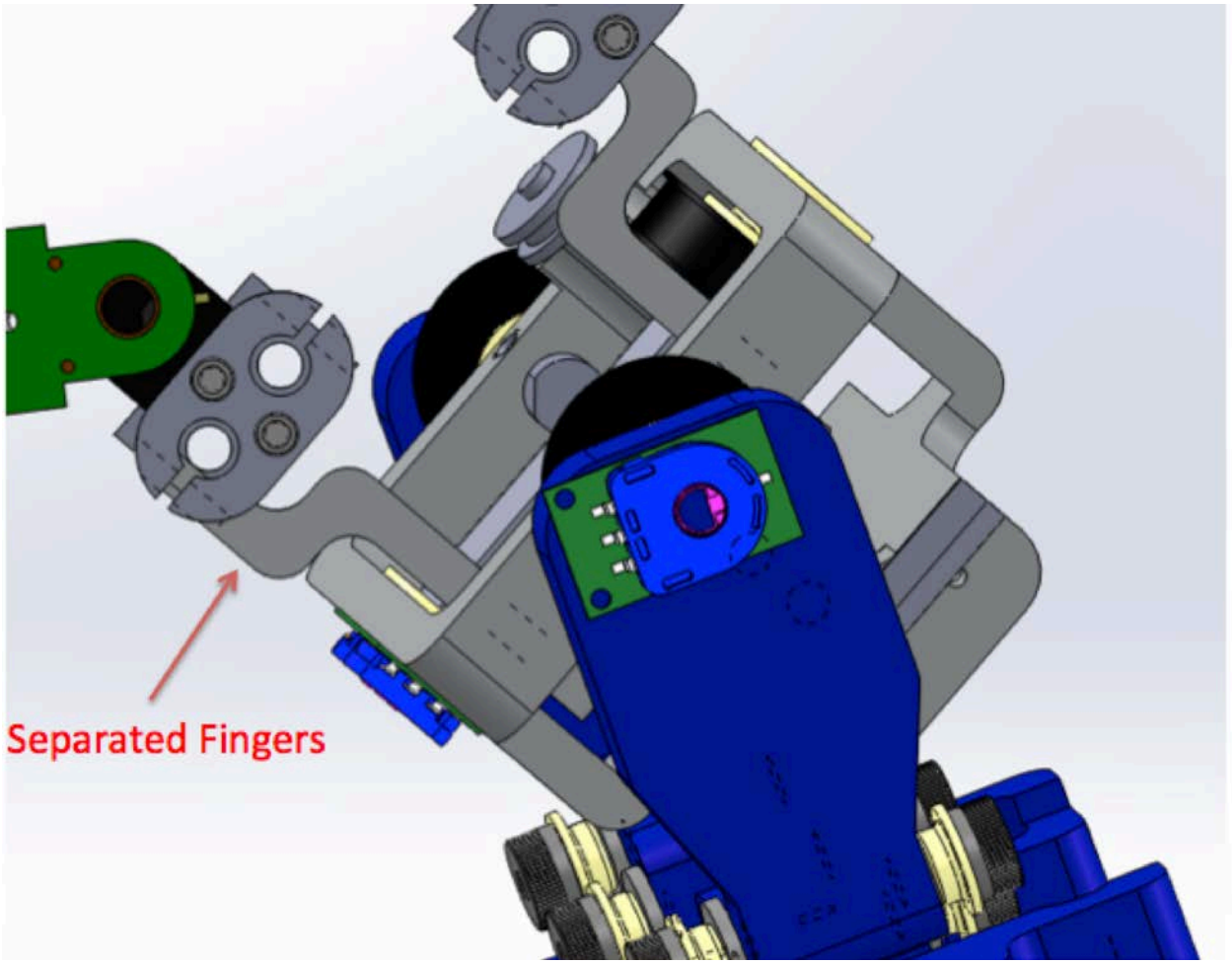

Figure 32: Third Design with separated Fingers

Forth Design

This design exchanged the large compressions springs for much smaller wave springs. By moving to smaller springs, the large and expensive to machine cage was removed and the springs are instead mounted directly below the pulley in a removable spring box. This removable spring box could be assembled separately from the wrist and then attached after it had been compressed. The center pivot was also simplified by moving the wave springs vertically on the inside. Two small pulleys were then used to redirect the

cable from the pivot pulley into the springs. Like the previous design the first pivot had one pulley on each side; one side for controlling its motion and the other for directing the cables for the inside yaw joint.

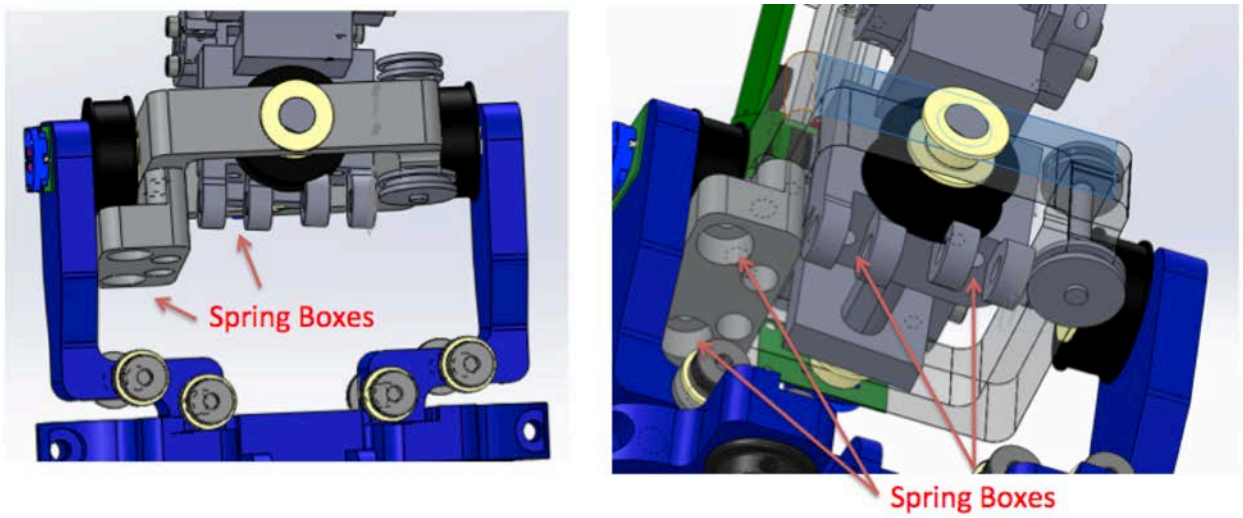

Figure 33: Forth Design incorporating Wave Springs

Fifth Design

The fifth design separated the cables for the inside yaw joint and moved one to each side of the center yaw pivot piece making the part more symmetrical and less complicated. This design also flipped the orientation of the springs so that the cable went straight down into the spring from the pivot pulley. Instead of using pulleys to redirect the cables to the second joint from the first, a Delrin director was used instead. This design also moved the springs on the first pitch pivot joint so that they are positioned further out horizontally as seen in the final configuration. Having the springs out to the sides reduces the pieces needed and the weight of the assembly. The springs also serve as mechanical stops for that axis.

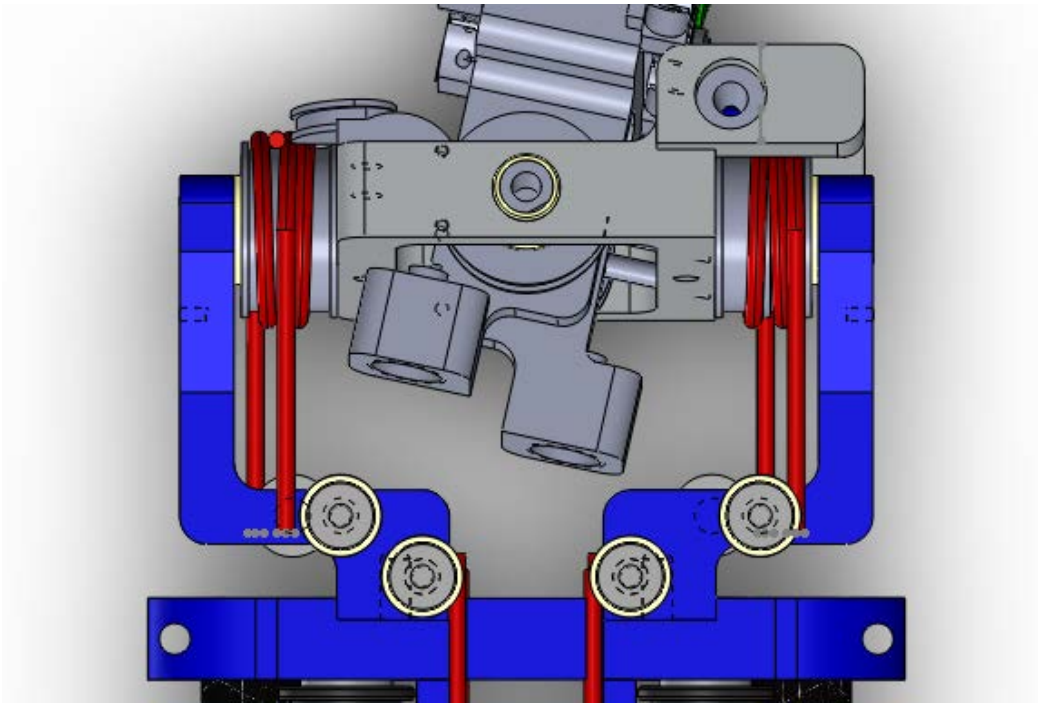

Figure 34 Fifth Design incorporating the wave springs into the pieces and rotating them

Transition to the Final Design

The primary differences between the fifth design and the final design are that the two pulleys on the sides of the first joint were replaced with four pulleys so that each cable has its own free spinning pulley and that the springs in the second yaw joint where rotated horizontally instead of vertically. Replacing the pulleys prevents the cables from sliding along the pulleys instead of spinning the pulleys, which reduces the inefficiencies in the system caused by friction. Rotating the springs in the second yaw joint makes the inner assembly smaller which increases the joint's range of motion. The major issue with this system was its limited range of motion.

2.4 Finger Modules

The finger modules are composed of the two unique links of the finger. This section begins with an overview of the design requirements for this module. After this, there is a

discussion of material and cable selection, module design, and cable support structure design methodologies. This section continues with the system modeling and motor selection, accompanied by discussions on the design of the series elastic actuators used in this section of the manipulator. The section concludes with a discussion on the final assembly of the fingers and the evolution of the design of the finger modules during the project.

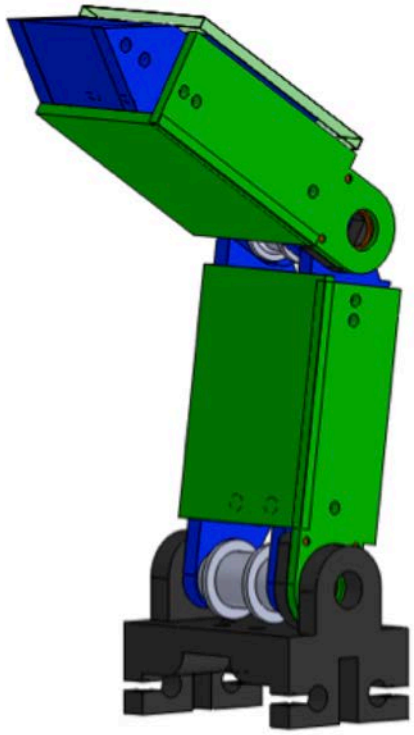

Figure 35:Two Link Finger Module

2.4.1 Design Requirements

Based on the design requirements, each module needed to be of comparable size to a human finger, incorporate series elastics, be easy to mount of the wrist, have two links and be dependent from the motion of the Wrist. The two-finger design was chosen because it is a simple system that still allows for up to 5 points of contact for large object, a

comfortable number of contact points for controlling most generic objects found in human environments. It also allows for two parallel contact lines for pinch grips to balance the forces. The fingers also need to be able to deflect easily on contact but be strong enough to grasp and hold a 1kg payload. Finally, the finger modules must be adequately covered in tactile sensors. Like the wrist, the motors for these modules are also located in the arm and cables are used to transfer the motion for the motor to the joint in the fingers. Additionally, because the motion of the fingers needs to be independent from the motion of the wrist, Bowden tubes are used to isolate the motion. A Bowden cable is a flexible hollow tube used to transfer the mechanical motion of an inner cable. Bowden cables are commonly used in bicycle brakes, cars, old remote camera shutter controls and aircraft. Based on the requirements, two of these finger modules are required in the final assembly. To satisfy the range of motion requirements, the first link is capable of moving 175 degrees, which is more than the minimum requirement of the motion of a human finger, relative to the base and the second link is capable of moving 90 degrees relative to the first link.

2.4.2 Material Selection and Manufacturing

The structural components in the finger modules are primarily made from 3D printed Polylactic Acid (PLA) plastic. PLA was used because it met the force requirement for the finite lement analysis for a safety factor of two for the expected loads and is readily available. The transition piece between the fingers and wrist, the slider, and finger spring box caps are all made from 6062 Aluminum. The majority of the fingers is 3D printed to reduce weight, cost and allow for future modifications. The three different parts are metal

because the forces and stresses that they experience during normal operation would break a 3D printed equivalent. This was confirmed through FEA's of the CAD model an example of which is in Figure 35. The Bowden Tubes are made from extension springs surrounded by a flexible plastic tube. The springs provide the rigidity that the Bowden needs and the tubing prevents the spring from kinking under maximum tension.

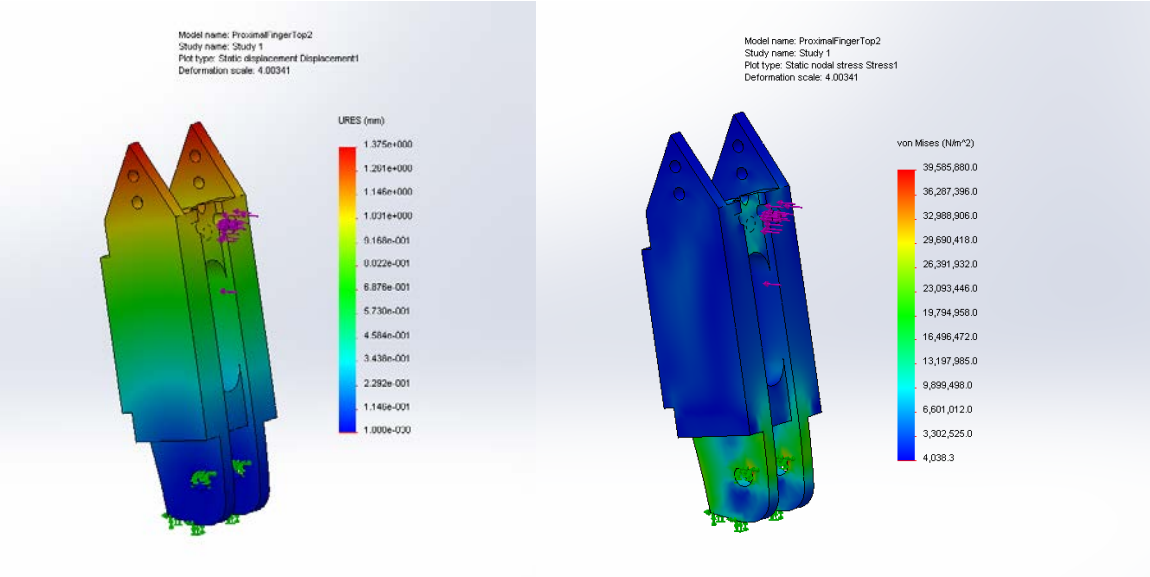

Figure 36 FEA of the first link of the finger

The spring boxes are attached to the fingers off center to increase the contact surface area of the fingers. The finger spring boxes are above the axles so that when the finger is folded at a 90 degree angle the contact area where the tactile sensors are is increased to help meet the requirement of having adequate sensor coverage as seen in Figure 36.

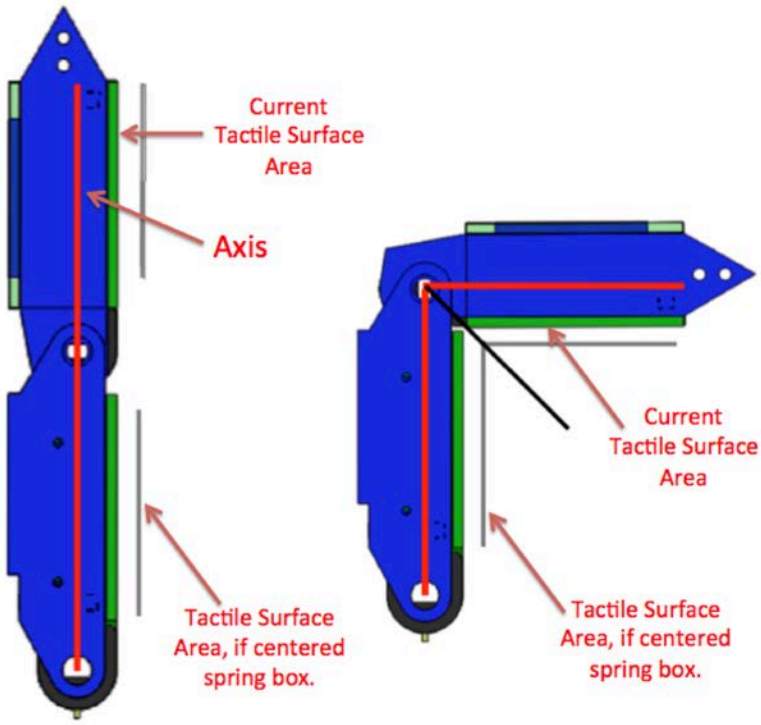

Figure 37: Tactile Sensor Coverage Area

2.4.3 Cable Routing

The cables for all of the joints in the fingers come from the four motors facing towards the wrist and finger modules. These cables are attached to four 0.4 inch diameter pulleys on the motors and are then routed from the motors to the tensioning blocks on the outside of the Wrist with Bowden cables. From the tensioning blocks the cables are then routed through the Bowden cables to the metal transition pieces where they are routed into the base of the fingers. Each joint has two cables controlling it, one for each direction of motion. One of the cables enters the finger link at the bottom and the other enters the at the top. From the metal cable routing piece, the first cable makes one turn around the base pulley then enters the spring box on the first link. Then it goes through the metal slider and attaches on the opposite side. The second cable makes one turn in the opposite direction

around the base pulley then it is pulled around the curve on the top edge of the link into the top of the spring box. From there it goes through the slider and attaches on the side of the slider closest to the wrist.

The next two cables control the second link in the finger module. Because these cables first wrap around the pulley for the first link, their motion is dependent on the first link of the fingers. After wrapping around the first pulley in opposite directions from each other, the cables then are routed up to the second pulley. When they make their turn around the first pulley, both cables rotate towards the center of the pulley so that they are lined up with the smaller second pulley. The first of these two cables makes half a turn around the second pulley and then enters the bottom of the second link. From there it goes into the metal slider and attaches to the far side. The last cable makes a full turn around the second pulley then enters the top of the spring box on the second link.

2.4.4 Finger Joints Knot Selection

The best method for attaching the cable to the slider is with a compressed knot and the best class of knots for this application is stopper knots. This type of knot is design to be tied in the middle or end of a cable and not move. By incorporating the opposite cable for that joint into the knot, it becomes more balanced and more secure around the slider. Ashley's Stopper Knot, Double Overhand Stopper Knot, and the Figure Eight knot where all tested before the Ashley's Stopper knot was selected. It was difficult to incorporate the middle of the other cable into the double overhand stopper knot in a secure way. The figure eight knot pulled through with very little resistance. The oysterman's knot was difficult to leave a reliably short teal that wouldn't get in the way of the springs in the spring box.

Figure 38 Ashley Stopper knot (30)

The Ashley's Stopper knot as seen in Figure 37 had several advantages over the other options. First, the harder the cable pulls on the knot, the more it clamped its own end against the metal. It was also easy to incorporate the middle of the other end into the cable, as seen in Figure 38.

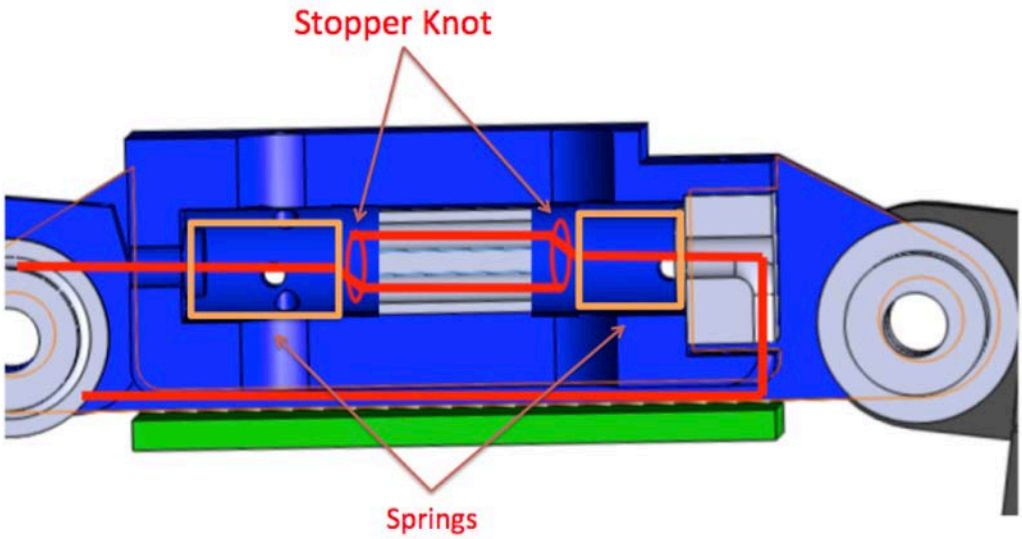

Figure 39 Stopper knot location in the fingers

2.4.5 Cable Selection

The tension requirements on the fingers are significantly smaller than the wrist. Additionally the space requirements in the finger require a thinner cable. For the Bowden tube to work correctly the difference between the inside diameter of the tube and the diameter of the cable need to be as close as possible. Due to the size limitation of the Bowden tubes available, 1mm was the smallest size of cable that could be used. For these reasons, a 1 mm 12 strand braided Dyneema cable was sought after. Dyneema was selected because of its small turning radius, low sliding friction, and low stretch. A more thorough discussion of Dyneema's material advantages is in the Cable selection section for the Wrist, 2.3.4 Cable Selection. A cable with 12 strands was desired because it would work with the Igus clamping method, which relies on a dense braid. Having a cable with less strands in the braid would prevent it from claiming properly because the braid would not have enough surface area in contact with the cone, an important components of the Igus clamping method.

Table 5 Cables tested

Cable	material	lbs	Diameter	Strains	Major Fault
FSE Robline Dinghy Control	Dyneem/Nylon	150	1.7mm	0	Unbraded Dynema
Atlandtic Braids Fling-it	Dynema/Polyurethance	300	1.4mm	8	Not shock resistant
Power Pro Braided Fishing Line	Spectra	80	.7mm	12	Too thin
Sporasub Dyneema Braid	Dynema	330	1mm	4	too few braids
Dynema Brain Yu Wei	Dynema	250	1mm	8	Couldn't find a supplier

In addition to being used in robotics applications, Dyneema cable is also used in fishing, parasailing, sailing, towing, and gliders. After extensive research, five different cables were ordered that had diameters ranged from 0.68 mm to 1.3 mm. All of these cables were braided and were made from Dyneema. Some of the other samples ordered claimed to be braided Dyneema surrounded by a Polyester double braided covering,

however upon delivery it was discovered that the interior Dyneema was simply stranded and not braided. Only one of the cables ordered had the desired 1mm diameter. While all of the ordered cables meet the strength requirement, many of them didn't have 12 braided stands. For example, the .68mm cable had 10 stands and the 1mm cable only had four. Because of size restriction, the 4 strand 1mm braided was selected despite the clamping issues.

2.4.6 Bowden Selection

A Bowden cable is a type of flexible tubing that is capable of transmitting linear mechanical energy across a distance. In this project, Bowden cables are used to decouple the fingers from the wrist joints. The Bowden cable begins at the upper arm, bypasses the wrist joints, and grounds again at the base of the finger. Bowden cables have many practical applications and can be commonly found on bicycle brakes and shifters, old camera shutters, personal gliders, and cars. Since it had been predetermined that the maximum cable that could be used in the fingers was 1.3mm, all of the tubes ordered and tested had an ID of at least 1.3mm.

2.4.7 Tested Bowden Tubes

The first Bowden tubes tested where the bike brake cable, shifter cable, and camera cable. Bike brake cable consists of three different layers. The outer is a thin plastic shell that holds the layer below it together. The next layer is a flat piece of metal that has been spiraled around the inner plastic tube. This metal support layer provides most of the support to the tube. The final layer is a smooth plastic tube that the cable slides inside. The

shifter cable has a similar structure however instead of having a coiled metal layer, there was a ring of metal rods forming the support layer. The camera shutter cable was the thinnest but still too stiff for this application. It was quickly determined that all of these tubes were too stiff to make the tight turn radiuses required because of the metal layer. However, the metal inserts made them easily meet the tension requirements.

Figure 40 Bicycle break and shifter Bowden cables (31)

It was then determined that a simple smooth plastic tube may be sufficient for this application. Because of the low tension requirements for the fingers, in theory there would not be enough tension on the cable for a metal layer to be necessary. Smooth plastic tubes that were both considered both firm and flexible where acquired. The following tubes were all selected because they meet this requirement.

Once the tubes arrived, it was easy to eliminate most of them with simple tests. Tubes that were too rubbery were easily compressed under tension, and had a large friction coefficient that added to the torque requirements in the system. Tubes that were too soft were immediately eliminated because they compressed around the inner cable when bent. This compression adds extra, unpredictable friction in the tube. Tubes that were stiff and had memory were also eliminated. Memory means that the tube will hold the position it is moved to. Having memory increases wear on the tube and reduces the

number of life cycles of the system before failure. The following chart summarizes the tubes that were immediately eliminated and the reason. Quantitative assessment of internal friction was not include due to its difficulty to measure.

McMaster Part	flexibility	turn diameter	interior	compressibility	memory	stretchy
52355K41	Durable White Tubing Made with Teflon® ® FEP 1/16" ID, 1/8" OD, 1/32" Wall					
	very	1	average	average	low	average
2129T11	Clear FEP Tubing 1/16" ID, 1/8" OD, .030" Wall Thickness					
	stiff	1.125	smooth	resistant	high	Not
9685T1	High-Pressure White Nylon Tubing .073" ID, 1/8" OD, .026" Wall Thickness					
	very	0.5		average	low	Very
5583K43	Abrasion-Resistant White ETFE Tubing .062" ID, 1/8" OD, .031" Wall, Semi-Clear White					
	average	1	smooth	average	average	average
1883T4	Miniature Clear EVA Tubing .05" ID, .09" OD, .02" Wall Thickness					
	very	0.5		very	low	Very
5173K39	Vacuum-Rated Nylon Tubing .078" ID, 1/8" OD, .024" Wall Thk, Semi-Clear White					
	stiff	2.5	rough	resistant	high	Not
5181K31	Crack-Resistant Polyethylene Tubing 1/8" ID, 3/8" OD, 1/8" Wall Thickness, White					
	stiff	6	rough	no	high	Not
51085K49	High-Pressure PEEK Tubing .062" ID, 1/8" OD, .031" Wall Thickness, Tan					
	stiff	3	rough	no	high	Not
9446K11	Choose-A-Color PVC Tubing, Blue, 1/16" ID, 1/8" OD, 1/32" Wall Thickness					
	average	0.75		very	slight	slightly
5119K78	High-Temperature Viton® Fluoroelastomer Tubing, Firm, 1/16" ID, 1/8" OD, 1/32" Wall					
	very	0.5	very sticky	very	low	Very
5006K61	High- Strength Clear PVC Tubing, 1/16” ID, ⅛” OD, 1/32” Wall Thickness					
	very	0.5	smooth	very	low	Very
51245K21	Durable Santoprene Rubber/Plastic Tubing, Food & Beverage 1/16” ID, 3/16” OD					
	very	1		easily	none	Very

The final two tubes that were selected where Durable White Tubing made with Teflon and Abrasion-Resistant White ETFE Tubing. Both of these tubes were installed in the assembly and tested there. The first tube was capable of making the required turns. However, because of its stiffness it was applying a force onto the finger modules that was

effecting the motion of the Wrist. Because of this, it was replaced with the Abrasion-Resistant White ETFE Tubing. When on the assembly, this tubing compressed under the tension making its length variable and unreliable. A new Bowden Cable was needed.

Next, extension springs were selected and ordered for testing. Extension springs are extremely flexible while still having a rigid frame, making them a good option for this application. Three different spring constant values were tested; 7.6, 1.4, and 1.2. The smallest extension springs that were able to be acquire had an OD of ⅛ inches. When the springs were placed in the assembly, the weakest spring had the tightest bend radius and put very little force on the wrist assembly when under tension. Unfortunately, under maximum tension the spring loop would form a 90 degree angle and kink out of place. Near the clamps, it also would kink under maximum tension. By kinking, the length of the spring was reduced which added random and unpredictable slack to the cabling. To prevent the spring from kinking, a flexible plastic tube, Laboratory Clear Tygon PVC Tubing, was added to the outside of the springs. This tube was flexible enough that it didn't impede the cables path or apply a force on the wrist assembly during tension, while still holding the spring in place.

2.4.8 Kinematic Modeling

The kinematics calculations for the Fingers were done in Mathcad. The goal of these equations was to determine the required joint torques for use in motor selection. Unlike for the calculations for the wrist, dynamic models were not created for the fingers and only the static equations were considered. This is because the dynamic forces on all of the other joints were consistently two times larger than the static values.

$$Length = 1.2\ inches \quad (19)$$

$$Pulley_{Finger} = 7mm \quad (20)$$

$$Pulley_{Motor} = .5inches \quad (21)$$

$$FJ1_{torque} = \frac{Length*g*load}{Pulley_{Finger}} = 99.636\ N \quad (22)$$

$$FJ1_{motor} = FJ1_{torque} * Pulley_{motor} = 0.633\ N * m \quad (23)$$

$$Length = 2.4\ inches \quad (24)$$

$$FJ2_{torque} = \frac{Length*g*load}{Pulley_{Finger}} = 170.804\ N \quad (25)$$

$$FJ2_{motor} = FJ2 *\ Pulley_{motor} = 1.08\ N * m \quad (26)$$

The final Equations (23) and (26) show a maximum static torque for the fingers of 1.08 Nm. This number was considered when selecting the motors and springs for the fingers.

2.4.9 Motor Selection

Similar to the motors for the wrist, the motors for the fingers were selected based on the maximum static torques determined in the section above. The maximum torques were then converted to the tension in the cable, then back to the required torque from the motor. The motor speed was calculated based on desired speeds of the fingers. The biggest limiting factor on the selected motor was the size. All six of the motors for the wrist and fingers need to fit in the upper arm. The final motor requirements and the chosen motor specifications can be seen in Table 1. To simplify the motor procurement and mounting design, all of the motors ordered meet the requirements for all six joints and can be used interchangeably. The selected motors all have a maximum power output of 24W, a nominal torque 1500 mNm, a no load speed of 12400 rpm, and a maximum efficiency of 85.9%. To

keep the motor operating in the peak range for this application, the motor was paired with a 243:1 gearbox.

Table 6: Selected Motors for the Fingers.

Joint	Required		Actual		Safety Factor
	Torque(Nm)	Speed(rpm)	Torque(Nm)	Speed(rpm)	
Finger joint 1	0.633	16.809	1.5	38.03	2.37
Finger Joint2	1.08	16.809	1.5	38.03	1.39

2.4.10 Series Elastic Actuators

The majority of each of the finger links is a spring box. These spring boxes are inspired by the spring boxes found in traditional linear based series elastic modules like seen in Obrero. This styles was also used in the elbow and upper arm rotation of the Sensitive manipulation Platform seen in Figure 34.

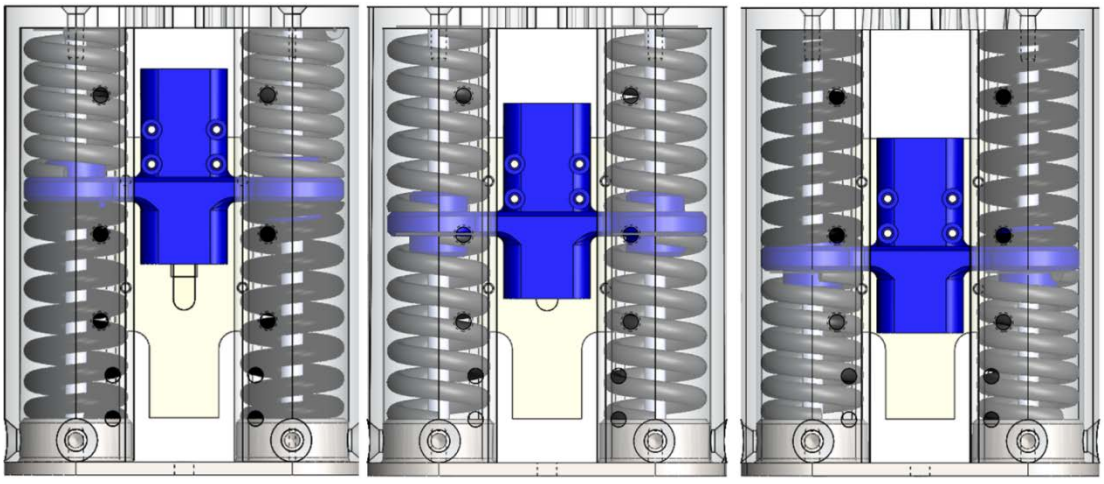

Figure 41 Elbow Pivot Joint SEA from the Sensitive Manipulation platform (11)

Unlike these modules which contain four springs, each spring box contains 8 springs. These springs apply a force to the spring case and the slider. The slider is attached

to the cables and its motion compresses half the springs and releases tension from the other half. Because the springs all start at half compression, no pre-compression is necessary. Unlike the spring boxes used in lower half of the Sensitive Manipulation platform the spring boxes in the fingers use eight springs instead of four. Four of the springs are weak springs and the other four are slightly stiffer springs. This creates two different ranges of stiffness in the joint. The first range is very sensitive and can be used to detect very light contacts, like when the manipulator is grasping a tube of paper. The second range allows it to still have compliance when lifting heavy objects. If only the weak spring was used it would quickly over saturate when lifting heavy objects or need to be extremely long. Using only a single spring constant wouldn't provide the sensitivity that this kind of research requires. The disadvantage of using two different springs is that when the weaker spring over saturates, a nonlinear range occurs. Together, the force displacement chart would look similar to the one show in Figure 34.

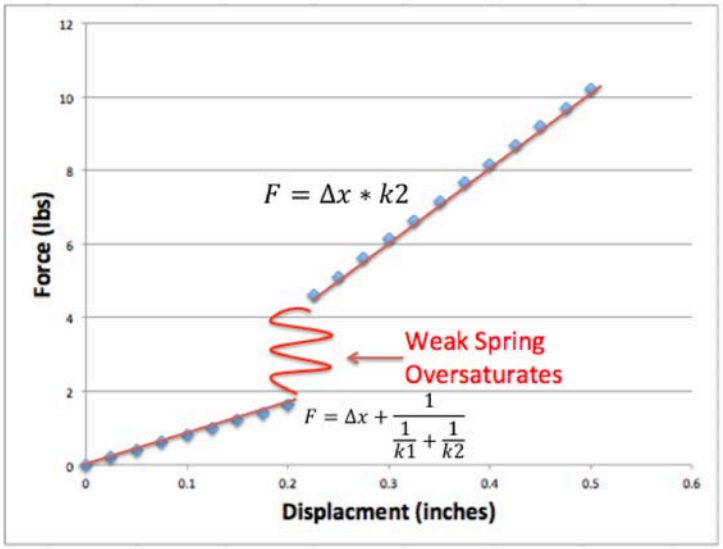

Figure 42: Force displacement chart for the Spring boxes

To avoid having two linear ranges with a non-linear range in the middle, a nonlinear spring could be used with a force displacement chart that would look similar to the one show in Figure 35. However, this type of spring would be extremely expensive to have made custom for this project in such a low quantity.

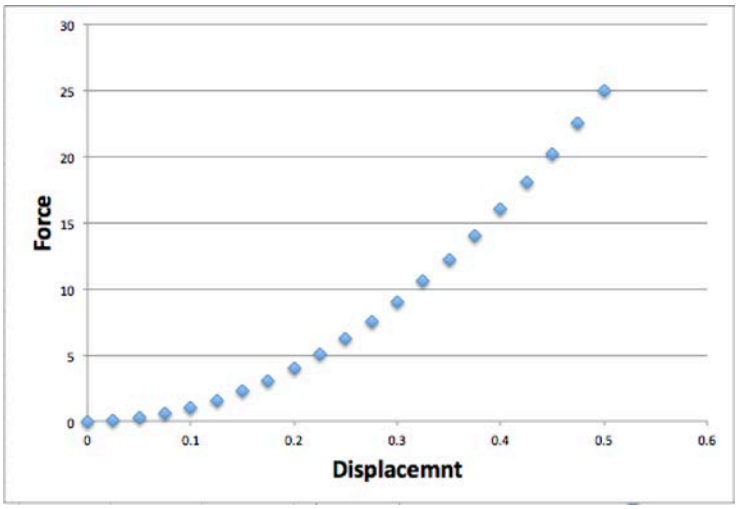

Figure 43: Force displacement curve for a non linear spring

2.4.11 Spring Selection

Two different springs were used in the fingers. A very weak spring was selected to detect delicate objects more accurately. A stiffer spring was selected to help sense heavier objects and larger contact forces. Unlike the other springs in the wrist, the math to calculate the spring constants for these two different spring constants is in the equations below. The two springs are in series with each other.

The calculations for the spring constant for the fingers were less straightforward. The fingers required a spring constant that would allow a high level of sensitivity and deformation for sensing very delicate objects. The fingers also need to be able to have an elastic element when grasping heavier objects. To satisfy both of these requirements, two

springs in series where selected. This creates two different linear ranges of sensitivity with a nonlinear range in the middle when the weaker spring becomes over saturated, and the entire spring assembly takes on the spring constant of the stiffer spring. The equation for springs in Series is Equation (27).

$$k_{net} = \frac{1}{\frac{1}{k_1}+\frac{1}{k_2}} \quad (27)$$

Given that the heaviest pay load the fingers will try to grasp is 1kg. It is important that the heavy springs doesn't over saturate. This week spring was chosen experimentally to be 13.3 lbf/in with a free length of .25 inches and a solid length of .073. Given that the links of the finger are comparable to the links of Go-bot and the total length of a human finger the heavy spring needs to have free length around .35 inches and a solid length around .13 inches. In order to meet the requirement Equation (28) was used. Force is divided by four because of the four springs of this type in the spring box.

$$k = \frac{F}{4*\Delta x} \quad (28)$$

This equation was used to solve for a 40 lbf/in spring constant. The final spring used was .313 inches long with a solid length of .125, and a spring rate of 39.2 lbf/in. The differences between the desired spring and used spring were compensated by modifying the size of the inside of the spring box in the link.

2.4.12 Assembly and Tensioning

One of the most important and frequently overlooked parts of the design process is engineering the assembly and tensioning strategy. The advantage to the spring box based fingers used in this project is that the series elastic elements themselves are pre-assembled independently of the arm and then assembled together. Because of this pre-assembly

process, the actually assembly of the module, once that step has been completed, is relatively easy. Another key aspect of the assembly process is the tensioning system.

Having an intelligent cable routing path was especially important for this model to keep the motion of the fingers independent from the wrist while still having the motors located in the arm. The routing of the cables also needed to allow for a tensioning system that can take up the three percent stretch that occurs in the cable during normal operation.

The assembly process for the spring box is as outlined in the following steps. First the cable is measured out then inserted into sliders and tied off with the Ashley's Stopper knot on each side. Then the cables are threaded through the bottom of the spring box link and through the metal cap. The springs are then inserted into the spring boxes. Two of each kind of spring are put on each side of the slider within the spring box. Having springs on both sides of the slider helps balance the force. Once the springs are in place, the top of the spring box is installed, pre-compressing the springs halfway, and the two locking screws are put in. Because the springs all start at half compression, no additional compression is necessary during the rest of the cabling process. The finally assembled box is seen in Figure 42.

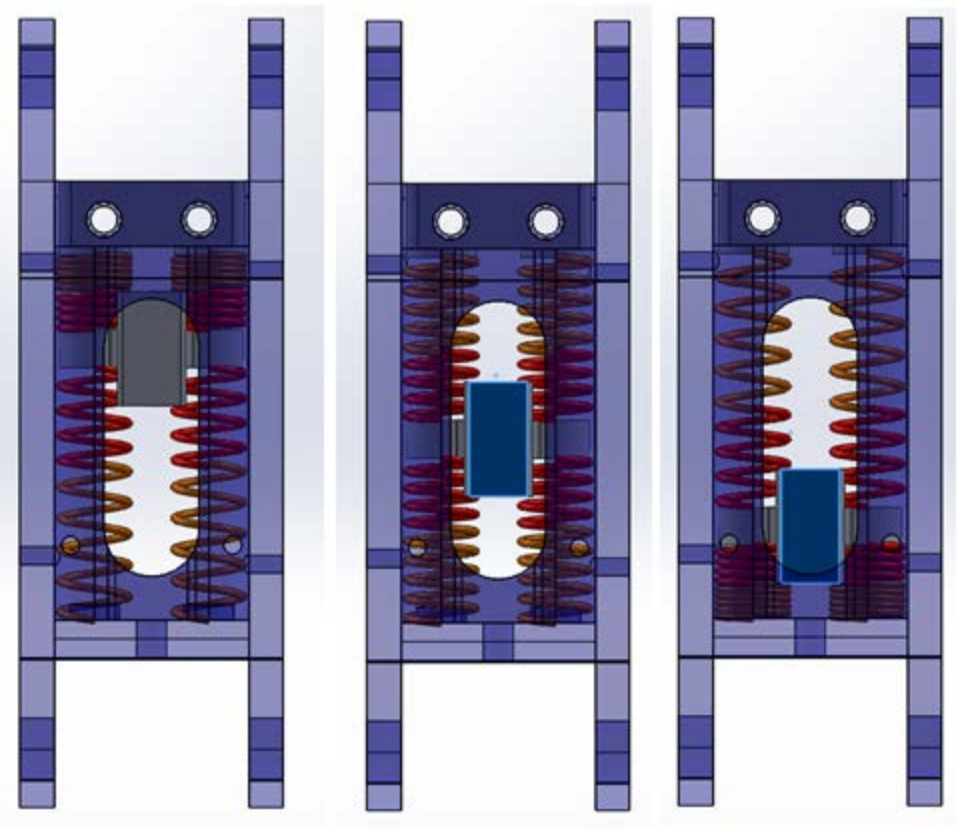

Figure 44 Finger Spring assembly

The tensioning system for the wrist relies on shortening the cable to the joint. The tensioning system for the Finger module does the opposite and lengthens the path the cable needs to travel. The flexible region of the Bowden cables works best over shorter distances, because it is easier to control the required turning radii and the motions the cable moves through. To reduce the region the cable must pass through, the Bowden cable is secured to the top of the support piece on the wrist. The tensioning system is then mounted to the back side of the wrist support piece above the potentiometer. There are three components to the tensioning system. Two 3D printed grounding parts and a hollow screw. The two grounding parts are spaced with a 1 inch gap between them. The hollow screw is then threaded all the way in to fill the gap. This assembly can be seen in Figure 43.

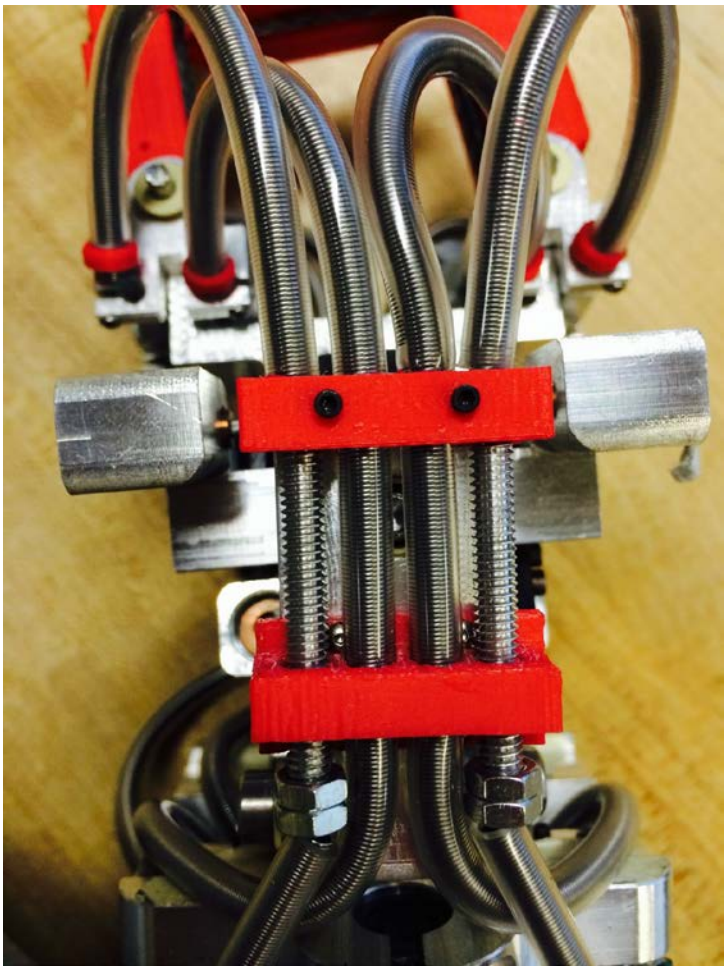

Figure 45 Finger tensioners

The cable loop is then completed after it has been attached to the motor are tightly as possible. The screw is unscrewed, lengthening the path of the cable and taking up the slack. This tensioning mechanism is only located on one of the cables in each joint and is responsible for taking up to tension in both cables caused by the 3% stretch. The unit at full extension can be seen in Figure 44.

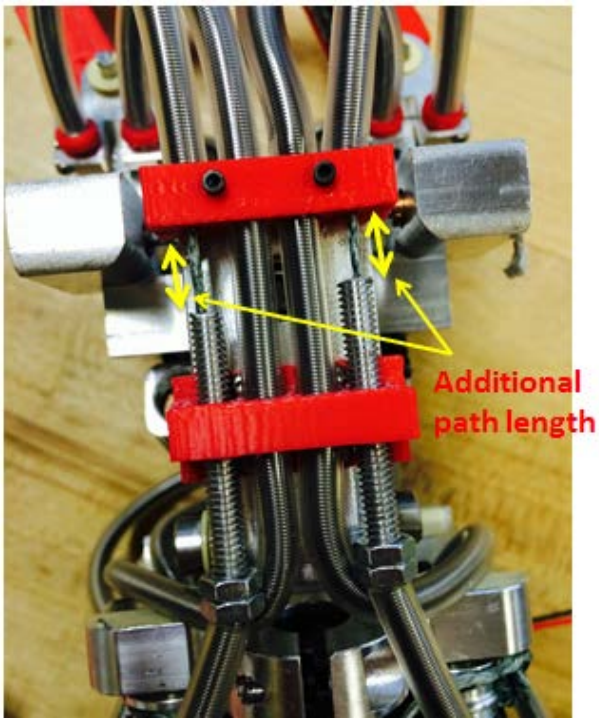

Figure 46 Finger tensioners fully extended

2.4.13 Evolution of Design

Like the wrist module, this module also went through several design revisions. The fingers themselves were originally going to be very similar to the fingers used in Go-bot seen in Figure 45. The fingers in Go-bot were designed to manipulate small, lightweight Go pieces. These fingers are made from 3D printed material and use the simplified series elastic modules defined in the background section as the third hybrid approach. The goal of this platform is the manipulate 1kg objects. The thin plastic pieces and delicate design of the Go-fingers were unsuited for use in this project without modification.

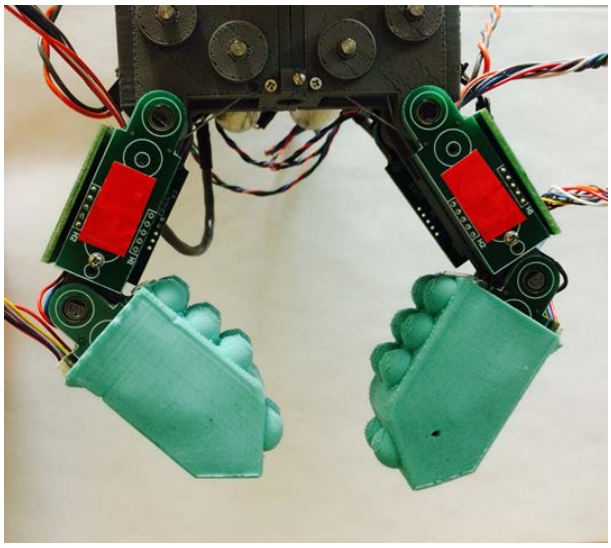

Figure 47 GoBot fingers

First design

The first design was inspired robotiQ robotics hand (31). This hand uses linkages to translate the motion of the motors to the finger links. A 3D printed prototype was created to test the mechanics of this concept. This design was quickly eliminated because it added an unnecessary level of complexity. The best way to translate the motion from the motor module to the fingers is with Bowden cables. Having the cables actuate a linkage makes the system unnecessarily complex.

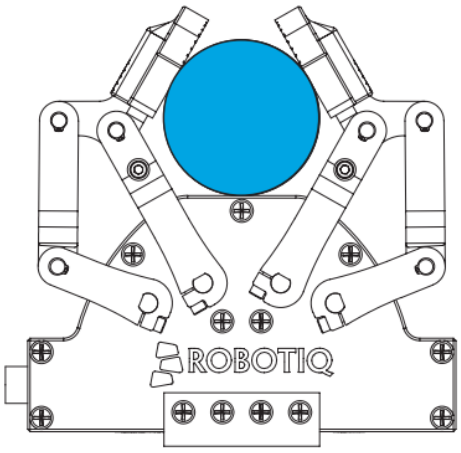

Figure 48: First Design of the Finger (31)

Second Design

The second design for the finger module was an upgrade on the original Go-bot finger. This upgrade increased the size the springs and moved them to the center of the finger as seen in Figure 47. By moving them to the center, the width of the link was reduced, making them more comparable to the size of a human finger. The joints were also thickened to support the additional stress caused by the heavier payload.

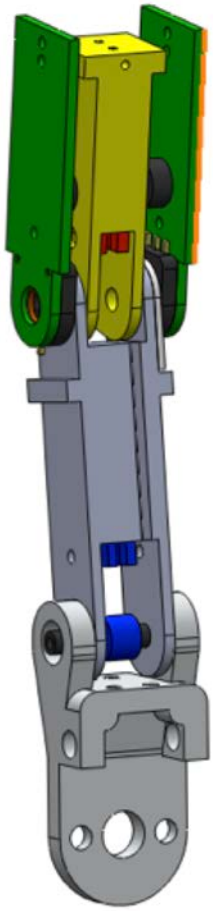

Figure 49: Second Design of Finger smaller version of the Go-bot fingers

Third Design

Having one spring on each side of the joint makes the fingers very thick and reduced the potential contact area for the tactile sensors. For the third design, the springs were both moved to the top of the joint. This thickened the joint slightly but significantly increased the contact surface area, which was more important dimension. This design was prototyped on the laser cutter and heavily influenced the final design.

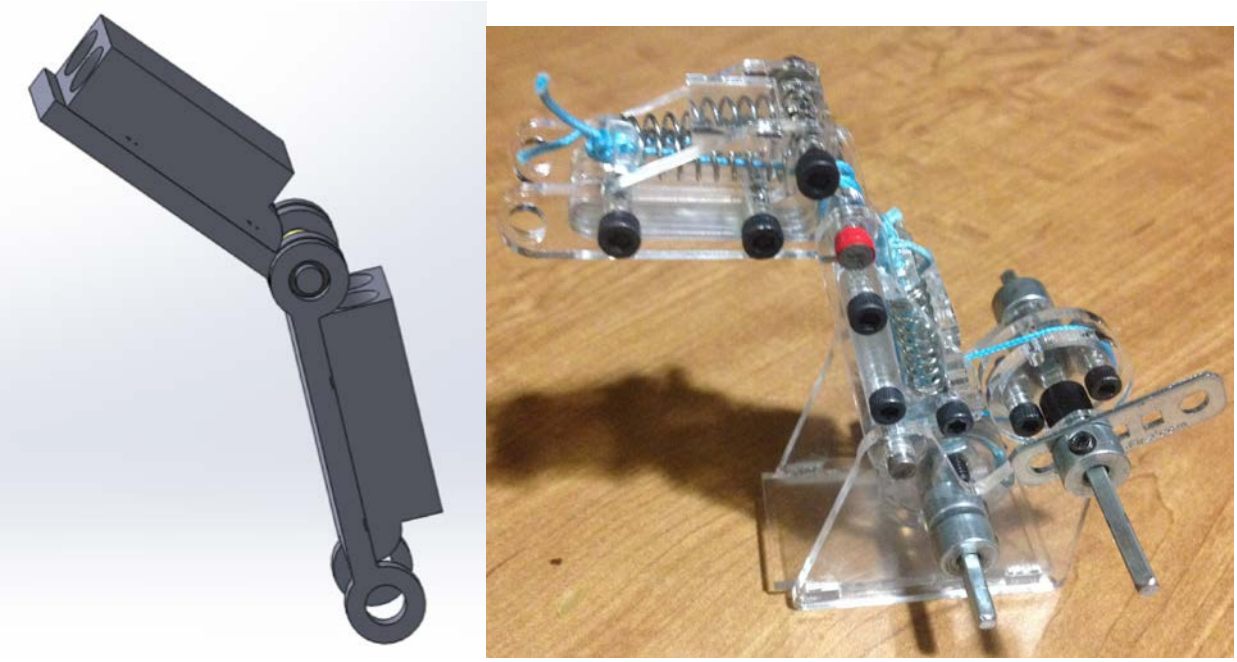

Figure 50 Third Finger design, CAD and laser cut concept

Transition to the Final Design

Instead of using only two springs like in the third Design, the final design incorporates eight springs. Having eight springs in a contained spring box makes it easy to assemble because the springs are already pre-compressed. By using two different springs, a larger range of forces can be measured by the series elastic element. Having a spring box instead of using two parallel springs means that the two different cables enter the spring assembly from different ends instead of the same end, which affects the cable routing.

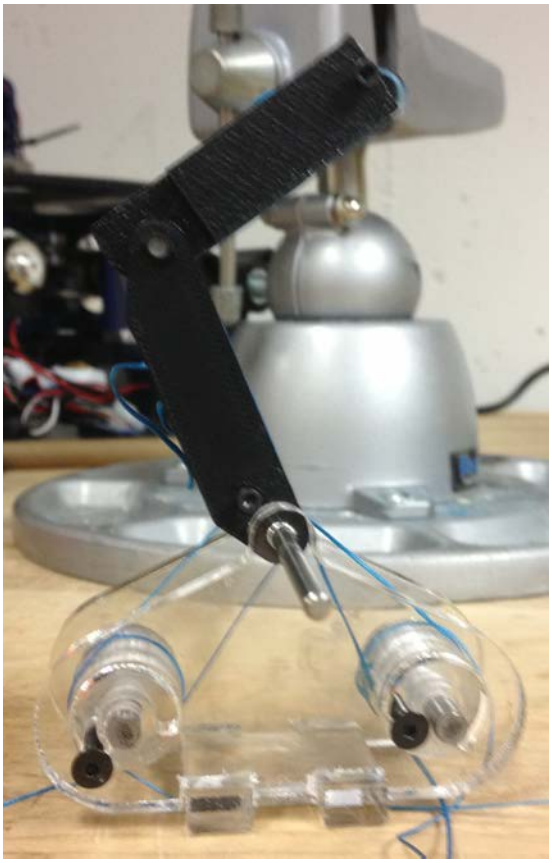

Figure 51: Concept exploration for final design

2.5 Motor Module

The motor module section supports the six motors that drive the six degrees of freedom of the arm. It is clamped into position by the final joint of the Sensitive Manipulation platform. The primary goals of this module are to intelligently position the motors so that the cables from their pulleys can be easily tensioned and routed to their corresponding joints.

2.5.1 Motor Module Requirements

To reduce the torque requirements on the shoulder, elbow, and wrist, all of the motors for the wrist and fingers were placed in the upper arm. To aesthetically match the lower arm,

all of the motors need to fit in a 3-inch diameter 4.5 inch long shell. The complete motor assembly can be seen in Figure 51. The primary goal of this module is to hold the motors, motors pulleys, and direct the cable routing towards the joints. Another requirement is that this module be easy to assemble and that the tensioning pieces in the middle of the module be assessable. To make the assembly process easier, all of the motors are designed to be removable without effecting the tension on the cable. This is especially important when tensioning the wrist cables. It must be able to interface with the Sensitive manipulation platform, as seen in Figure 50.

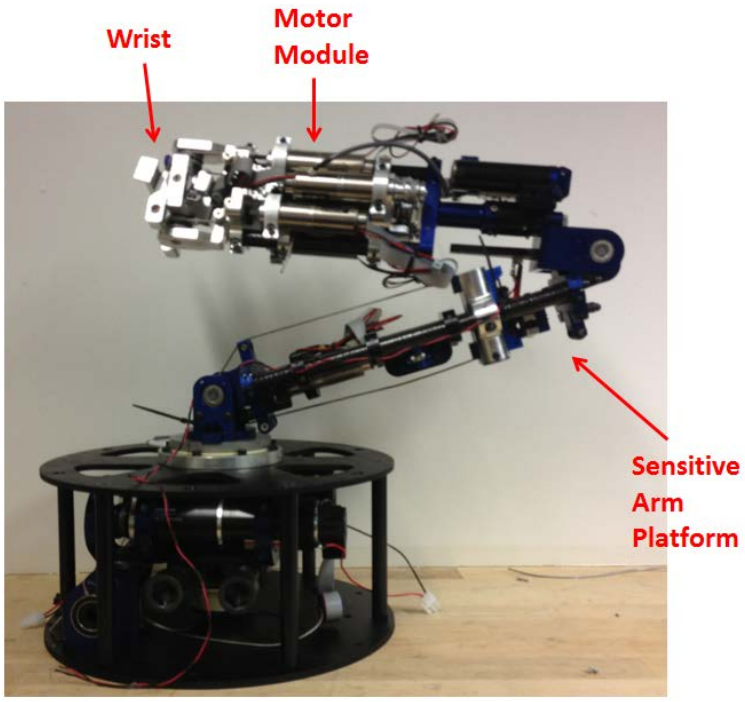

Figure 52: Wrist and Motor Module created in thesis as attached to the Sensitive Arm Platform

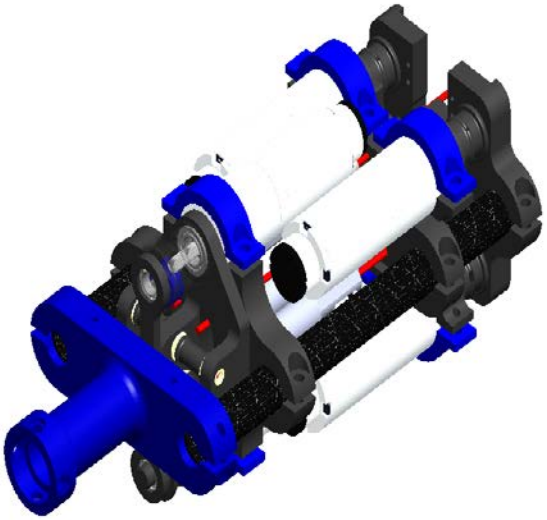

Figure 53: Complete motor module

2.5.2 Primary Components

The structural components for this module are made from two half inch diameter carbon fiber tubes and three 6062 Aluminum support pieces. The lower half of the Sensitive Manipulation platform is supported by two carbon fiber tubes with the other elements clamped on to them. To make the two links of the arm both interface correctly and look like they aesthetically were designed for each other, a similar structure was used in the new section of the arm. The far end of the carbon fiber tube is clamped into the wrist rotation joint on Sensitive Manipulation Platform and the near end is clamped onto a plate that attaches to the wrist module. The two support pieces on the wrist that support the pivots screw into this final piece.

2.5.3 Motor Attachment and Cable Routing

Each of the motors is a cylinder 0.87 inches diameter by 3 inches in length. The configuration, which allowed for the largest and most powerful motors, was in a circle as

seen in the Figure 52. Other configurations, such as mounting the motors perpendicularly in the slot between the carbon fiber tubes were also considered, but proved to be less space efficient and heavier than the circular configuration.

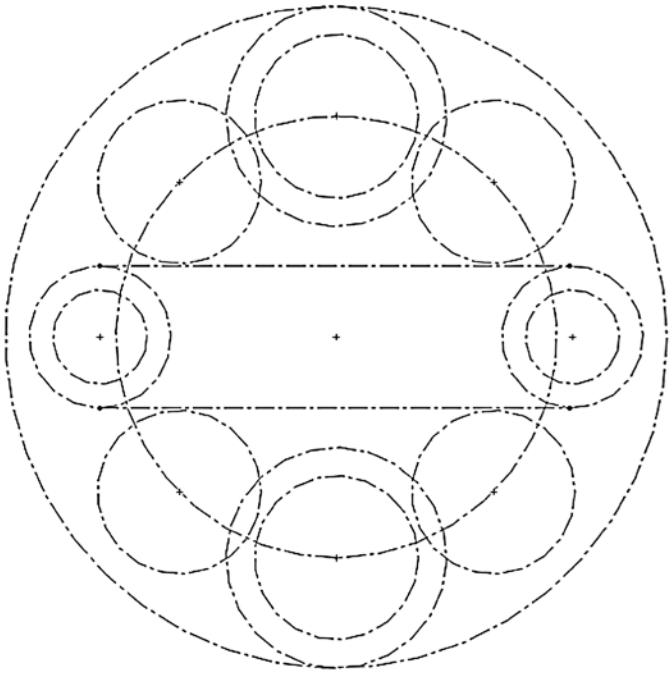

Figure 54: Circulate orientation of the motors

Igus developed a terminating method of Dyneema that works by inserting a cone into the center of the Dyneema braid, then compressing the braid between the cone and the walls of a conical hole. However, the outer Igus brass piece was too large to fit in the small pulleys of the motor. So instead a conical hole was added to all of the motor pulleys using a 5 degree 1/16 end mill, so this same technique could still be used. A cross section of the motor pulley can be seen in Figure 53. This method of combining the conical hole into the pulley was first used in the biped robot Caminante (10).

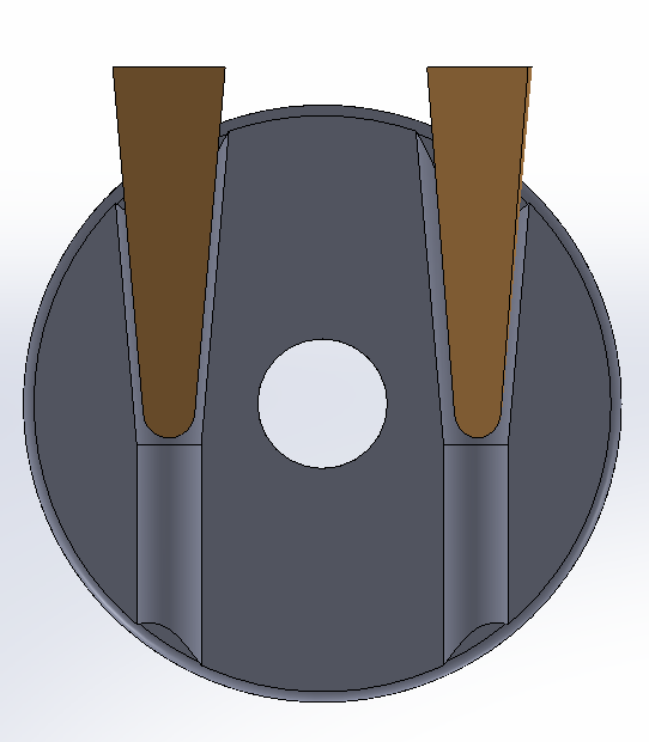

Figure 55 Cross section of motor pulley

2.5.4 Wrist motors

To make room for the motor pulleys that control the cables, the two motors for the wrist were oriented facing down the arm and the four motors for the fingers were oriented facing up the arm. This means that the cables from the wrist are sent through the center of the motor module. The metal clamp that holds the rear two motors also hold the corresponding cable rerouting pulleys. The two-motor-clamps can be seen in Figure 54 with the four rerouting pulleys. The most important consideration was that the cables exited the motor module in the correct position for them to be wrapped around the 0.75 inch diameter pulleys at the wrist.

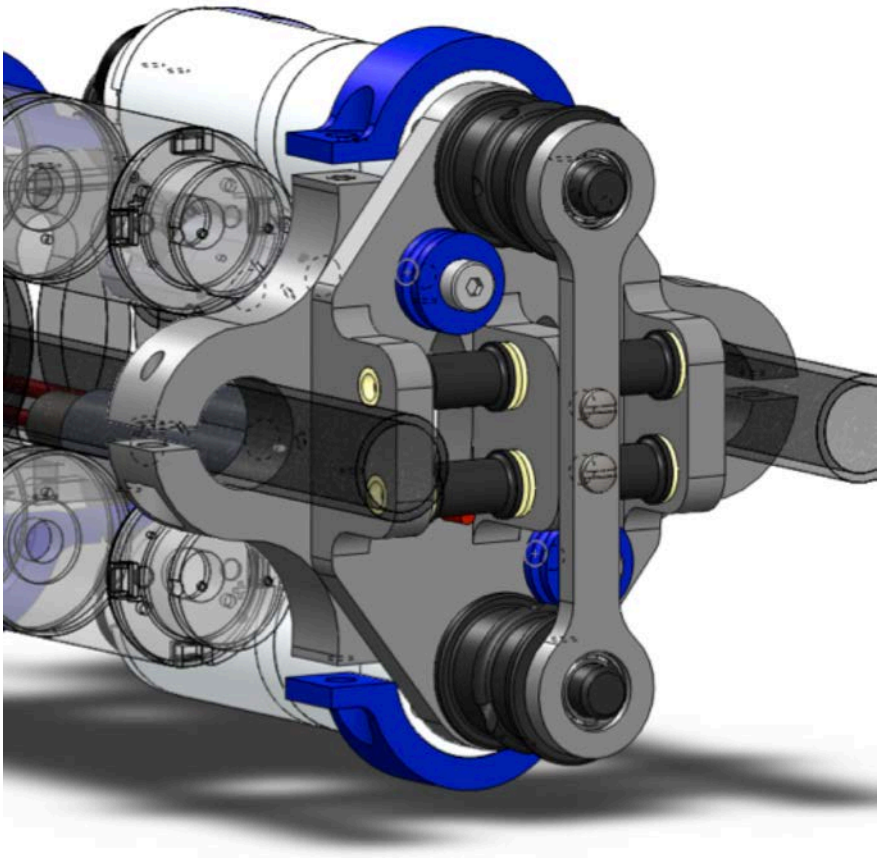

Figure 56 Two motor rear clamp

2.5.5 Finger Motors

The four motor clamps can be seen in Figure 55. Instead of having rerouting pulleys like for the Wrist, these cables are instead directed to the Bowden cable starting clamps. The piece supporting the finger motors also needed to allow the cables from the wrist motors to safety pass through to the wrist joint.

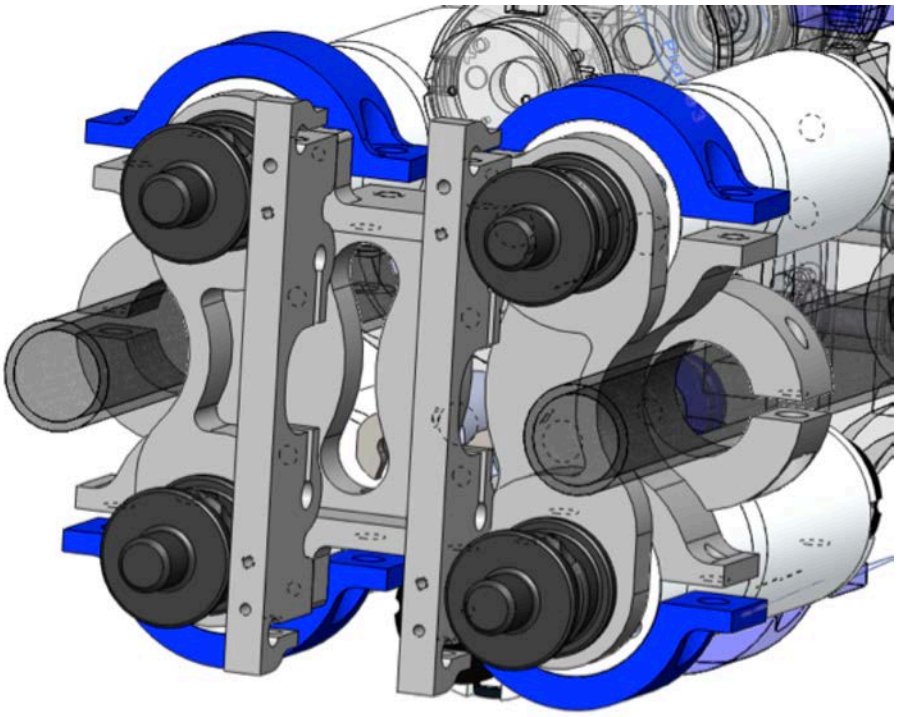

Figure 57 four motor forward clamp

2.4.6 Assembly

This entire module is largely assembled by clamping the different components together. Clamping instead of screwing the components together makes the assembly easier because it reduced the amount of required precision. The primary reason the pieces are clamped together is because the carbon fiber tubes could not have screws driven into them. Having the motors clamped as well allows them to be easily removable. Clamping the motors at the gearboxes has the added benefit of supporting them better than simply bolting into on one face. The pulleys are held into place by two bearing surfaces.

Chapter 3 Electronics

The electronics used in this project measure the position of the joints, springs, and tactile sensor deformation. This thesis's contribution to the electronics were the system architecture and linear potentiometer sensor selection. This information is then used in closed loop controllers and as feedback in the navigation and grasping algorithms. The following two sections outline the electrical architecture and the selection of the linear potentiometers to measure the spring displacement.

3.1 Electrical Architecture

A block diagram of the electrical architecture of the system can be seen in Figure 56. This architecture was designed in conjunction with an electrical engineering student in the lab. This electrical system was developed to be both space efficient and be able to quickly respond to sensor readings. Instead of having a few critical boards with more functionality, several small boards were developed instead. Having many smaller boards allows the final assembly to be more compact, instead of having large surface areas for the electrical boards. An external PC handles all of the higher level processing, navigation, and controls.

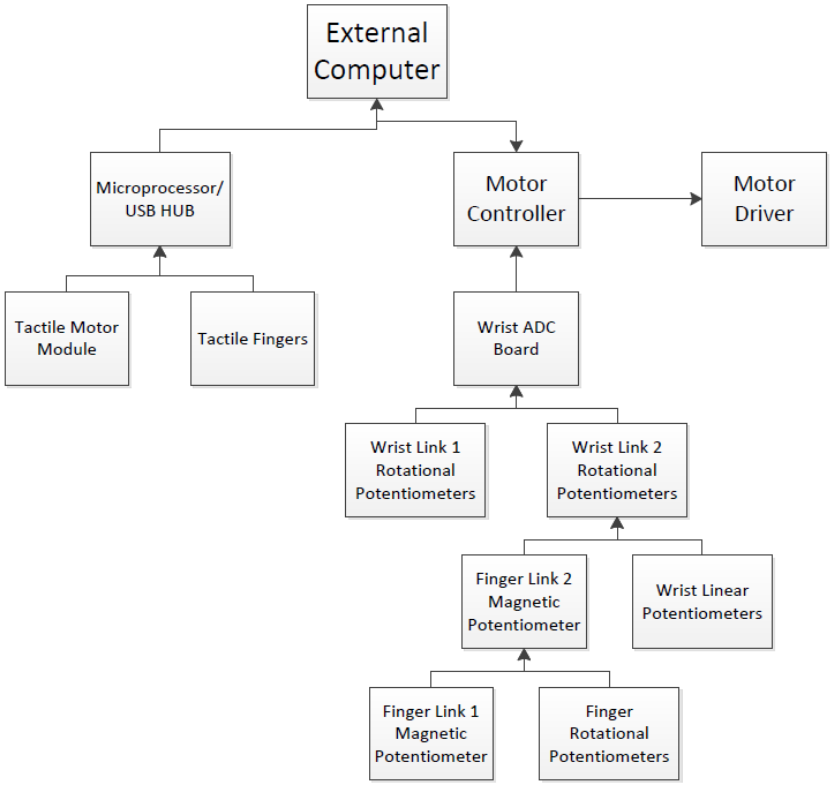

Figure 58: Electrical Diagram

The electrical engineering student Ennio Claretti also designed all of the boards themselves, including custom motor controllers and drivers. Custom motor were used because of both the space limitations and for their built in capacity to read for all from the potentiometers and motor encoders. Each of these motor controllers has a LPC2148 microcontroller capable of sending a PWM signal to the motor drivers based on either a position PD controller based on the potentiometer readings from the joint positions and/or encoders from the motors or a force based PD controller based on readings from the linear potentiometers measuring the spring deflection. Both of these PD controllers run at 1kHz. Each of the motors controllers is capable of controlling three of the six motors. These controllers send a PWM control signal to the custom motor driver. A custom motor driver

was used because of space limitations. Each motor driver is capable of running three 24V brushed DC motors.

All of the sensor information from the tactile sensors is sent directly to the PC computer over USB. USB was selected because of its ability to reduce the number of cables to the PC and because of its high transmission rate. A high transmission rate is important for quickly transmitting tactile information from the fingers and shell each of which sampled at 100 Hz.

3.2 Linear Potentiometer Sensor selection

The small size of the springs used in both the fingers and wrist and the small size of the components themselves made finding small sensors with high resolutions a requirement for the success of the platform. Not having reliable sensors or a high resolution would significantly limit the capabilities of the system and would affect the accuracy of the controllers. Inexact readings would produce imprecise results.

A variety of different sensors were tested for their sensitivity to small motions. The springs on the wrist compress 3mm under maximum load. All of the sensors discussed below had their resolution tested over a range of 2mms.

Table 7 Sensors Tested

Sensor Type	counts	noise
Linear potentiometer	30	8
IR photo transistor	50	10
photo transistor	20	6
QRE1113 line sensor	32	3
NSE5310 and AS5311 Magnetic Linear Sensor	NA	NA

The first sensor tested was an IR photo transistor with an IR LED. It produced a 50 count range over the 2 mm of travel at close range with a noise level of 10 counts on a 10

bit ADC. Two different photo resistors were tested with a red LED light. Both of them produced a 20 count range over the 2mm traveled at close range with a noise level of 6 counts on a 10 bit ADC. The QRE1113 analog board produced a 32 count range over the 2 mm travel at close range with a noise level of 3 counts on a 10 bit ADC. All of these values were gathered over multiple tests with a cover to reduce the ambient noise and on a laser cut test rig to ensure measureable linear motion.

Two different linear magnetic Hall Effect sensors were also tested, the NSE5310 and AS5311 from ams.com. The output duty cycle of the sensor related to the positioning of the magnet. With the magnets available in lab and without a linear guide system to guarantee linear motion, about 1500 counts were measured for the 2mm traveled (total 12 bits over 6 mm). Based on the data sheet, these chips will produce 2 um of resolution with a small magnet and PCB. The hall effect sensor with the smaller package size (AS5510) was chosen for measuring the displacement on all of the springs seen in Figure 58.

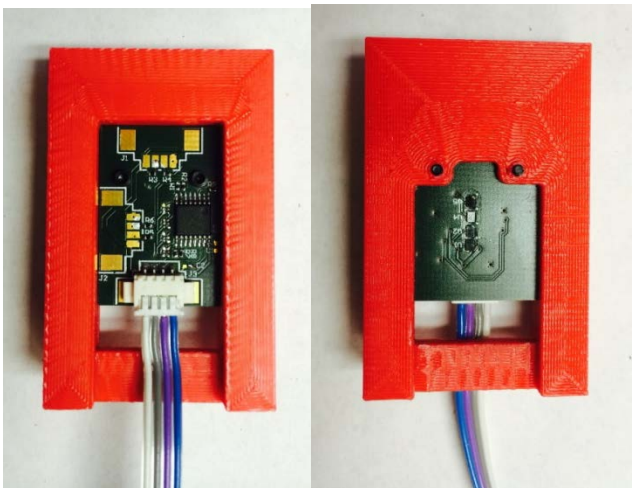

Figure 59 Magnetic Sensor Board Ready to be calibrated on the Manual Mill

The final magnetic boards where calibrated using on a manual Mill. Because of the rang of motion of the spring in the fingers four sensors in a line are used to detect the

position of the magnet. At any point along its path the magnet is in the linear range of at least one magnetic sensor. The linearized graph of the sensor readings over a 12 mm displacement can be seen in Figure 57.

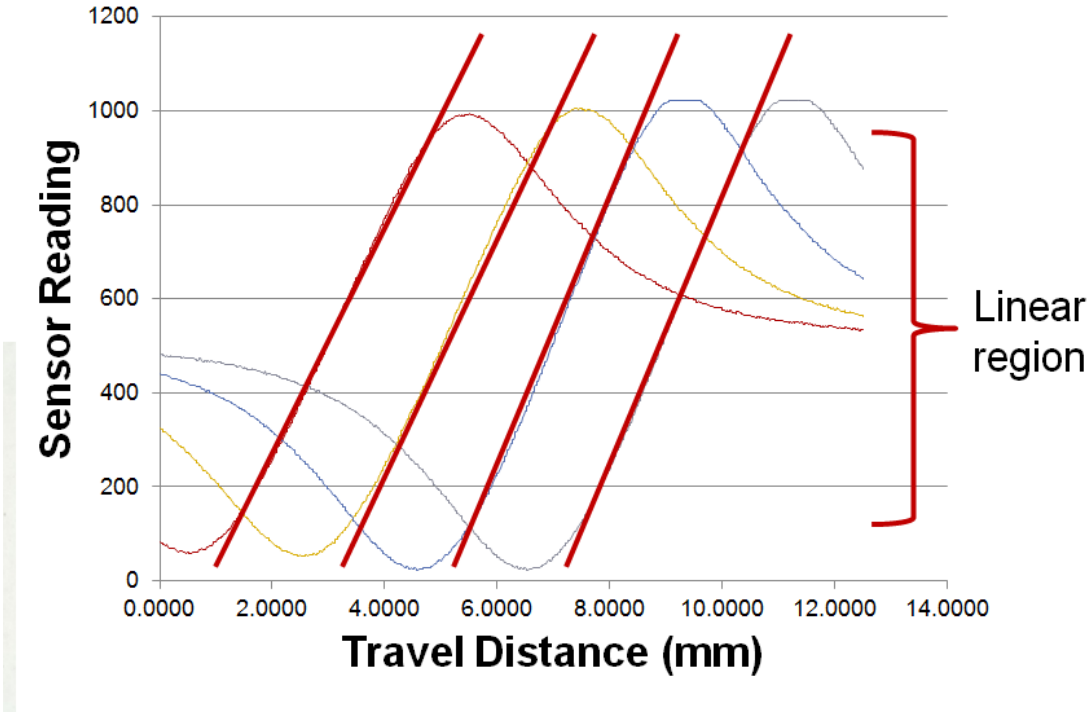

Figure 60 Linear Sensor Calibration Data

Chapter 4 Tactile Sensor Integration

One of the most important requirements for the system to have is adequate sensor coverage. The research that this platform is being developed for is based on tactile feedback and sensitivity. The eventual goal of this research is to eventually have sensitivity equivalent or better than that of humans. Fingers have the finest resolution on the body, with less than 5 mm of resolution, because they are used for tasks that require dexterity and fine manipulation. Large extremities like the thigh, back, legs, or arm have a much lower resolution of around 40mm. These resolutions were determined by pricking the skin with two needles and determining what the minimum distance apart they need to be for the brain to distinguish them as being two separate points. Adequate sensor coverage is defined for this project as having coverage that maximizes the surface area with sensor coverage without interfering with any of the joints range of motion and having a tactile sensor resolution that is either comparable to a human's or as dense as the current sensor technology allows. The contributions of this thesis are mold creation and placement of the tactile sensors.

4.1 Fingers

To satisfy the requirement of being adequately covered, the fingers will have deformable tactile sensors as described in section 1.3.2 on five of the sides: front, back, both sides, and the top. Unfortunately, the size of the surface mount components prevents the inside of the dome from being less than 6mm in diameter. The molds for the rubber dome are also 3D printed on a printer that requires the distance between each dome to be 1 mm. Based on these restrictions and the available surface area, the highest density of

domes possible on the front and back of the fingers is a grid of three by four domes. The sides can have a strip of four domes each. The top of the fingers are triangles with 45 degree slopes, each of these slopes has a row of the domes. The fingers with maximum coverage of domes can be seen in Figure 58.

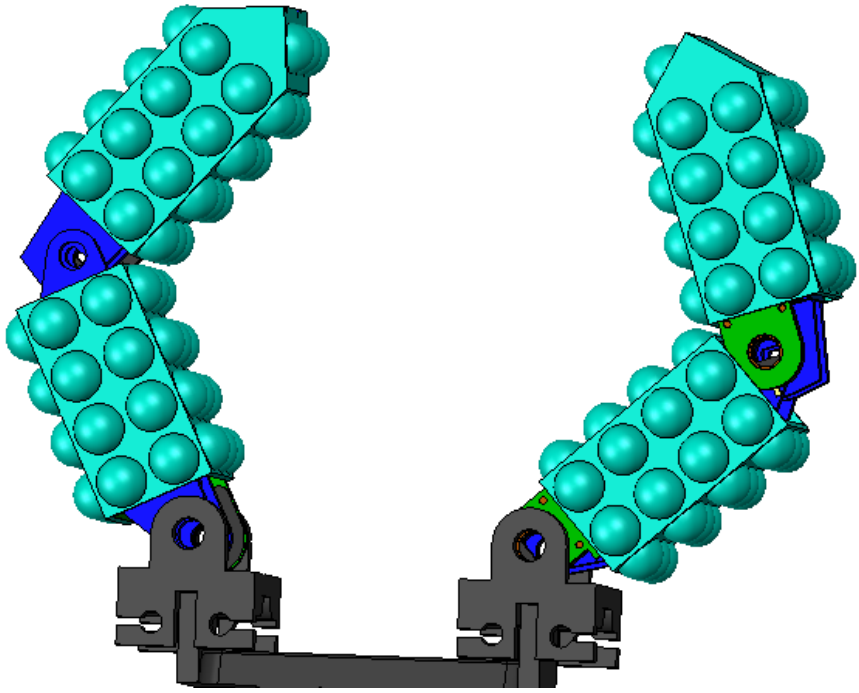

Figure 61 Fingers cover in tactile sensors

This scope of this project does not include the production of the actual sensors themselves, but does include the molds for the rubber domes as they relate to the mechanical design of the manipulator. The domes on the fingers are located on all of the large sides of the fingers. This makes the mold complex to both design and assemble. The after the rubber has been poured the inside the mold, support for the domes needs to be ~~slide~~ located perpendicular to outside wall of the mold. This means that each side of the final rubber piece needs to have its own mold, which can be connected together around a central core, which provides the required support.

The mold for the lower link is composed of five different pieces. To assemble them, a combination of dipping the center pieces, and pouring into the outer pieces was used. This process is extremely messy and difficult to assemble, however only two of each type of mold is needed, one for each of the fingers. If these were going to be made in larger quantities, an injection molding system would be used to fill a sealed mold, reducing waste material. Using injection molding would reduce the number of necessary pieces in each mold. The material used is too viscous to be injected by hand, so the manual assembly process is the only one available for the limited production quantities required by this project.

4.2 Motor Module

In addition to tactile sensors on the fingers, the motor module and parts of the wrist module will be covered in a tactile sensing shell. This shell will be helpful for impact detection, during recovery from unintentional collisions and during contact navigation. The shell is composed of five separate pieces; two on the lower half of the arm covering the wrist rotation, one on top of the elbow joint, and two on the top half of the arm covering the motor module and part of the wrist. This can be seen in Figure 59. The shell covers as much of the wrist as it can without interfering with its range of motion.

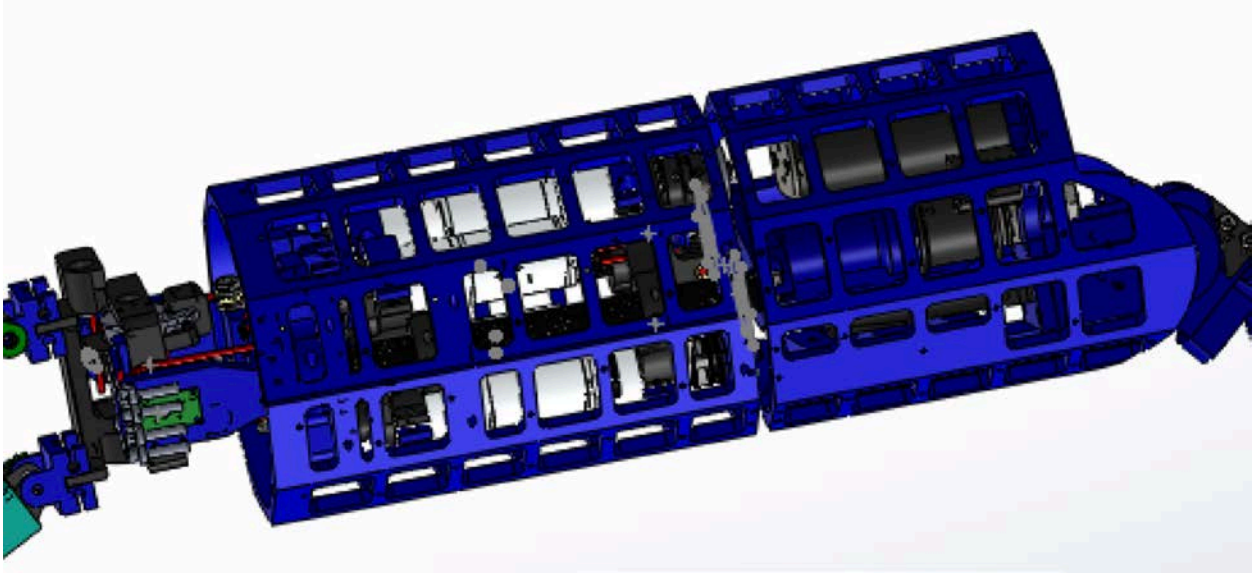

Figure 62: Motor Module and Wrist rotation Shells

This shell is made of a 3D printed plastic, decagon netting that supports the tactile sensing boards, which are covered in the rubber domes. The lower decagon shell is 141.6 mm long, with an outer diameter of 100 mm, and a side width of 30.5mm. The upper decagon shell is 172 mm long with the same diameter and width. The distance between each tactile sensing dome is based on the sensitivity of a human arm. As discussed in the Chapter introduction different parts of the human body have different levels of sensitivity. Each sensor has a diameter of 17mm spaced 19 mm apart, which is a higher density of sensors than the approximately 40 mm of resolution in a human arm. The molds for the rubber component that goes with these shells are in Figure 60. These molds are significantly simpler than the ones for the finger because the domes are only in one dimension.

Figure 63 Motor Module shell Molds

The upper shells are designed to clamp onto the carbon fiber tubes that form the basis of the motor module structure. It is significantly easier to assemble the tactile shell as two separate pieces that screw into each other and clamp onto the carbon fiber tubes than as a single ring that slides over the other modules. The motor clamp pieces also stick out slightly and fit through a gap in the netting, making sliding impossible. The lower shell does not have the convenient carbon fiber tube to clamp onto. Instead, this pair of shells screws into mounting holes on the metal components themselves. The shells covered in tactile sensors can be seen in Figure 61.

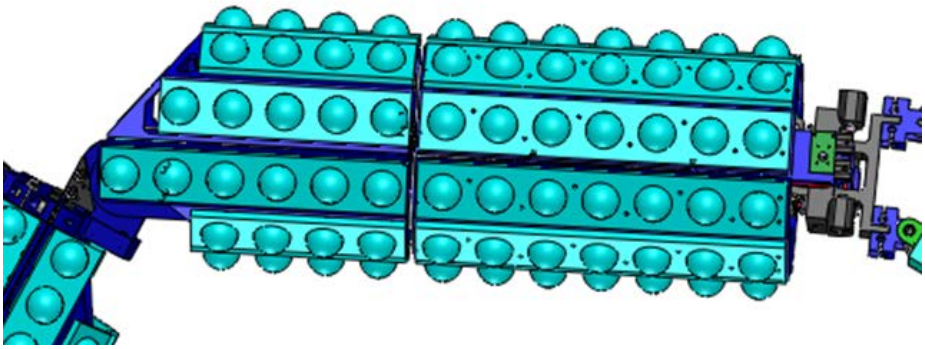

Figure 64 Motor Module/ Upper Arm covered in Tactile Sensors

Chapter 5 Sensitive Manipulation

The primary applications for the completed platform will be research in contact navigation and manipulation in dynamic environments. It will be used to investigate new methods and algorithms that utilize exploration and sensitivity to perform tasks in a dynamic environment. This section addresses the potential implementations of software for this platform. The types of implementation discussed below will use the sensors to control an event driven manipulation. The following section describes a proposed process for using the additional sensors for navigation and manipulation. This thesis only coved the development of position control and force control.

Traditional manipulation relies on having an accurate model of the environment and mostly pre-computed navigation and grasping strategies. This strategy depends on having a static environment, as any changes in the environment void the pre-computed to strategy. These changes add computation time and uncertainty. Changes in the environment can occur when collisions either move objects or lead to unpredictable torque dynamics. Sensitive manipulation on the other hand has real time reactions. It replaces the complex models with reaction based sensor feedback and simple equations. Also it embraces contract because instead of adding uncertainty to the system, contacts can provide significant amounts of information about the operating environment. Contact can give sensitive platforms information about the location, size, friction coefficient, and weight of anything they come in contact with. Based on the location of the contact along the arm, the skew forces can also be calculated to improve the dynamic model instead of adding uncertainty. A sensitive platform can also use the tactile information it gathers to regulate the external forces it creates during contact.

A generalized procedure for navigating with tactile feedback is shown in Figure 62. This procedure was developed based on the research conducted on contact Navigation at Georgia Tech. Since this arm will be operating without an exact model of its environment, its first action will be to move in the direction it believes the goal is in. This direction can be determined by using either vision or some previously known information about its environment. If a contract force is encountered on the outside of the fingers or wrist, the arm then adjusts its trajectory so that it can use the contact to navigate around the obstacle. Different contact profiles give indications of the orientation of the object, which is then used to choose the most appropriate response based on this contact during the rest of the navigation.

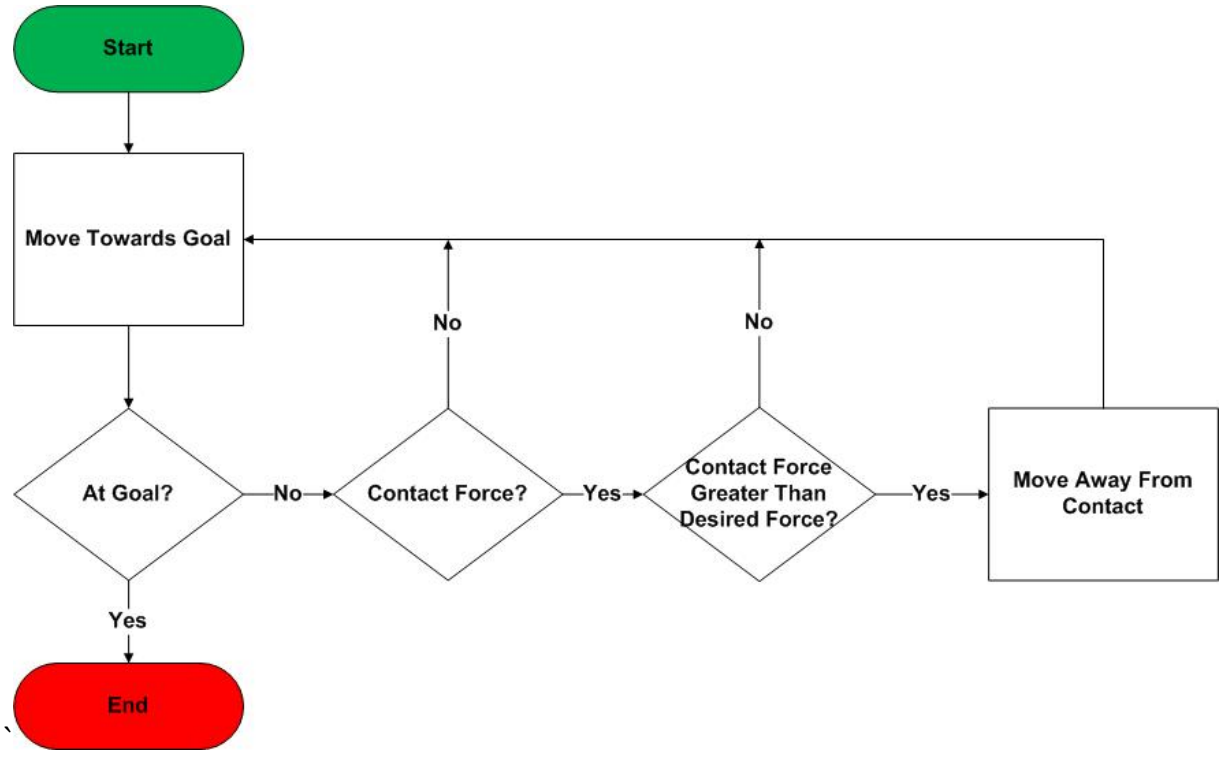

Figure 65: Flow chart for navigation Decisions

Once the arm has maneuvered the gripper close to its goal, the tactile sensors on the fingers are used to explore the area in search of the object to be grasped. This procedure was inspired by the algorithm used for grasping on the robot Obrero. Once the object has been located, the fingers are then used to examine the object to find an acceptable grasping location. A generalized procedure for this route is outlines in Figure 63.

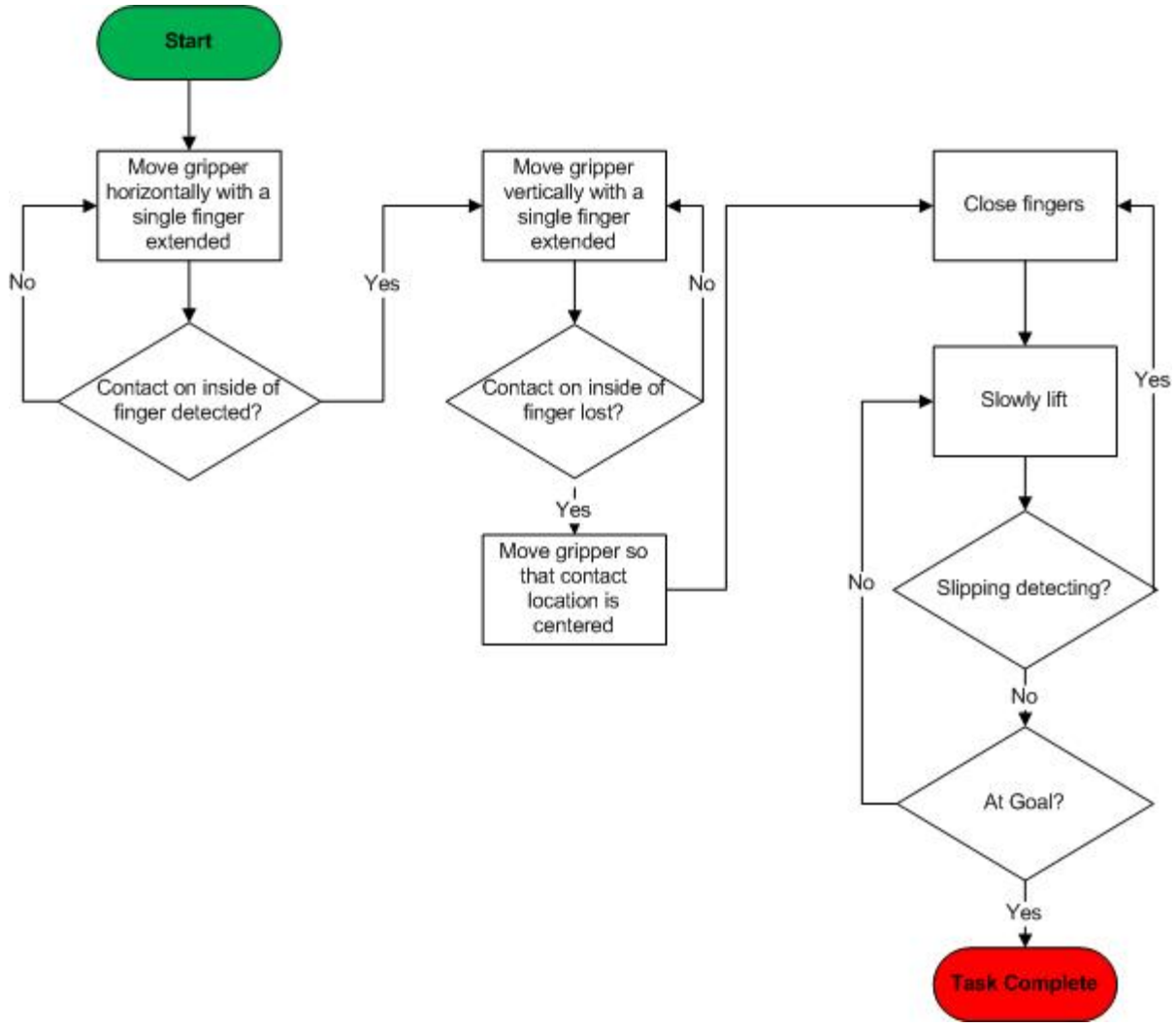

Figure 66: Flowchart for Grasping Decisions

At the lower level, a hybrid of closed looped controls are used to regulate the motor output. The hybrid is created by a weighted summation of the two controllers throughout the workflow. These controllers are weighted differently depending on the phase the arm is

in and how the arm needs to respond to the different types of sensor feedback. These controllers include position control, velocity control, torque control, contact force control, impedance position control, impedance velocity control, and impedance force control.

5.1 Position Control

Position control is the most basic controller mode. This controller computes the PWM output for the motors using a basic PID (Position Integral Derivative) controller based purely on the difference between the desired joint position and the current measurement of the joint position. These measurements are gathered from both the potentiometers at the joints and the encoders on the motor. The controller also limits the maximum output velocity. This is the only type of controller that will be implemented as part of this thesis.

5.2 Velocity Control

Velocity control is very similar to position control. It also computes the PWM signal for the motor based on inputs to a basic PID controller. However, the difference is that instead of the difference in desired position and measured position, the desired velocity and measured velocity are taking into consideration instead. This type of controller can also be implemented based on a desired acceleration.

5.3 Torque Control

Torque control directly controls the robot joint torques. This controller uses the measured displacement from the series elastic springs to determine this joint torque. Like

the position control and the velocity control, the torque control also uses a basic tuned PID controller. This controller also imposes a maximum acceleration.

5.4 Contact Force Control

The contact force controller uses the input from the tactile feedback for the control loop. This controller is more intelligent than the others because it needs to understand the location of the contact force vector and treat the contract point as a joint in a closed kinematic loop, connecting the arm and obstacle. The contact force between the arm and obstacle is regulated by slightly shifting position of the arm perpendicularly in relation to the obstacle.

5.5 Impedance Position Control

Impedance controllers work by treating the manipulator as if it has impedance and the environment as if it has admittance, which is equivalent to have having a virtual spring and dampening system that affects the output of the controller. Using this type of controller, the equilibrium position and stiffness/damping of a virtual spring can be controlled.

$$\tau_d = -k_{stiffness}(q - q_d) - k_{damping}\dot{q} + \tau_{offset}$$

$$PWM = PID(\tau - \tau_d) + PWM_{offset}$$

The reference torque is tracked by a PID algorithm and is computed based on desired position and the set stiffness/dampening parameters (Hooke's law). These stiffness and dampening parameters can be tuned to make the robot react like a spring while still controlling the desired joint position. This controller also considers the arm trajectory

vectors. This platform already has springs built into the joints so this type of controller is only used when a different amount of stiffness is desired. The force control with the series elastic elements creates a very similar behavior to this controller.

5.6 Impedance Velocity Control

The impedance velocity control is equivalent to the impedance position control but instead of using the desired position to determine the output, the integrated velocity is used. This controller also takes into consideration the trajectory of the arm's acceleration. Integrating the measurements from the series elastic actuator position can be used to generate a similar output as this type of controller. This does not mean that this control would never be used in this type of application. There may be scenarios where using it in conjunction with one of the other types of controllers could be beneficial for accomplishing a specific task.

Chapter 6 System Validation

Throughout both the design and testing process, different components and assemblies were constantly being tested to confirm they were capable of meeting their corresponding design requirements. This was both an iterative process that was used to confirm that the selected components were capable of meeting the requirements and as a final confirmation that the final assembly met the design requirements.

6.1 Design for Sensitive Manipulation

This platform was designed for sensitive manipulation research-manipulation and path planning with the help of tactile feedback in unstructured environments. The sensors and joints were all designed with specific properties to ensure that the arm will behave and react in a way best suited for this type of research. The upper arm is covered in 116 tactile sensors and the fingers are covered in 70 tactile sensors designed to precisely sense the platforms contacts with its environment. Also, all of the joints were designed with built in compliance.

6.2 Mimic Human Ranges and Size

The arm and fingers were designed to be approximately the size of a small human arm with fingers comparable to human fingers. Figure 67 shows the fully assembled platform side by side with a human hand for scale.

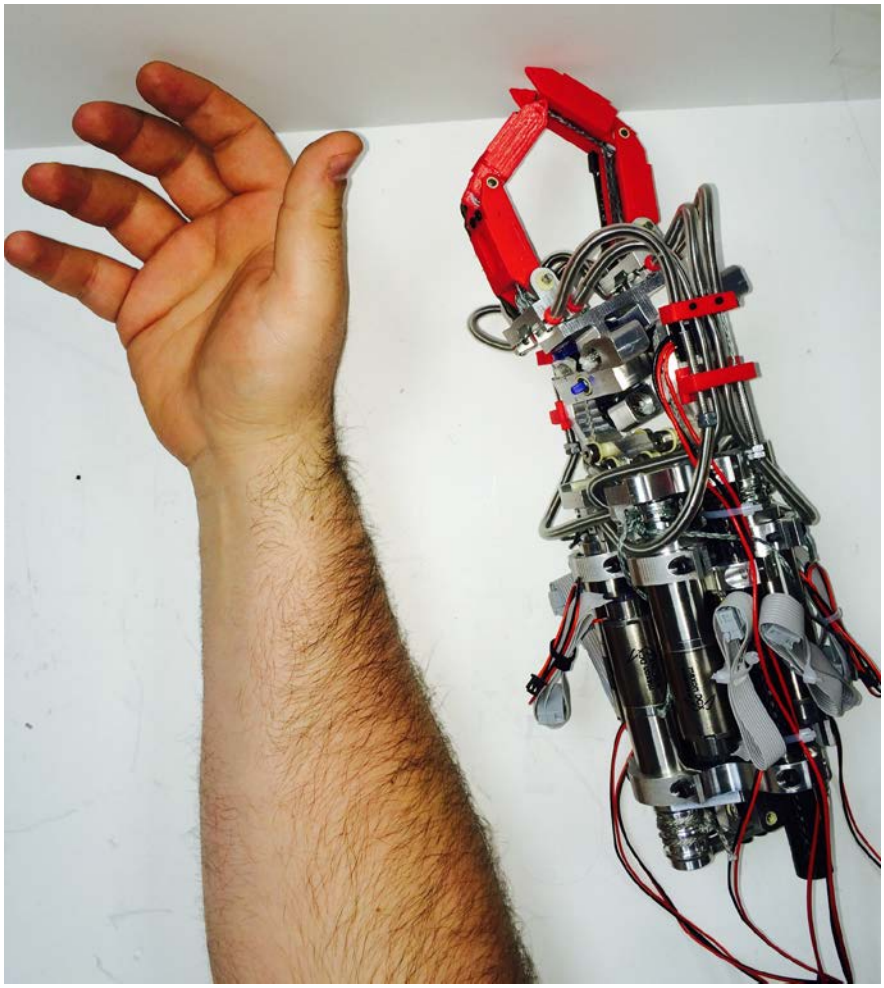

Figure 67 Size comparison to a human

This was achieved by having the motor Module fit in a 5-inch long space, making the completed upper link of the arm 0.3 m in length. The joint deflection was also designed to replicate that of a human. Table 6 shows the range of motion of each joint and the corresponding human joint.

Table 8 Joint Range of Motion

Joint	Robotic Arm	Human Arm
First Wrist Pitch	140 to -140	0 to 270
Second Wrist Yaw	75 to -75	0 to 100
First Finger Link	140 to -40	0 to 140
Second Finger Link	105 to -105	0 to 180

6.3 Tactile Sensor Coverage

The goal of this project is to create a platform for sensitive manipulation research. For this platform to perform optimally as a research platform, it is important that it be adequately covered with tactile sensors. The upper arm is encompassed by two prototype decagon shells, the lower shell has 46 tactile sensors evenly distributed across it. The upper shell has 70 tactile sensors. The density of the tactile sensors is 24mm apart, which is denser than the 40mm sensory resolution of a human's arm. The process for determining this resolution was discussed in section 1.3.2 Tactile Sensing in Humans .

The resolution on human finger is 5 mm. Currently, the smallest size tactile module that can be made is 6.5 mm. Because of this, adequate sensor coverage for the fingers is simply the highest density of sensors possible on the outside surface, given the technological restrictions. The inside of the fingers have 24 tactile sensors. The sides have eight sensors each. The back of the fingers have 24 tactile sensors, and the tip has six tactile sensors. Since the highest density possible of covering the maximum amount of surface area as possible without restricting the motion of the fingers was achieved, this requirement is satisfied.

6.4 Manipulate 1 kg Payload

One of the requirements for the system is that is capable of handling a one kilogram payload. This was tested by strapping a 1kg payload to the fingers and seeing if the wrist was capable of its full range of motion. To test the strength of the fingers weights were attached to the finger joints and they were powered through their maximum torque range of motion.

6.5 Degrees of Freedom

This system was designed to have a range of motion similar to the motion of a human in terms of degrees of freedom in the arm. The manipulator on the other hand was only required to consist of two fingers with two links each. All of these degrees of freedom allow the system to have high maneuverability and be capable of manipulating most objects in a dynamic environment.

6.7 Integration of Series Elastic Actuators

The robot successfully has series elastic actuators integrated into every joint. Instead of using the traditional impedance controllers, this system can directly measure the torque at each joint instead of interpolating the current from the motor. The compliance in the system has also been extensively tested. A large external force on each of the joints visually compresses the corresponding spring without effecting the position of the motor, demonstrating that the series elastic element is correctly integrated. The displacement of the springs could also be measured using the linear magnetic potentiometers mounted above them. The springs in the wrist where chosen based on the dynamic forces they will experience, while the finger springs were selected for their sensitivity.

6.8 Confirmation of Finger Material Strength

The base structure of the fingers was made from 3D printed material. 3D printed material is more fragile than many of the other material choices for this project. The fingers built off the work done for Go-bot, which also used 3D printed material. However, Go-bot was built to manipulate small, lightweight Go pieces. This platform is designed to maneuver

1kg objects and will experience larger strain and stresses. To test the strength of the 3D printed fingers, successively larger weights were suspended off the finger module until it broke. The largest weight that the finger held successfully was 14 kg. 14 kg is significantly larger than the dynamic load that a 1kg payload could produce at the speeds the arm will be moving, so the 3D printed material is sufficient for this application.

6.7 Overall System Performance

The whole system has been tested as individual modules. Each joint has been powered multiple times and run through its full range of motion and bottomed out the springs without any permanent harm or slack being added to the system. The wrist module and finger modules were also tested individually by running both motors at the same time and correcting for the dependence of the second joint in the module on the first joint. As a whole, the robot has been successfully designed to be robust, reliable, and capable of both sensing light contact and surviving unanticipated collisions without breaking key structural members.

Chapter 7 Conclusion and Future Work

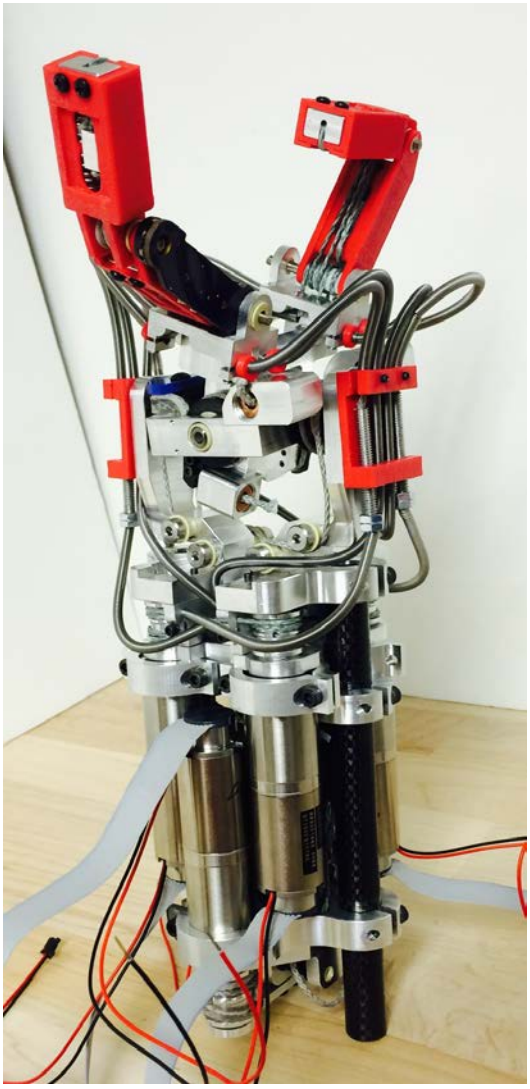

Figure 68: Fully assembled Wrist and Fingers

The goal of this thesis was to design a state of the art platform, shown in Figure 64, specifically developed for sensitive manipulation. This platform contained a two-degree of freedom wrist, and two two-degree of freedom fingers, all of which utilized series elastic actuators in order to intelligently respond to both intentional and unintentional contact. The series elastics add an important level of compliance that is necessary both when

working in a human environment alongside humans and for contact based navigation and grasping. This platform also utilizes 116 large tactile sensors around the motor module and 70 small sensors on the fingers. These tactile sensors are capable of detecting both shear and normal forces, which is important detecting the difference between sliding contact and direct pressure. This differentiation is key for both contact navigation and sensitive grasping.

In the process of this design, the system was modeled to aid in the selection of motors, springs, materials, and other important design decisions. An extensive material selection process was undertaken for several of the critical mechanical components, such as the Bowden tubes and the cables, which included extensive research and testing on samples before a final component set was selected. A similar process was undertaken for the electronic components of the system, including the sensors. My major specific contributions of this thesis are as follows: a completed 2-degree of freedom wrist/hand and finger system with a tension able cabling system and series elastic elements for articulation with integrated sensors for position and joint force feedback made with inexpensive parts and materials and with ease of assembly in mind.

While this system has been fully developed and each individual link tested, there are still several tasks remaining to prepare this platform for its role as a research tool. The tactile sensors designed as part of this project need to be fabricated and integrated into the platform. A more complete flexible tactile shell that covers the wrist without restricting its motion also should be developed so that contact at any location on the assembly can be detected. The sensors designed into the initial sensitive arm project still need to be manufactured and integrated into that system as well. Manipulation algorithms need to be

developed to demonstrate the full capabilities of the manipulator and allow it to begin its function as a research platform. The tasks that are left to reach this point are:

- Develop a tactile sensor mounting shell with more coverage for the motor modules
- Design tactile sensor boards for the shell and fingers
- Full integrate all electronics, including the motors controller boards and sensor mapping boards.
- Investigate a simpler method to tension the cables for the fingers. A tensioner that can extend the path or decrease the size of the cable to a greater degree than the current system would better maintain the tension in the cable.
- Implement and evaluate manipulation algorithms utilizing the feedback available from the tactile sensors and series elastic elements.

At the conclusion of this thesis, the groundwork for further sensitive manipulation research using a platform specifically designed for this purpose will be in place. This groundwork encompasses a completed six-degree of freedom arm with a two finger gripper. Work is still needed, but once the platform is completed and the tactile sensors are integrated, this robot will serve as an important platform for furthering the field of sensitive robotics research.

References

1. *World Robotics-Industrial Robotics.* 2013.
2. *Series elastic actuators for high fidelity force contorl.* **J. Pratt, B. Krupp, and C. Morse.** 3, s.l. : Inductrial Robot: An International Journal, 2002, Vol. 29.
3. **Julian Keil, Nadia Muller, Niklas Ihssen, Nathen Weisz.** *On the Variability of the McGurk Effect: Sudiovisual Integration Depends on Prestimulus Brain States.* Konstanz : Oxford Journals, 2012.
4. **E Kemp, CC, Edsign,A Torres-Jara.** *Challenges for robot manipulation in human environments.* s.l. : Robotics & Automation Magazine, 2007.
5. *Contact sensing and grasping performance of compliant hands.* **A. M. Dollar, L. P. Jentoft, J. H. Gao, and R. D. Howe.** 1, s.l. : Autonomous Robots,, 2009, Vol. 28.
6. *Human-inspired robotic grasp control with tactile sensing.* **J. M. Romano, K. Hisiao, G. Niemeyer, S. Chitta, and K. J. Kuchenbecker.** 6, s.l. : IEEE Trasactions on Robotics, Vol. 27.
7. **Gomez, E. Torres-jara and G.** *Fine Sensative manipulation.* s.l. : Autralasian Conferance on Robotics and Automation, 2008.
8. **Torres-Jara, E.** *Sensitive Manipulation.* 2007.
9. *A Sensative Approach to grasping.* **Torres-Jara, L. Natale and E.** s.l. : Proceedings of the sixth international workshop epigenetic robotics, 2006.
10. **Chernyah, V.** *The Design and Realization of a Sensative Walking Platform.* s.l. : Worcester Polytechnic Institue , 2012.
11. **Cochran, Nigel.** *The Development of a Sensative Manipulation Pltform.* s.l. : Worcester Polytechnic Institue , 2013.
12. **Kawamura, Dr. Kazuhiko.** *Expert Village.* [Online] November 2008. http://www.engineering.com/Videos/VideoPlayer/tabid/4627/VideoId/2130/Who-Invented-The-Robotic-Hand.aspx.
13. **Monkman, G. J., et al., et al.** Robot Grippers. s.l. : Wiley-VCH, 2007.
14. **RobotWorx.** The History of Robotics in Research. *RobotWorx Experts in Automation.* [Online] http://www.robots.com/education/research-history.
15. **Mellon, Carnegie.** Unimate. *Robot Hall of Fame.* [Online] 2003. http://www.robothalloffame.org/inductees/03inductees/unimate.html.
16. **Ernest, Heinrich.** *MH-1, A computer-Operated mechanical Hand.* Cambridge : Massachusetts Institute of Technology, 1961.
17. **Museum, Computer History.** History of Robots & Artificial Intelligence. *Computer History.* [Online] Computer History Museum, 2006. http://www.computerhistory.org/timeline/?category=rai.
18. *A survey of tactile human-robot interactions.* **Argall, Brenna.** 10, s.l. : S, 2010, Vol. 56. 0921-8890.
19. **A. Jain, M. Killpack, A. Edsinger, and C. Kemp.** *Manipulation in Clutter with Whole Arm Tactile Sensing.* s.l. : The International Journal of Robotics Research, 2013. 10.1177/0278364912471865.
20. **Antonis Morales, Mario Prats and Javier Felip.** *Grasping in Robotics.* Cassino : University of Cassino, 2013. 2211-0984.

21. **Paulos, Eric.** *Trends in Grasping.* Berkeley : University of California.
22. **Ackerman, Evan.** IROS 2013: JPL's Microspine Rock-Climbing Robot. *IEEE Spectrum.* [Online] November 2013. http://spectrum.ieee.org/automaton/robotics/military-robots/iros-2013-jpls-microspine-rockclimbing-robot?utm_source=feedburner-automaton&utm_medium=feed&utm_campaign=Feed%3A+ieeespectrum%2Fautomaton+%28Automaton+-+IEEE+Spectrum%29.
23. **Roach, John.** *Three-fingered iRobot hand points to strong, nimble future machines.* s.l. : NBC News, 2013.
24. **Williamson, M.** *Series elastic actuators.* 1995.
25. **Banks, E. Torres-Jara and J.** *A simple and scalable force actuator.* 2005.
26. **LaMote, R. S. Johansson and R. H.** *Tactile detection thresholds for a single asperity on .* s.l. : Somatosensory Research, 1983.
27. **Johansson, G Westling and R.S.** *Responses in glabrous skin mechanoreceptors during precision grip in humans.* Umea, Sweden : University of Umea, 1987.
28. **Crowder, R. M.** Tactile Sensing . *Automation and Robotics.* [Online] 1998. www.southampton.ac.uk/~rmc1/robotics/artactile.htm.
29. Sensory Systems: Interactive Summaries. *Life, The Science of Biology.* [Online] Life. http://bcs.whfreeman.com/thelifewire8e/content/cat_010/45010-01.htm?v=chapter&i=45010.01&s=45000&n=00010&o=.
30. **Fred, David J.** *Tying illustration for Ashley's stopper knot.* Wikipedia, s.l. : 2006.
31. 2-Finger Adaptive Robot Gripper- 85. *Robotiq.* [Online] Robotiq, 2013. http://robotiq.com/en/products/industrial-robot-gripper/.

Appendix A: Arduino Test code

Position Control one finger

```
#include <Wire.h>

int motorSpeed1 = 9;
int motorSpeed2 = 10;
int motorDirection1 = 11;
int motorDirection2 = 12;
int potPin1 = A1;
int potPin2 = A2;
int joint1start;
int joint2start;
int pot1start;
int pot2start;
int intjoint1error=0;
int intjoint2error=0;

void setup() {
  Wire.begin();       // join i2c bus (address optional for master)
  Serial.begin(115200);  // start serial for output
  pinMode(motorSpeed1, OUTPUT);
  pinMode(motorSpeed2, OUTPUT);
  pinMode(motorDirection1, OUTPUT);
  pinMode(motorDirection2, OUTPUT);
  pinMode(potPin1, INPUT);
  pinMode(potPin2, INPUT);
  //  setPwmFrequency(motorSpeed1, 2);
  //  setPwmFrequency(motorSpeed2, 2);
  //  pot1start = analogRead(potPin1);
  //  pot2start = analogRead(potPin2);

}

void loop() {

  //clear values to ground
  Wire.begin();
  Wire.beginTransmission(B0101000);
  Wire.write(B01000000);
  Wire.endTransmission(true);
  Wire.begin();
  Wire.requestFrom(B0101000, 2);
  //  while (Wire.available()) {
```

```
//    int a = Wire.read();
//  }
Wire.endTransmission(true);


//read from port 1 on ADC
Wire.begin();
Wire.beginTransmission(B0101000);
Wire.write(B00100000);
Wire.endTransmission(true);
Wire.begin();
Wire.requestFrom(B0101000, 2);    // request 6 bytes from slave device #2

  int flag = 1;
char msga, msgb;
while (Wire.available())   // slave may send less than requested
{
  if (flag) {
    flag = 0;
    msga = Wire.read(); // receive a byte as character
    //      Serial.print("msga ");
    //       Serial.println(msga,DEC);
  }
  else {
    msgb = Wire.read(); // receive a byte as character
    // Serial.print("ch2 ");
    //Serial.println(ch2,DEC);
  }

}
Wire.endTransmission(true);

int c = msga & 0x0F;
c = c << 8;
c = c + msgb;
Serial.print("c ");
Serial.print(c);        // print the character
Serial.print("\t");



//clear values to ground
Wire.begin();
Wire.beginTransmission(B0101000);
Wire.write(B01000000);
Wire.endTransmission(true);
```

```
Wire.begin();
Wire.requestFrom(B0101000, 2);    // request 6 bytes from slave device #2
//  while (Wire.available()) {
//    int a = Wire.read();
//  }
Wire.endTransmission(true);


//read from port 3 on ADC
Wire.begin();
Wire.beginTransmission(B0101000);
Wire.write(B10000000);
Wire.endTransmission(true);
Wire.begin();
Wire.requestFrom(B0101000, 2);  // request 6 bytes from slave device #2
char msgc, msgd;
flag = 1;
while (Wire.available())   // slave may send less than requested
{
  if (flag) {
    flag = 0;
    msgc = Wire.read(); // receive a byte as character
  }
  else {
    msgd = Wire.read(); // receive a byte as character
  }
}
Wire.endTransmission(true);

int b = msgc & 0x0F;
b = b << 8;
b = b + msgd;
Serial.print("b ");
Serial.print(b);
Serial.print("\t");  // print the character

int val1 = analogRead(potPin1);
int val2 = analogRead(potPin2);

val1 = map(val1, 0, 1023, -2048, 2048);
val2 = map(val2, 0, 1023, -2048, 2048);

int jointval1= c-2048;
int jointval2= b-2048;

//  intjoint1error = intjoint1error + (val1 - jointval1)/100;
```

```
  //  intjoint2error = intjoint2error + (val2 - jointval2)/100;
  //
  //  if(intjoint1error> 5000){
  //    intjoint1error =5000;
  //  }
  //
  //  if(intjoint2error> 5000){
  //    intjoint2error =5000;
  //  }
  //
  //  Serial.print("int J1 ");
  //  Serial.print(intjoint1error,DEC);
  //  Serial.print("\t");
  //
  //  Serial.print("int J2 ");
  //  Serial.print(intjoint2error,DEC);
  //  Serial.print("\t");

  int errorJoint1= (val1 - jointval1)/14 + intjoint1error/600;
  int errorJoint2= (val2 - jointval2)/14 + intjoint2error/600;

  Serial.print("errorJ1 ");
  Serial.print(errorJoint1,DEC);
  Serial.print("\t");

  Serial.print("errorJ2 ");
  Serial.println(errorJoint2,DEC);
 //  Serial.print("\t");

  if(errorJoint1 > 255){
    errorJoint1 =255;
  }

  if(errorJoint2 > 255){
    errorJoint2 =255;
  }
  if(c<2){
    analogWrite(motorSpeed1, 0);
  }
  else{
    analogWrite(motorSpeed1, abs(errorJoint1));
  }
  if(errorJoint1 >= 0){
    digitalWrite(motorDirection1, HIGH);
 //    Serial.print("Dir1 HIGH");
 //    Serial.print("\t");
```

```
  }
  else {
    digitalWrite(motorDirection1, LOW);
//    Serial.print("Dir1 LOW");
//    Serial.print("\t");
  }
  if(b <2){
    analogWrite(motorSpeed2, 0);
  }
  else{
    analogWrite(motorSpeed2, abs(errorJoint2));
  }
  if(errorJoint2 >= 0){
    digitalWrite(motorDirection2, HIGH);
//    Serial.println("Dir2 HIGH");

  }
  else {
    digitalWrite(motorDirection2, LOW);
//    Serial.println("Dir2 LOW");

  }


}
```

Position Control two fingers for Grasping

```
#include <Wire.h>

int motor1aPWM = 9;
int motor2aPWM = 10;
int motor1bPWM = 11;
int motor2bPWM = 12;
int motor1aDir = 2;
int motor2aDir = 3;
int motor1bDir = 4;
int motor2bDir = 5;
int desired1 = 0;
int desired2 = 0;

int current1a = 0;
int current1b = 0;
int current2a = 0;
int current2b = 0;
```

```
int desired1aOpen = 3325;
int desired1bOpen = 2742;
int desired2aOpen = 2548;
int desired2bOpen = 2177;

int desired1aClosed = 3034;
int desired1bClosed = 2282;
int desired2aClosed = 3060;
int desired2bClosed = 2914;

char PCA9546 = 0b1110011;

void setup() {
  Wire.begin();       // join i2c bus (address optional for master)
  Serial.begin(115200);  // start serial for output
  pinMode(motor1aPWM, OUTPUT);
  pinMode(motor2aPWM, OUTPUT);
  pinMode(motor1bPWM, OUTPUT);
  pinMode(motor2bPWM, OUTPUT);
  pinMode(motor1aDir, OUTPUT);
  pinMode(motor2aDir, OUTPUT);
  pinMode(motor1bDir, OUTPUT);
  pinMode(motor2bDir, OUTPUT);

}



void loop() {
  I2cChangeCh(PCA9546,1);
  getPot('a');
  I2cChangeCh(PCA9546,0b00001000);
  getPot('b');
  Serial.print("1a = ");
  Serial.print(current1a,DEC);
  Serial.print("\t");
  Serial.print("2a = ");
  Serial.print(current2a,DEC);
  Serial.print("\t");
  Serial.print("1b = ");
  Serial.print(current1b,DEC);
  Serial.print("\t");
  Serial.print("2b = ");
  Serial.println(current2b,DEC);
```

```
//  int errorJoint1a= (desired1 - current1a)/12;// + intjoint1error/600;
//  int errorJoint2a= (desired2 - current2a)/12;// + intjoint2error/600;
//  int errorJoint1b= (desired1 - current1b)/12;// + intjoint1error/600;
//  int errorJoint2b= (desired2 - current2b)/12;// + intjoint2error/600;
//
//  setMotor(motor1aPWM,motor1aDir,errorJoint1a);
//  setMotor(motor2aPWM,motor2aDir,errorJoint2a);
//  setMotor(motor1bPWM,motor1bDir,errorJoint1b);
//  setMotor(motor2bPWM,motor2bDir,errorJoint2b);

}

int I2cChangeCh(char addrs, char ch){
  Wire.beginTransmission(addrs); // transmit to device #4
  Wire.write(ch);              // sends one byte
  Wire.endTransmission(true);
}

void setMotor(int PWMch,int dirCh, int value){

  if(value > 255){
    value =255;
  }

  if(value > 255){
    value =255;
  }
  if(value <2){
    analogWrite(PWMch, 0);
  }
  else{
    analogWrite(PWMch, abs(value));
  }
  if(value >= 0){
    digitalWrite(dirCh, HIGH);
//    Serial.println("Dir2 HIGH");

  }
  else {
    digitalWrite(dirCh, LOW);
//    Serial.println("Dir2 LOW");
  }
}

void getPot(char finger){
```

```
 //clear values to ground
 Wire.begin();
 Wire.beginTransmission(B0101000);
 Wire.write(B01000000);
 Wire.endTransmission(true);
 Wire.begin();
 Wire.requestFrom(B0101000, 2);
 //  while (Wire.available()) {
 //    int a = Wire.read();
 //  }
 Wire.endTransmission(true);


 //read from port 1 on ADC
 Wire.begin();
 Wire.beginTransmission(B0101000);
 Wire.write(B00100000);
 Wire.endTransmission(true);
 Wire.begin();
 Wire.requestFrom(B0101000, 2);    // request 6 bytes from slave device #2

  int flag = 1;
 char msga, msgb;
 while (Wire.available())   // slave may send less than requested
 {
  if (flag) {
    flag = 0;
    msga = Wire.read(); // receive a byte as character
//          Serial.print("msga ");
//           Serial.println(msga,DEC);
  }
  else {
    msgb = Wire.read(); // receive a byte as character
//      Serial.print("ch2 ");
//     Serial.println(msgb,DEC);
  }

 }
 Wire.endTransmission(true);

 int c = msga & 0x0F;
 c = c << 8;
 c = c + msgb;

//  Serial.print("c ");
```

```
//     Serial.println(c,DEC);

 //clear values to ground
 Wire.begin();
 Wire.beginTransmission(B0101000);
 Wire.write(B01000000);
 Wire.endTransmission(true);
 Wire.begin();
 Wire.requestFrom(B0101000, 2);    // request 6 bytes from slave device #2
 //  while (Wire.available()) {
 //    int a = Wire.read();
 //  }
 Wire.endTransmission(true);


 //read from port 3 on ADC
 Wire.begin();
 Wire.beginTransmission(B0101000);
 Wire.write(B10000000);
 Wire.endTransmission(true);
 Wire.begin();
 Wire.requestFrom(B0101000, 2);  // request 6 bytes from slave device #2
 char msgc, msgd;
 flag = 1;
 while (Wire.available())   // slave may send less than requested
 {
  if (flag) {
    flag = 0;
    msgc = Wire.read(); // receive a byte as character
  }
  else {
    msgd = Wire.read(); // receive a byte as character
  }
 }
 Wire.endTransmission(true);

 int b = msgc & 0x0F;
 b = b << 8;
 b = b + msgd;

//  Serial.print("b ");
//     Serial.println(b,DEC);

 if(finger == 'a'){
  current1a = c;
  current2a = b;
```

```
  }
  else{
    current1b = c;
    current2b = b;
  }
}
```

Appendix B: Mathcad Spring and Motor Selection

$P_j := 4mm$

$P_m := 8.5mm$

$L_{j2} := 1.43in$ $P_w := \frac{.75}{2}in$

$load := .5kg$ $L_{j3} := 4in$

$L_{j1} := 3.27in$

$J1_{torque} := \frac{L_{j1} \cdot g \cdot load}{P_j} = 101.815\,N$

$J1_{speed} := \frac{\pi}{4}\frac{rad}{s}$

$J2_{speed} := \frac{\pi}{2}\frac{rad}{s}$

$J1_{motor} := J1_{torque} \cdot P_m = 0.865 \cdot N \cdot m$

$J2_{torque} := \frac{L_{j2} \cdot g \cdot load}{P_j} = 44.525\,N$

$J3_{torque} := \frac{L_{j3} \cdot g \cdot load}{P_w} = 52.302\,N$

$J2_{motor} := J2_{torque} \cdot P_m = 0.378 \cdot N \cdot m$

$J3_{motor} := J3_{torque} \cdot P_m = 0.445 \cdot N \cdot m$

$S1_{motor} := \frac{P_w}{P_m} \cdot J1_{speed} = 8.404 \cdot rpm$

$S2_{motos} := \frac{P_w}{P_m} \cdot J2_{speed} = 16.809 \cdot rpm$

$cir := \pi \cdot .75in$

$Dx := cir \cdot \frac{10}{360} = 0.065 \cdot in$

$k := \frac{J3_{torque}}{4 \cdot Dx} = 44.912 \cdot \frac{lbf}{in}$

Lee Spring: LHL 375D 04

Lee Spring: LC 051D 05 M

$L_{f1} := 1.2in$ $P_{f1} := 6mm$

$L_{f2} := 2.4in$ $P_{f2} := 7mm$

$P_W := .75in$

$L_W := 4.3in$

$P_{mf} := .5in$

load

$P_{mw} := .6in$

$$T_{f1} := \frac{L_{f1} \cdot g \cdot load}{\frac{P_{f1}}{2}} = 49.818\,N \qquad T_{f2} := \frac{L_{f2} \cdot g \cdot load}{\frac{P_{f2}}{2}} = 85.402\,N$$

$$F_{f1} := T_{f1} \cdot \frac{P_{mf}}{2} = 0.316 \cdot N \cdot m \qquad F_{f2} := T_{f2} \cdot \frac{P_{mf}}{2} = 0.542 \cdot N \cdot m$$

$$T_w := \frac{L_W \cdot g \cdot load}{\frac{P_W}{2}} = 56.225\,N$$

$$F_W := T_w \cdot \frac{P_{mw}}{2} = 0.428 \cdot N \cdot m$$

$cir := \pi \cdot 7mm$

$x := .35in - .23in = 3.048 \times 10^{-3}\,m$ $\qquad Dx := cir \cdot \frac{20}{360} = 0.048 \cdot in$

$$k := \frac{T_{f2}}{4 \cdot x} = 39.998 \cdot \frac{lbf}{in}$$

Appendix C: Magnetic Sensor Data

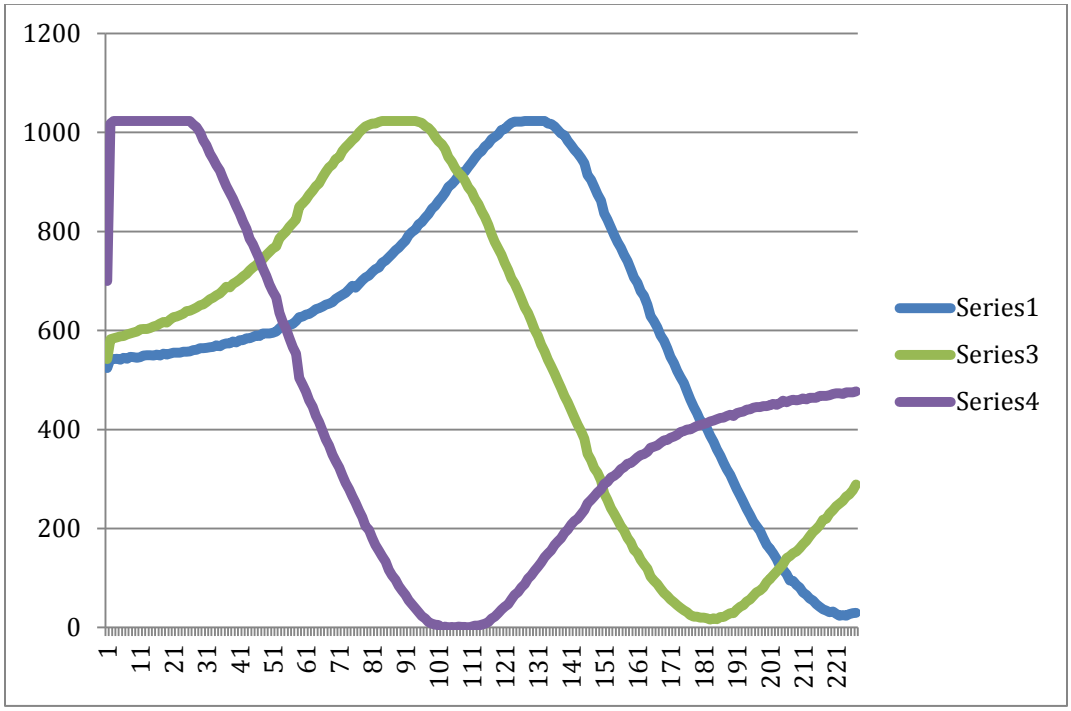

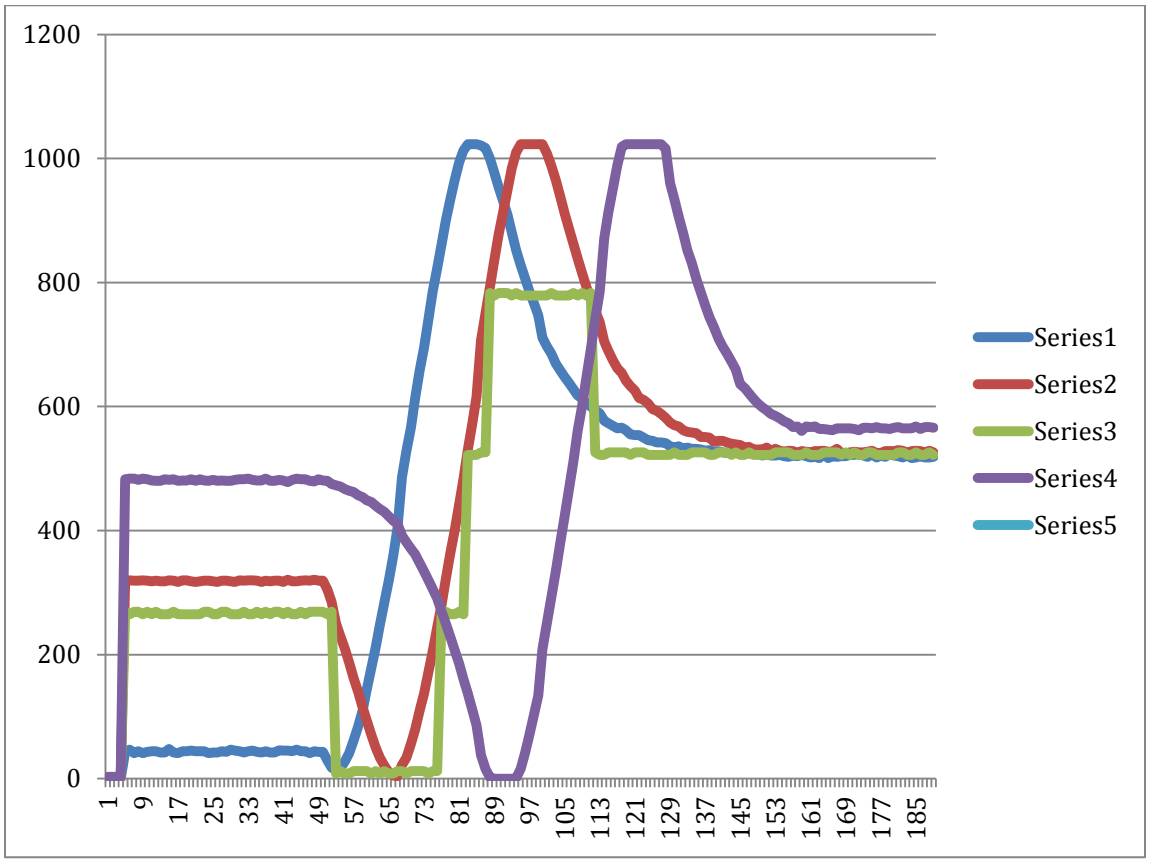

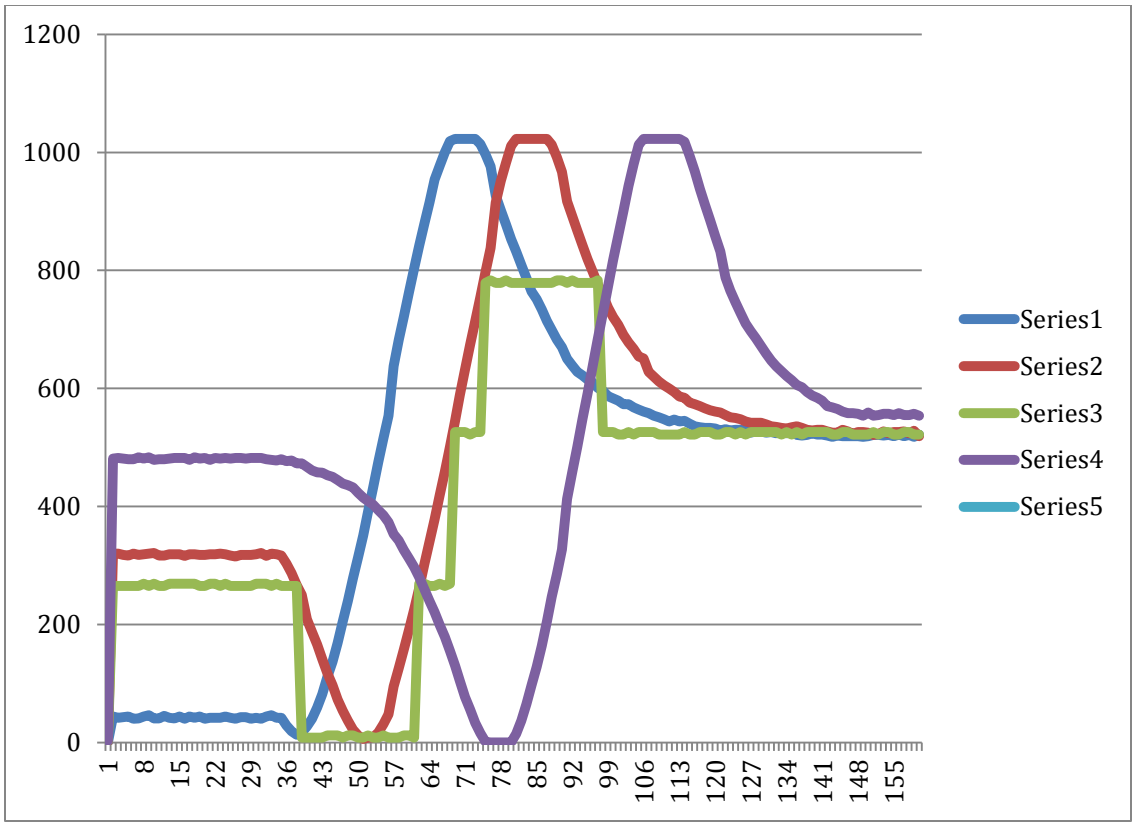
1200
1000
800
600
400
200
0
1
8
15
22
29
36
43
50
57
64
71
78
85
92
99
106
113
120
127
134
141
148
155
Series1
Series2
Series3
Series4
Series5

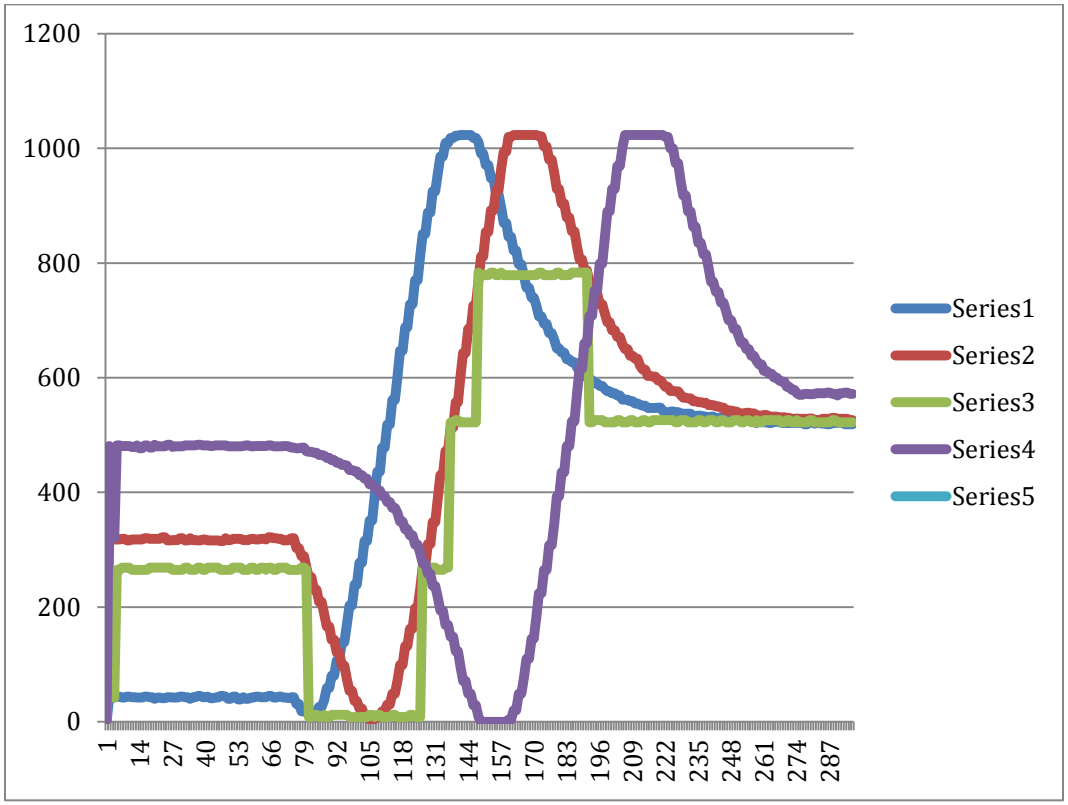
1200
1000
800
600
400
200
0
1
14
27
40
53
66
79
92
105
118
131
144
157
170
183
196
209
222
235
248
261
274
287
Series1
Series2
Series3
Series4
Series5

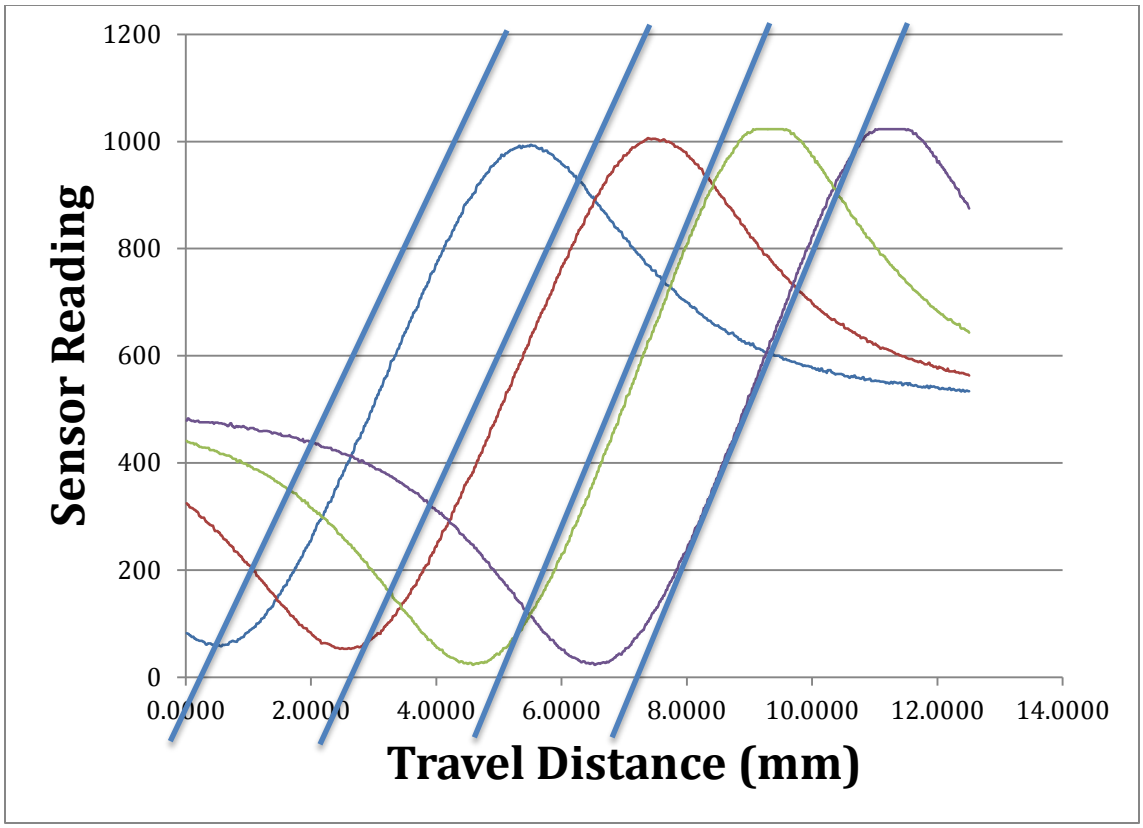
Sensor Reading
1200
1000
800
600
400
200
0
0.0000
2.0000
4.0000
6.0000
8.0000
10.0000
12.0000
14.0000
Travel Distance (mm)

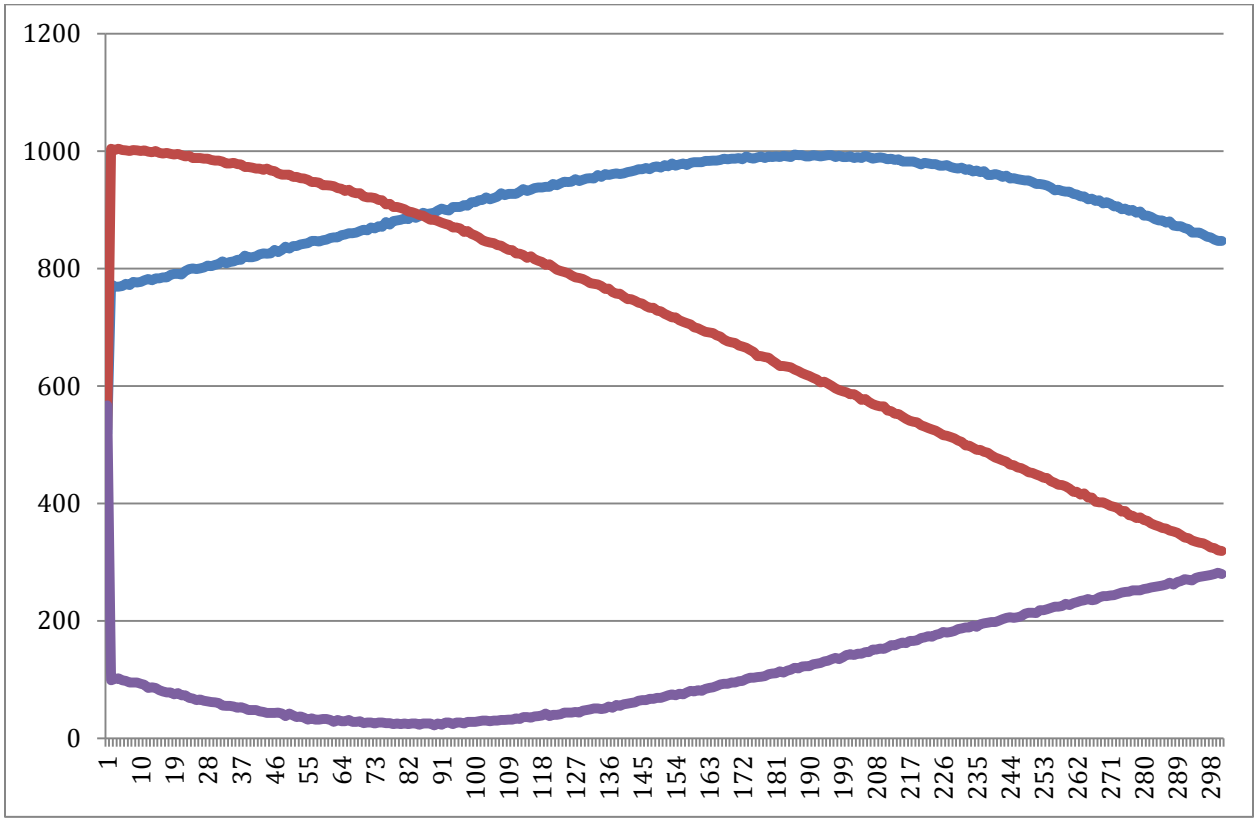
1200
1000
800
600
400
200
0
1
10
19
28
37
46
55
64
73
82
91
100
109
118
127
136
145
154
163
172
181
190
199
208
217
226
235
244
253
262
271
280
289
298